Supplementary Information

Hydroquinone-based Anion Receptors for Redox-Switchable Chloride Binding.

Daniel A. McNaughton[1], Xiaochen Fu [1], William Lewis[1], Deanna M. D'Alessandro[1] and Philip A. Gale[1,*]

[1] School of Chemistry (F11), The University of Sydney, Sydney, NSW 2006, Australia.
***** Correspondence: philip.gale@sydney.edu.au

1. Characterisation Data

^{1}H NMR and ^{13}C{^{1}H} NMR shown for each compound. High resolution mass spectrometry (HR-MS) using ESI is displayed for all compounds aside from the quinone species – which were characterised with APCI.

2,5-dimethoxybenzoyl chloride

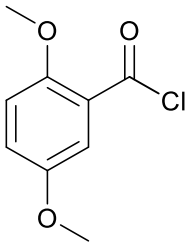

This compound was synthesised following a literature procedure [1]. 2,5-dimethoxybenzoic acid (1.00 g, 5.49 mmol) was dissolved in dry toluene (10 mL) and drops of DMF were added. The solution was stirred under N_2 atmosphere until all 2,5-dimethoxybenzoic acid had dissolved and was subsequently cooled to 0 °C in an ice bath. Following this, a portion on oxalyl chloride (0.732 g, 5.76 mmol) was added dropwise and the solution stirred at 0 °C for a further 30 minutes. The mixture was then stirred at room temperature for a further 2.5 hours before the solvent was removed on a rotary evaporator to leave a yellow oil (0.941 g, 4.69 mmol, 85%). ^{1}H NMR and mass spec were not obtained, as the product was used immediately for subsequent reactions.

2,5-dimethoxy-N-phenylbenzamide

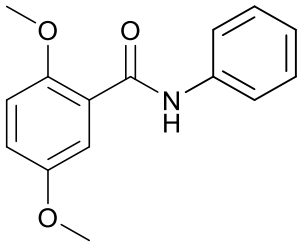

This compound was also synthesised following the same procedure [1]. 2,5-dimethoxybenzoyl chloride (1.00 g, 4.99 mmol) was dissolved in acetonitrile (18 mL) before a portion of K_2CO_3 (0.800 g, 5.79 mmol) was added. Subsequently, aniline (0.464 g, 4.99 mmol) was added and the mixture left to stir at room temperature for 2 days. The solvent was removed on a rotary evaporator before the resultant solid was redissolved in EtOAc and washed with 1M NaOH solution. The solvent was again removed, and the solid recrystallised from diethyl ether to yield the product (0.634 g, 2.47 mmol, 50%). The NMR spectra were found to be consistent with literature spectra.

2,5-dimethoxy-N-(p-tolyl)benzamide

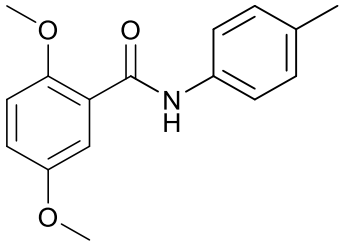

2,5-dimethoxybenzoyl chloride (0.941 g, 4.69 mmol) was dissolved in acetonitrile (20 mL) before a portion of K_2CO_3 (0.840 g, 6.08 mmol) was added. Subsequently, p-toluidine (0.502 g, 4.69 mmol) was added and the mixture left to stir at room temperature for 2 days. The solvent was removed on a rotary evaporator before the resultant solid was redissolved in EtOAc and washed with 1M NaOH solution. The solvent was again removed to leave a brown oil, which recrystallised from ether to yield a yellowish-white product (0.488 g, 1.80 mmol, 38%).

^{1}H NMR (400 MHz, $CDCl_3$-*d*) δ ppm 10.06 (1 H, s), 7.62 (2 H, d, J 8.4), 7.23 (1 H, d, J 3.0), 7.14 (2H, d, J 8.5), 7.08 (2 H, d, J 3.0), 3.86 (3 H, s), 3.75 (3 H, s), 2.27 (3 H, s); **^{13}C{^{1}H} NMR** (101 MHz, $CDCl_3$-*d*) δ ppm 162.8, 154.1, 151.5, 135.9, 133.8, 129.5, 122.4, 120.4, 119.8, 115.6, 113.3, 56.9, 55.8, 20.9.

LR-MS (ESI$^+$) *m/z* 294.16 $[M + Na]^+$, 565.20 $[2M + Na]^+$; **HR-MS** (ESI$^+$) calcd for $C_{16}H_{17}NO_3$ $[M+Na]^+$: 294.11061, found *m/z* 294.11205

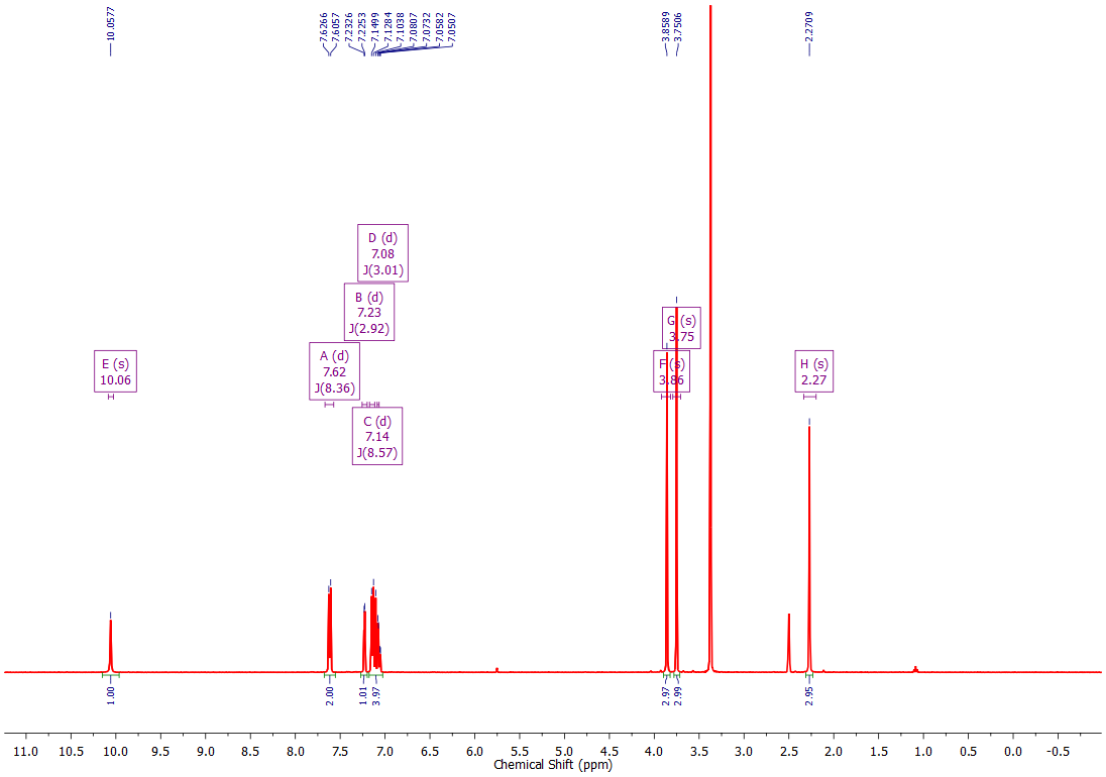

Figure 1. ^{1}H NMR (400 MHz) spectrum of 2,5-dimethoxy-N-(p-tolyl)benzamide in $(CD_3)_2SO_3$ at 298 K.

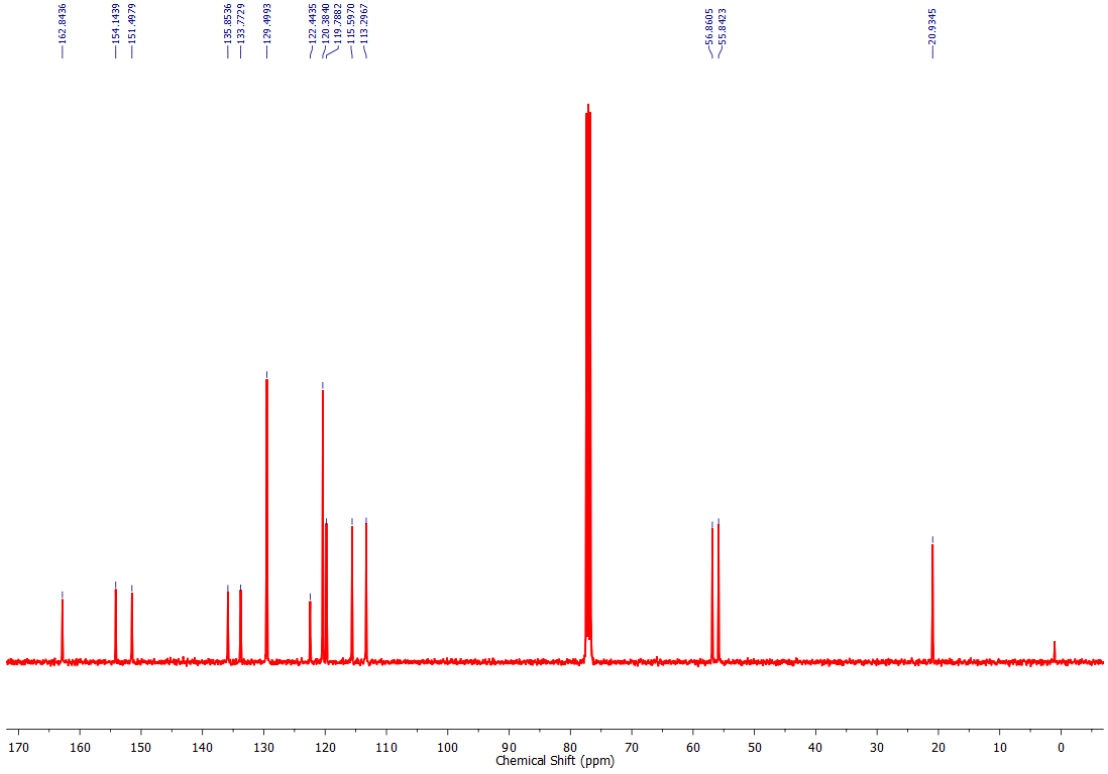

Figure 2. $^{13}C\{^{1}H\}$ NMR (101 MHz) spectrum of 2,5-dimethoxy-N-(p-tolyl)benzamide in $(CD_3)_2SO_3$ at 298 K.

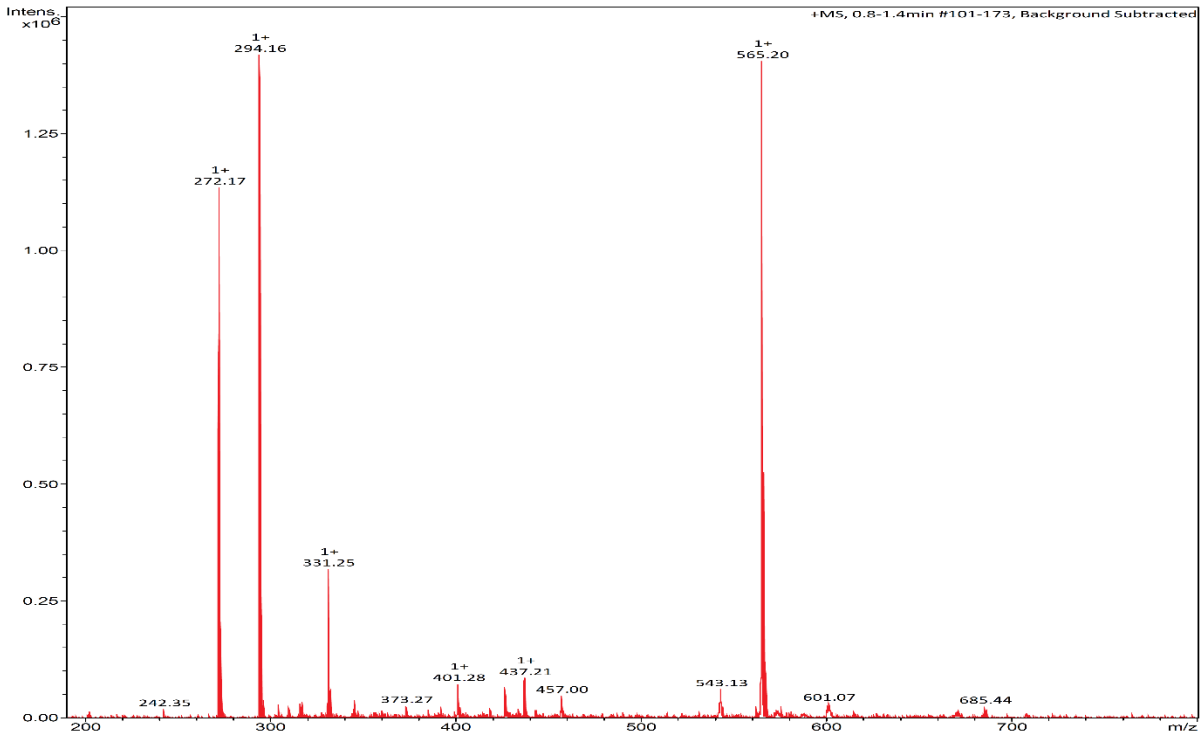

Figure 3. LR-MS (ESI^+) of 2,5-dimethoxy-N-(p-tolyl)benzamide.

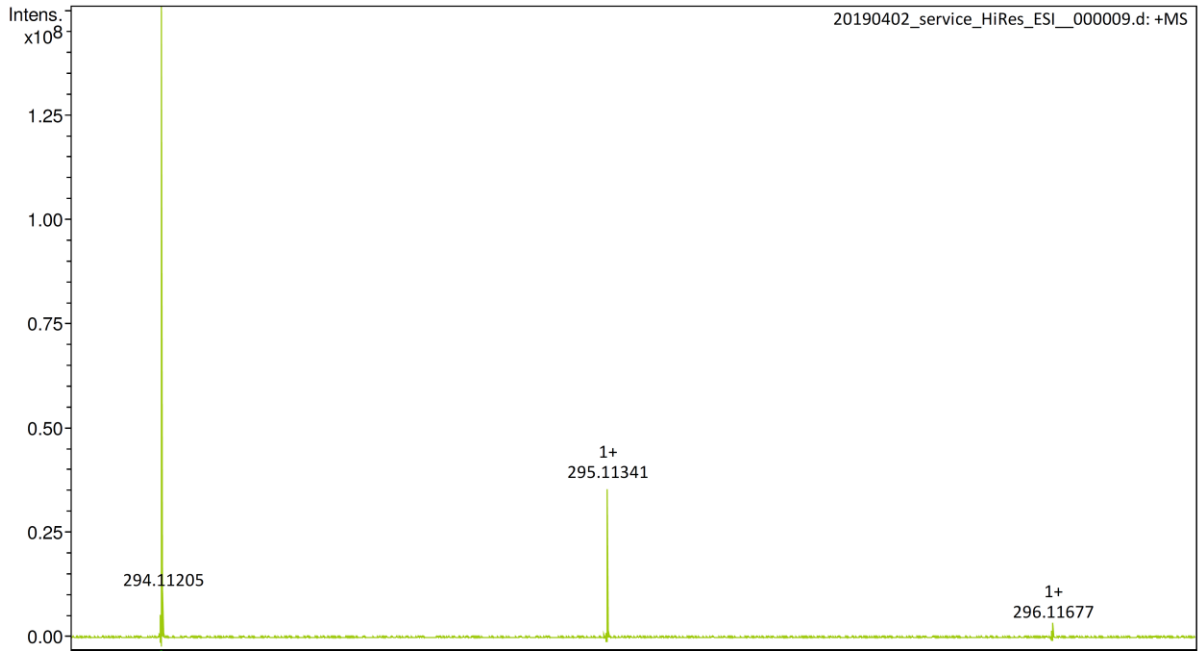

Figure 4. HR-MS of 2,5-dimethoxy-N-(p-tolyl)benzamide

N-(4-fluorophenyl)-2,5-dimethoxybenzamide

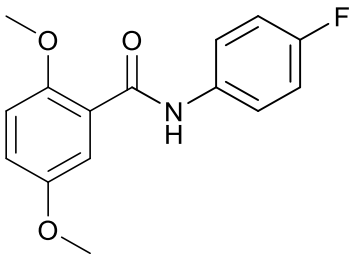

2,5-dimethoxybenzoyl chloride (0.690 g, 3.44 mmol) was dissolved in acetonitrile (20 mL) before a portion of K_2CO_3 (0.625 g, 4.52 mmol) was added. Subsequently, 4-fluoroanline (0.382 g, 3.44 mmol) was added and the mixture left to stir at room temperature for 2 days. The solvent was removed on a rotary evaporator before the resultant solid was redissolved in EtOAc and washed with 1M NaOH solution. The solvent was again removed, and the solid recrystallised from ether to yield a fine, white crystalline product (0.515 g, 1.87 mmol, 55%).

^{1}H NMR (500 MHz, DMSO-d_6) 10.17 (1 H, s), 7.76 (2 H, dd, J 9.0, 5.1), 7.21 (1 H, d, J 3.0), 7.18 (2 H, t, J 8.9), 7.12 (1 H, d, J 9.0), 7.07 (1 H, dd, J 9.0, 3.0), 3.85 (3 H, s), 3.75 (3 H, s); **^{13}C{^{1}H} NMR** (101 MHz, DMSO-d_6) δ ppm 164.4 (s), 158.7 (d, J 240.1), 153.5 (s), 151.1 (s), 135.8 (d, J 2.5), 125.7 (s), 122.0 (d, J 7.8), 117.8 (s), 115.7 (d, J 22.2), 115.0 (s), 114.0 (s), 56.9 (s), 56.1 (s).

LR-MS (ESI$^+$) *m/z* 298.13 $[M + Na]^+$, 573.16 $[2M + Na]^+$; **HR-MS** (ESI$^+$) calcd for $C_{15}H_{14}FNO_3$ $[M+Na]^+$: 298.08554, found *m/z* 298.08499.

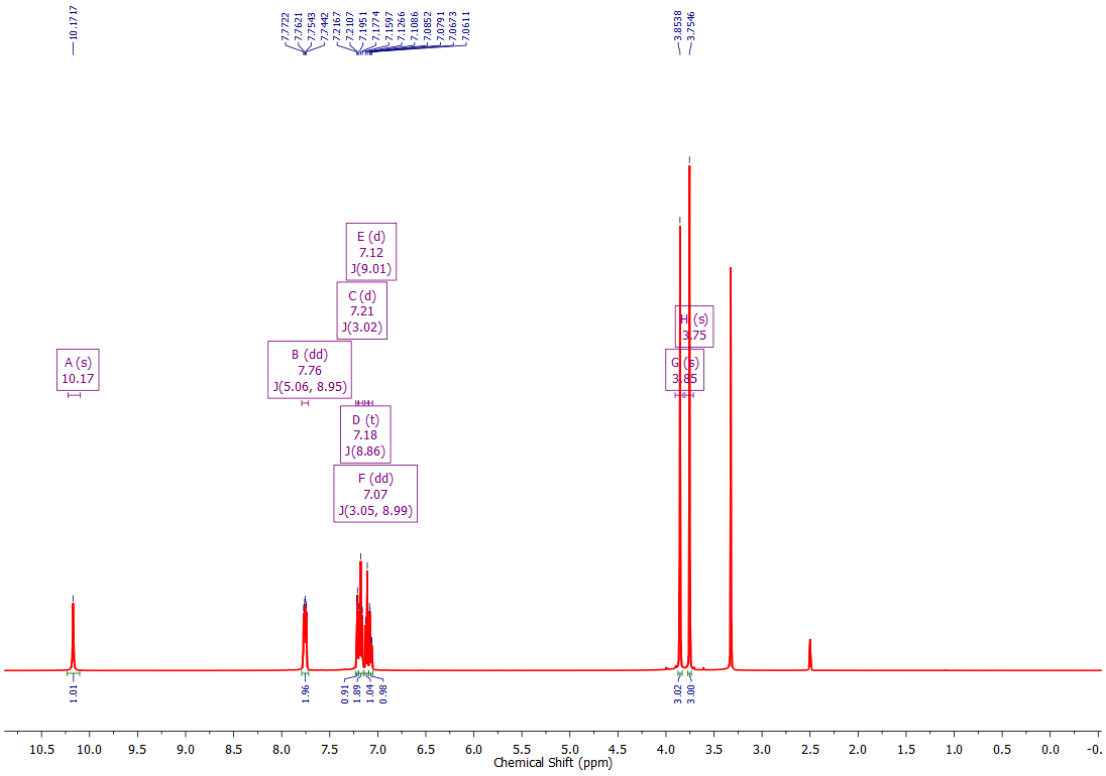

Figure 5. ^{1}H NMR (500 MHz) spectrum of N-(4-fluorophenyl)-2,5-dimethoxybenzamide in $(CD_3)_2SO_3$ at 298 K.

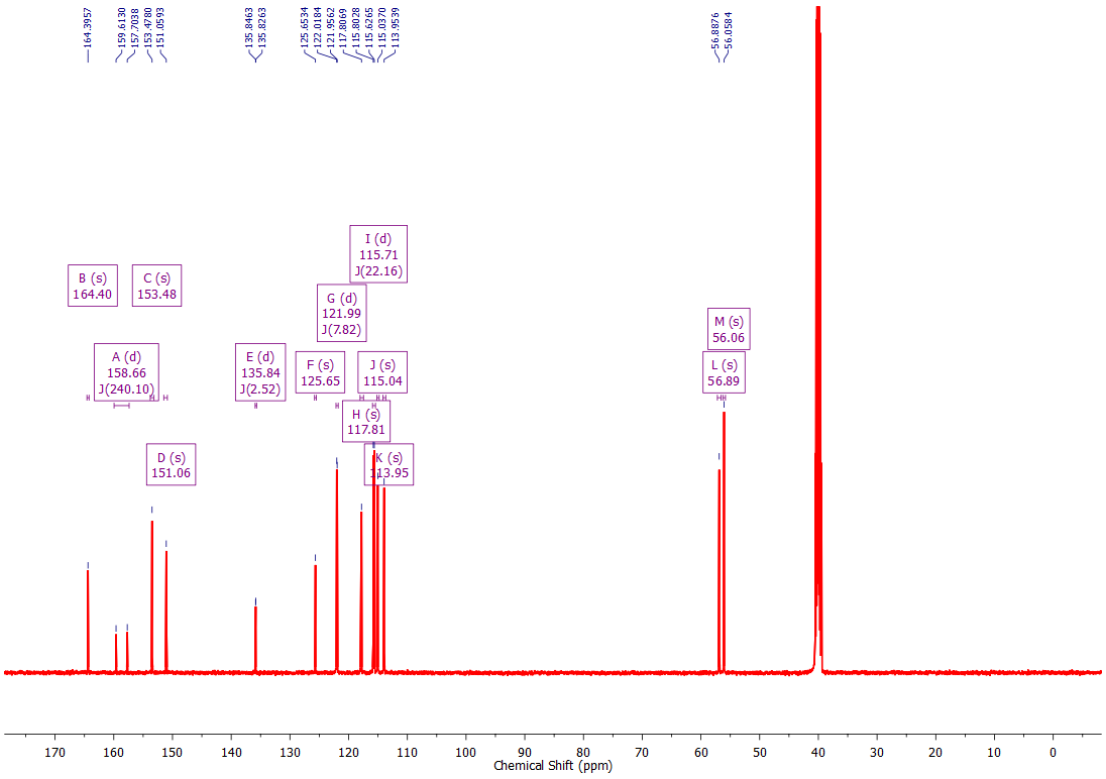

Figure 6. $^{13}C\{^{1}H\}$ NMR (101 MHz) spectrum of N-(4-fluorophenyl)-2,5-dimethoxybenzamide in $(CD_3)_2SO$ at 298 K.

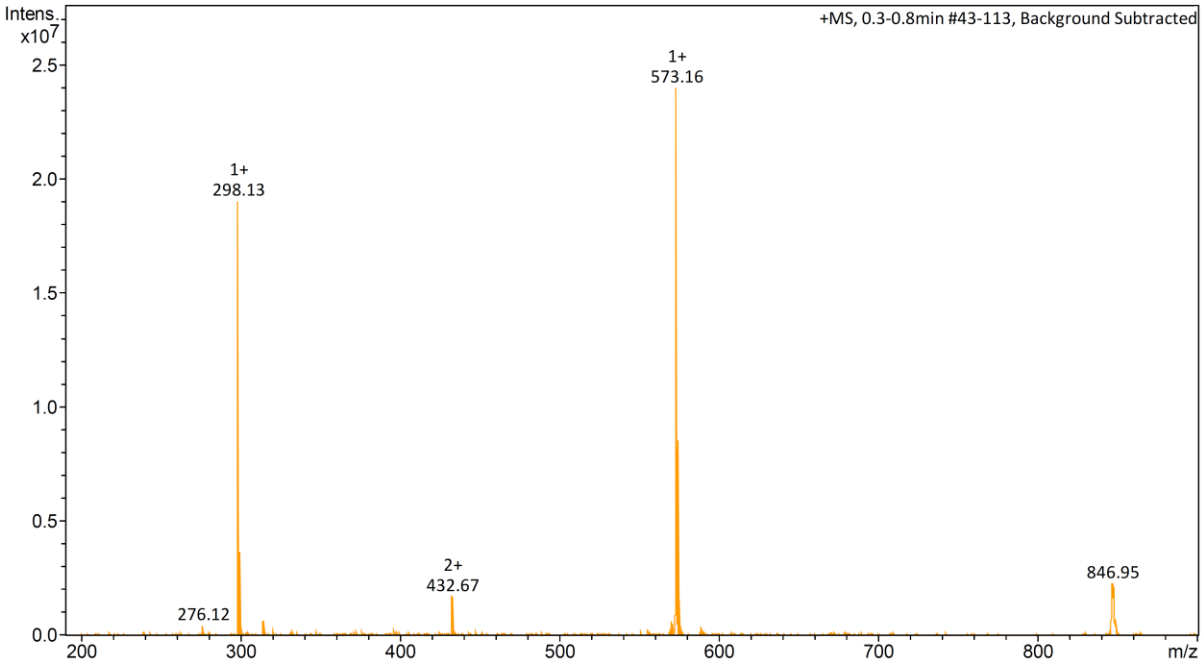

Figure 7. LR-MS (ESI$^+$) of N-(4-fluorophenyl)-2,5-dimethoxybenzamide.

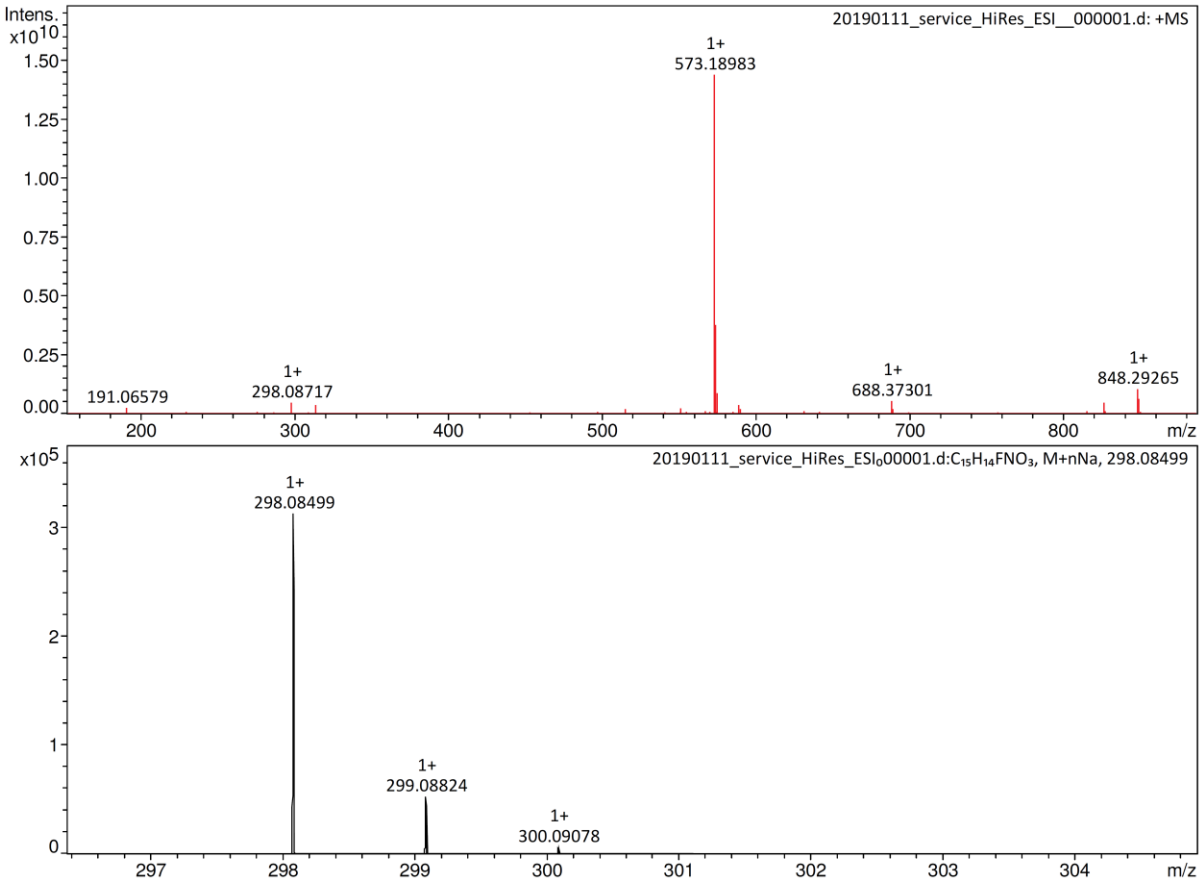

Figure 8. HR-MS (ESI$^+$) of N-(4-fluorophenyl)-2,5-dimethoxybenzamide.

N-(3,5-bis(trifluoromethyl)phenyl)-2,5-dimethoxybenzamide

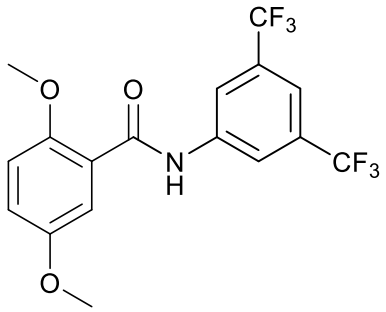

2,5-dimethoxybenzoyl chloride (1.00 g, 4.99 mmol) was dissolved in acetonitrile (20 mL) before a portion of K_2CO_3 (0.892 g, 6.45 mmol) was added. Subsequently, 3,5-(trifluoromethoxy)aniline (1.1143 g, 4.99 mmol) was added and the mixture left to stir at room temperature for 2 days. The solvent was removed on a rotary evaporator before the resultant solid was redissolved in EtOAc and washed with 1M NaOH solution. The solvent was again removed, and the solid recrystallised from ether to yield a dark yellow product (1.357 g, 3.45 mmol, 69%).

^{1}H NMR (500 MHz, DMSO-*d*$_6$) δ ppm 10.72 (1 H, s), 8.46 (2 H, s), 7.79 (1 H, s), 7.24 (1 H, d, J 2.9), 7.15 (1 H, d, J 9.0), 7.12 (1 H, dd, J 9.0, 2.9), 3.86 (3 H, s), 3.76 (3 H, s); **^{13}C{^{1}H} NMR** (101 MHz, $CDCl_3$-*d*) δ ppm 165.6 (s), 153.5 (s), 151.2 (s), 141.3 (s), 131.2 (q, J 32.8), 124.9 (s), 123.7 (q, J 272.8), 120.0 (d, J 3.0), 118.5 (s), 116.8 (dt, J 7.3, 3.7), 115.1 (s), 114.0 (s), 56.9 (s), 56.1 (s).

LR-MS (ESI^+) *m/z* 416.12 $[M + Na]^+$, 809.05 $[2M + Na]^+$; **HR-MS** (ESI^+) calcd for $C_{17}H_{13}F_6NO_3$ $[M+Na]^+$: 416.06973, found *m/z* 416.06918

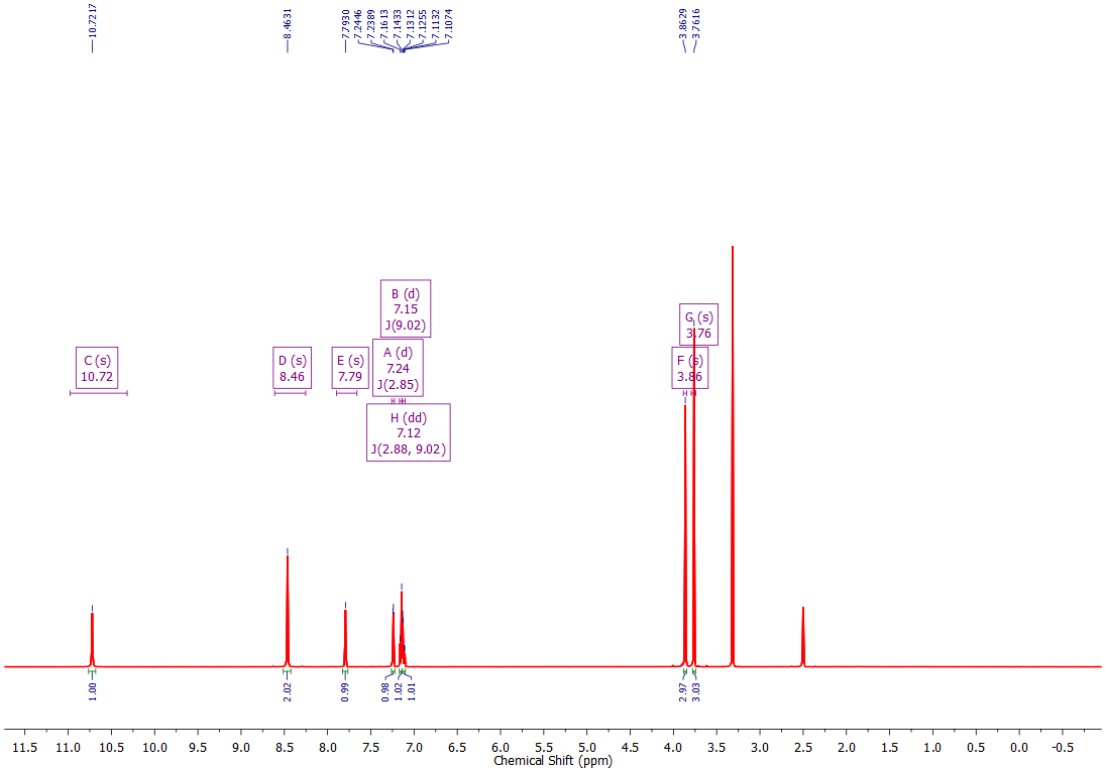

Figure 9. ^{1}H NMR (500 MHz) spectrum of *N*-(3,5-bis(trifluoromethyl)phenyl)-2,5-dimethoxybenzamide in $(CD_3)_2SO$ at 298 K.

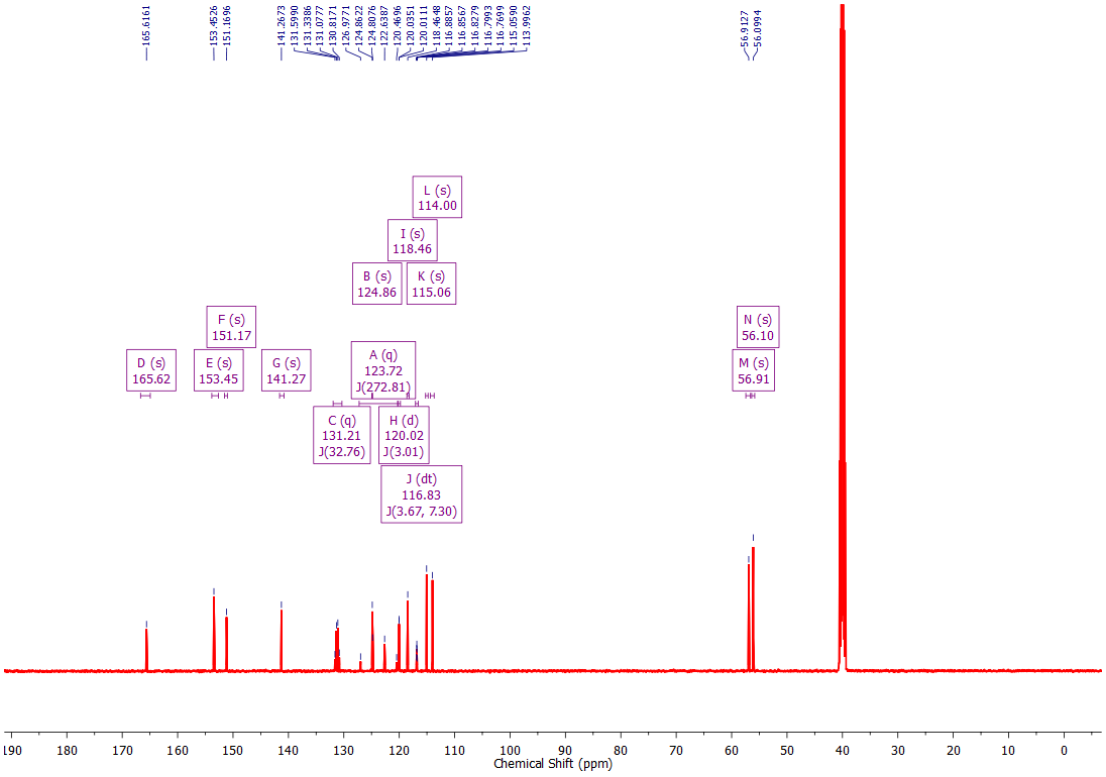

Figure 10. ^{13}C{^{1}H} NMR (101 MHz) spectrum of *N*-(3,5-bis(trifluoromethyl)phenyl)-2,5-dimethoxybenzamide in $(CD_3)_2SO$ at 298 K.

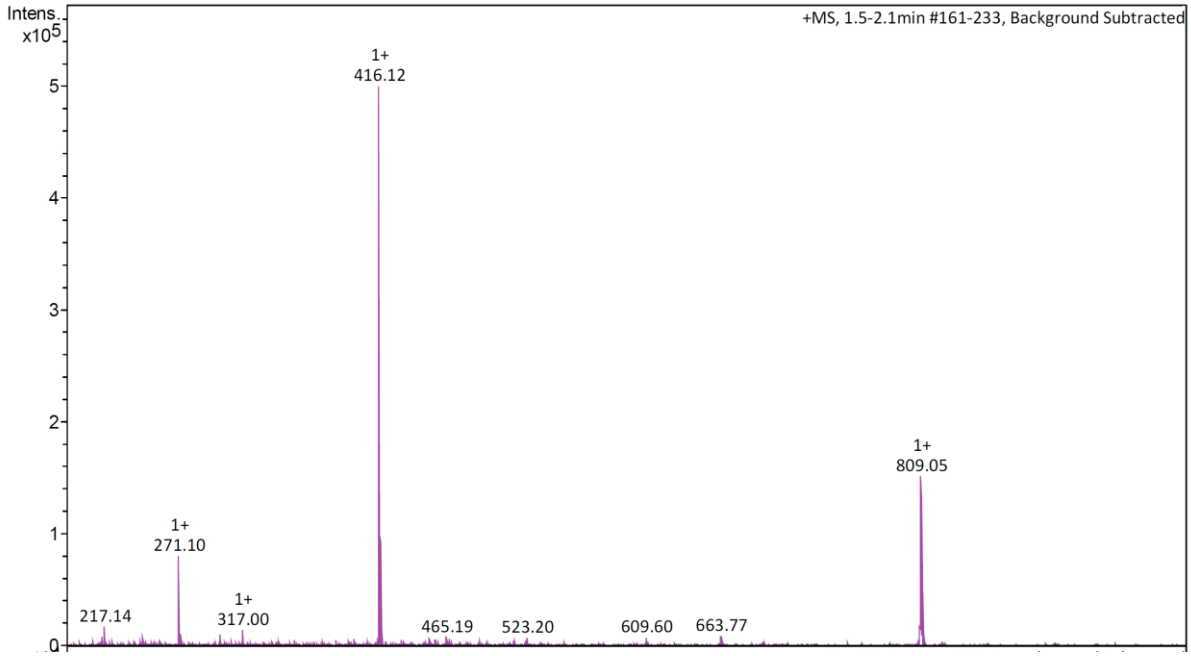

Figure 11. LR-MS (ESI$^+$) of *N*-(3,5-bis(trifluoromethyl)phenyl)-2,5-dimethoxybenzamide.

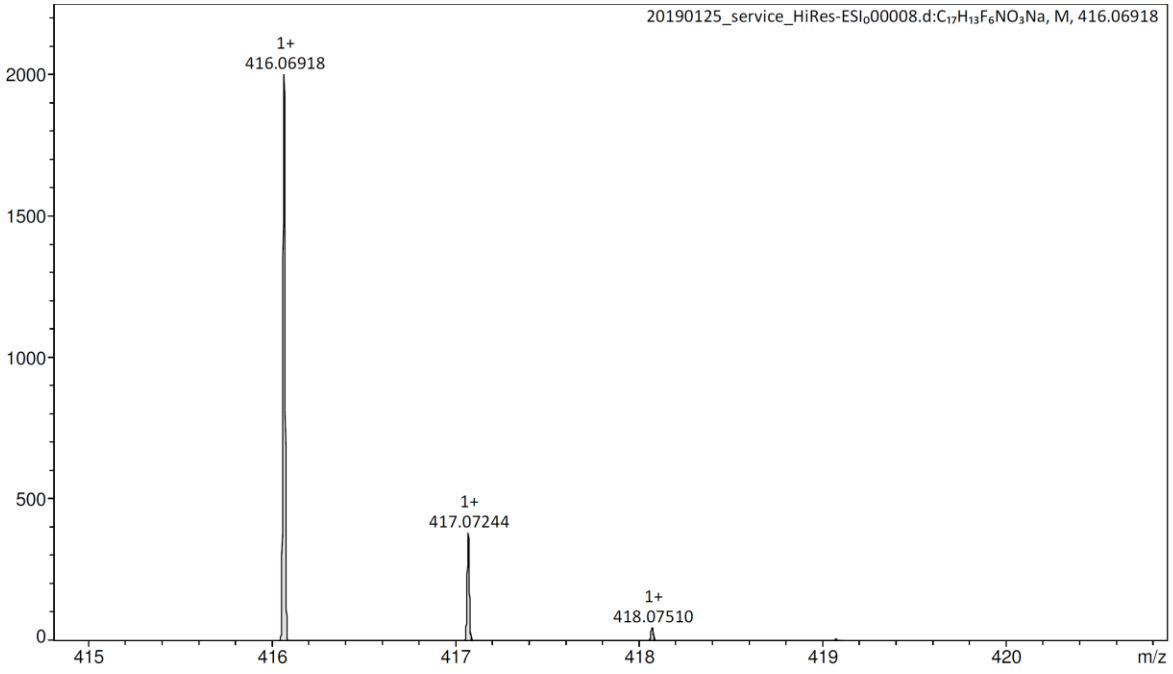

Figure 12. HR-MS (ESI$^+$) of *N*-(3,5-bis(trifluoromethyl)phenyl)-2,5-dimethoxybenzamide.

2,5-dihydroxy-*N*-phenylbenzamide

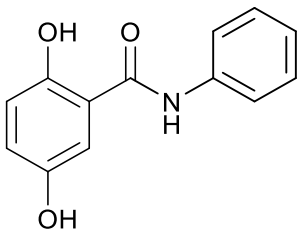

This compound was synthesised following literature procedure [1]. 2,5-dimethoxy-N-phenylbenzamide (0.418 g, 1.62 mmol) was dissolved as much as possible in dry DCM (5 mL), and the solution was cooled to 0 °C under a N_2 atmosphere. Subsequently, BBr_3 (1.947 g, 7.77 mmol) in 1M DCM solution (7.7 mL) was added dropwise, and the mixture sustained at 0 °C for 1 hour. The solution was allowed to warm to room temperature and stirred for another 5 hours. Following this, the solution was poured into a conical flask and deionised water (20 mL) was poured in to elicit the formation of a precipitate. This mixture was stirred for 15 minutes, and deionised water was also added to the original rbf to collect any residue. Next, the precipitate was filtered using a Büchner funnel and the solid washed with hexane (3 x 30 mL). The solid was collected from the filter paper and dried under vacuum to afford a brown solid (0.358 g, 1.56 mmol, 96%). The NMR spectra were consistent with those previously obtained in the literature.

2,5-dihydroxy-N-(p-tolyl)benzamide

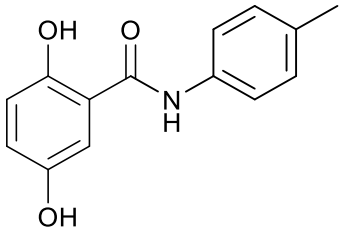

2,5-dimethoxy-N-(p-tolyl)benzamide (0.198 g, 0.74 mmol) was dissolved as much as possible in dry DCM (7 mL), and the solution was cooled to 0 °C under a N_2 atmosphere. Subsequently, BBr_3 (1.052 g, 4.2 mmol) in 1M DCM solution (4.2 mL) was added dropwise. The clear solution immediately changed to milky white and the temperature was sustained at 0 °C for 1 hour. The solution was allowed to warm to room temperature and stirred overnight. Following this, the solution had turned back to clear and was poured into a conical flask before deionised water (20 mL) was poured in to elicit the formation of a whitish-brown precipitate. This mixture was stirred for 15 minutes, and deionised water was also added to the original rbf to collect any residue. Next, the precipitate was filtered using a Büchner funnel and the solid washed with hexane (3 x 30 mL). The solid was collected from the filter paper and dried under vacuum to afford a whitish-brown solid (0.164 g, 0.67 mmol, 92%).

^{1}H NMR (400 MHz, DMSO-d_6) δ ppm 10.32 (1 H, s), 7.57 (2 H, d, J 8.3), 7.36 (1 H, d, J 2.8), 7.15 (2 H, d, J 8.3), 6.88 (1 H, dd, J 8.8, 2.9), 6.81 (1 H, d, J 8.8), 2.27 (3 H, s); **^{13}C{^{1}H} NMR** (101 MHz, DMSO-d_6) δ ppm 165.9 (s), 150.8 (s), 149.8 (s), 135.8 (s), 133.2 (s), 129.3 (s), 120.9 (s), 120.7 (s), 117.9 (s), 114.7 (s), 114.5 (s), 20.5 (d, J 16.1).

LR-MS (ESI^+) 266.10 $[M + Na]^+$; **HR-MS** (ESI^+) calcd for $C_{14}H_{13}NO_3$ $[M+Na]^+$: 266.07931, found *m/z* 266.07876

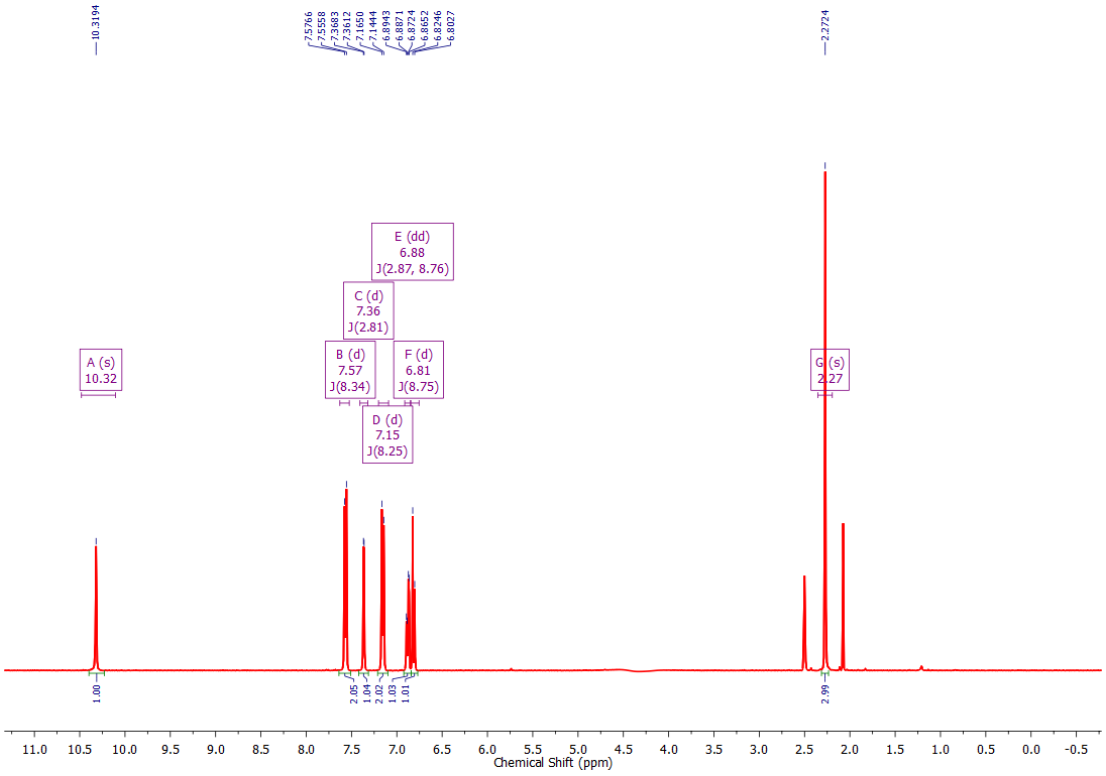

Figure 17. ^{1}H NMR (400 MHz) spectrum of 2,5-dihydroxy-N-(p-tolyl)benzamide in $(CD_3)_2SO$ at 298 K.

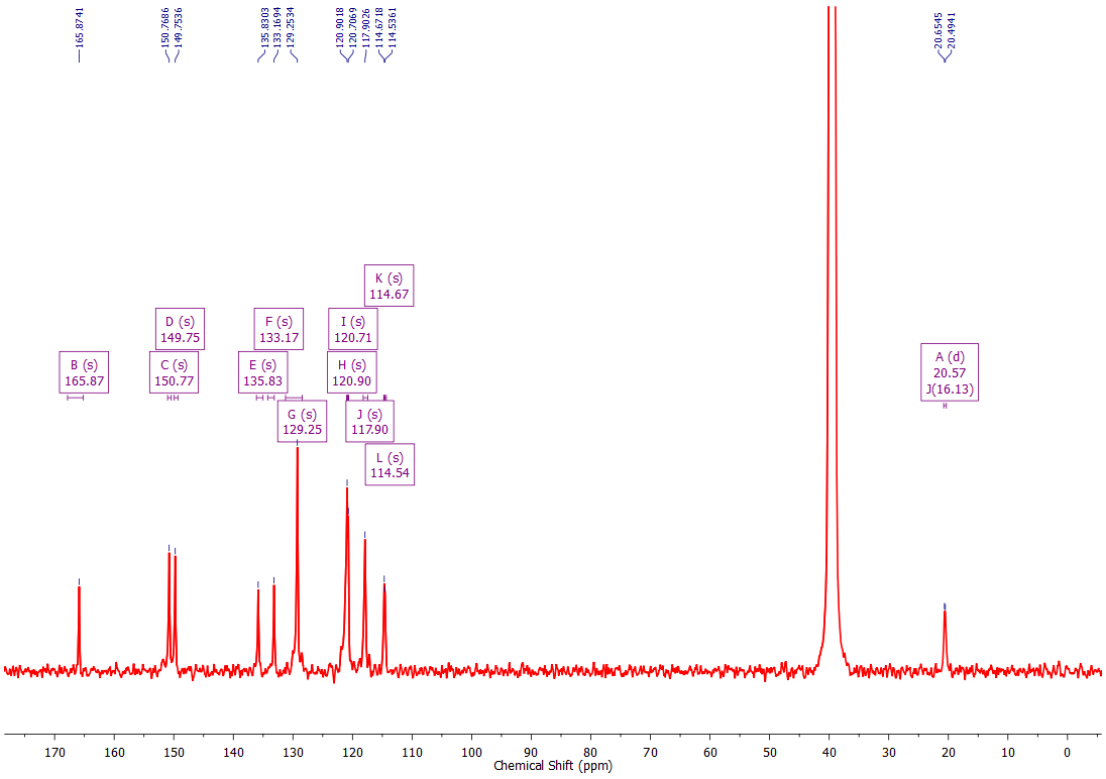

Figure 18. $^{13}C\{^{1}H\}$ NMR (101 MHz) spectrum of 2,5-dihydroxy-N-(p-tolyl)benzamide in $(CD_3)_2SO$ at 298 K.

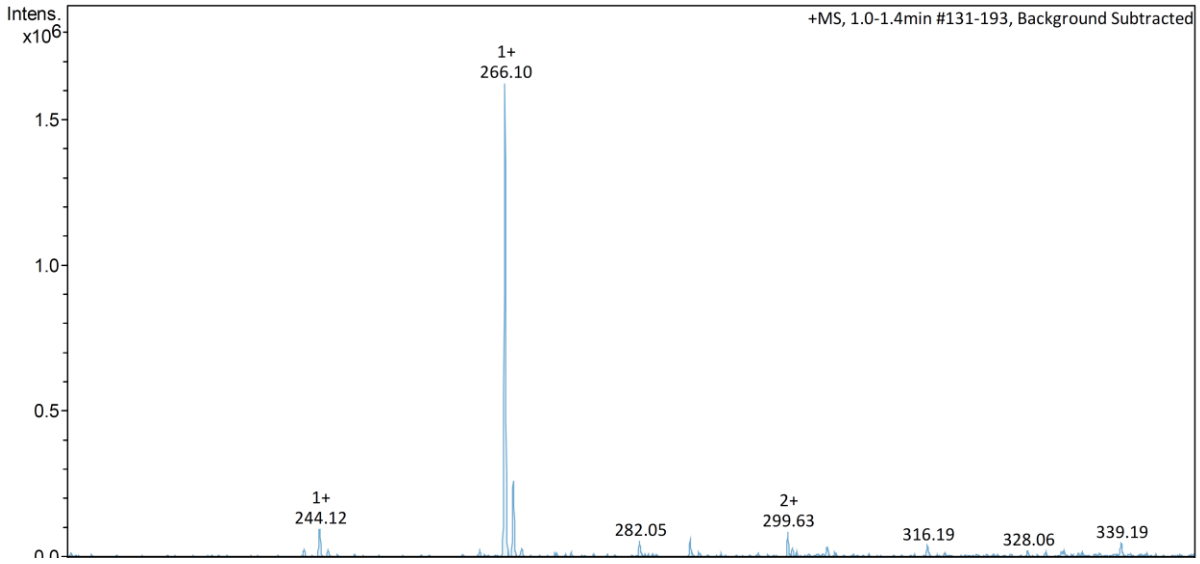

Figure 19. LR-MS (ESI$^+$) of 2,5-dihydroxy-N-(p-tolyl)benzamide.

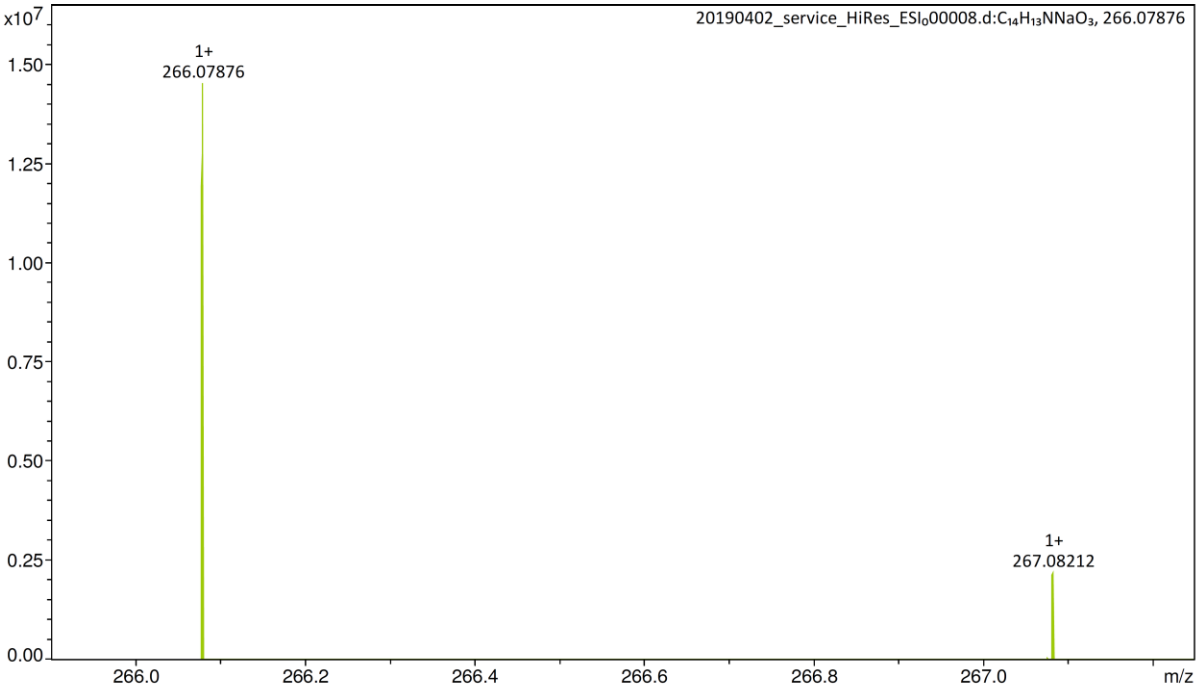

Figure 20. HR-MS (ESI$^+$) of 2,5-dihydroxy-N-(p-tolyl)benzamide.

N-(4-fluorophenyl)-2,5-dihydroxybenzamide

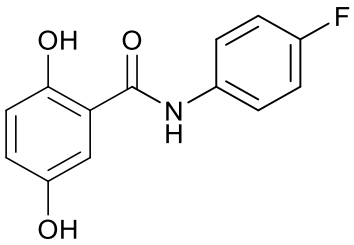

N-(4-fluorophenyl)-2,5-dimethoxybenzamide (0.045 g, 0.16 mmol) was dissolved in dry DCM (6 mL), and the solution was cooled to 0 °C under a N_2 atmosphere. Subsequently, BBr_3 (0.213 g, 0.85 mmol) in 1M DCM solution (1 mL) was added dropwise. The purple solution immediately changed to dark brown and the temperature sustained at 0 °C for 1 hour. The solution was then allowed to warm to room temperature and stirred overnight. Following this, the solution was a lighter brown in colour and was poured into a conical flask before deionised water (20 mL) was poured in to elicit the formation of a precipitate. This mixture was stirred for 15 minutes, and deionised water was also added to the original rbf to collect any residue. Next, the precipitate was filtered using a Büchner funnel and the solid washed with hexane (3 x 30 mL). The solid was collected from the filter paper and dried under vacuum to afford a whitish-brown solid (0.034 g, 0.14 mmol, 83%).

^{1}H NMR (500 MHz, DMSO-d_6) δ ppm 11.00 (1 H, s), 10.39 (1 H, s), 9.09 (1 H, s), 7.71 (2 H, dd, J 9.0, 5.0), 7.34 (1 H, d, J 2.9), 7.19 (2 H, t, J 8.9), 6.88 (1 H, dd, J 8.8, 2.9), 6.82 (1 H, d, J 8.8); **^{13}C{^{1}H} NMR** (101 MHz, DMSO-d_6) δ ppm 166.4 (s), 159.0 (d, J 240.7), 151.2 (s), 150.1 (s), 135.1 (d, J 2.6), 123.1 (d, J 7.9), 121.6 (s), 118.3 (s), 118.2 (s), 115.8 (d, J 22.2), 114.9 (s).

LR-MS (ESI$^-$) *m/z* 246.07 [M - H]$^-$, 493.18 [2M - H]$^-$; **HR-MS** (ESI$^-$) calcd for $C_{13}H_{10}FNO_3$ [M-H]$^-$: 246.05653, found *m/z* 246.05719.

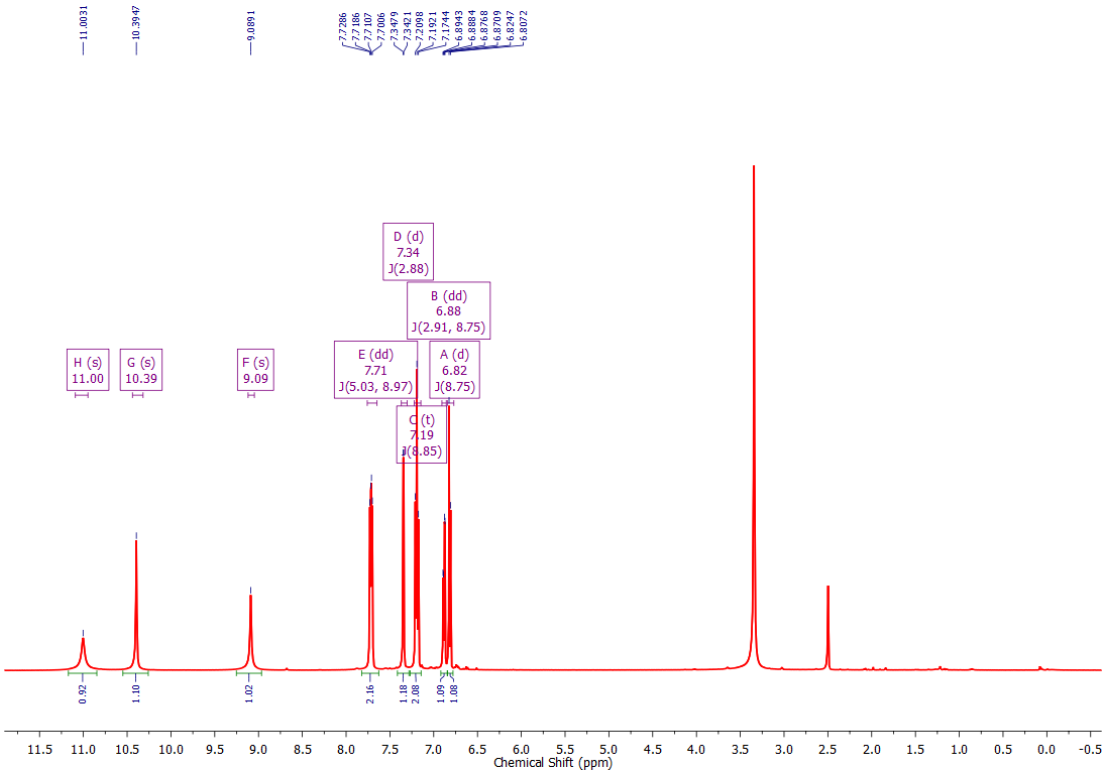

Figure 21. ^{1}H NMR (500 MHz) spectrum of N-(4-fluorophenyl)-2,5-dihydroxybenzamide in $(CD_3)_2SO$ at 298 K.

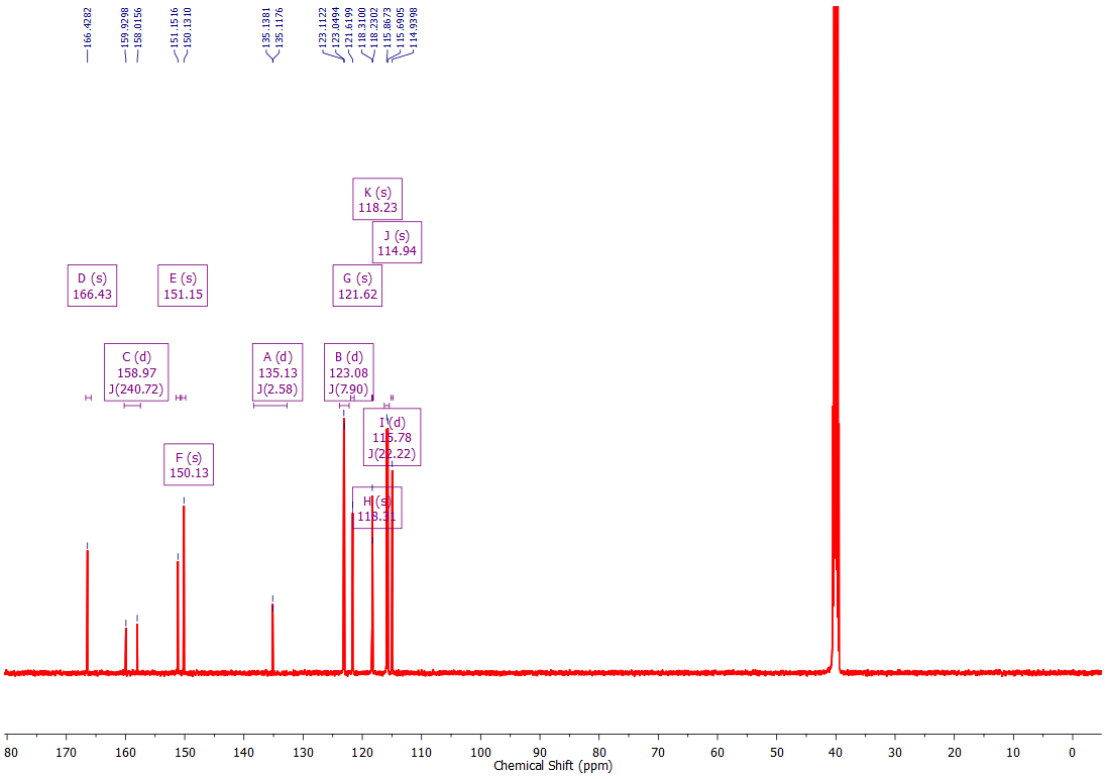

Figure 22. ^{13}C{^{1}H} NMR (101 MHz) spectrum of N-(4-fluorophenyl)-2,5-dihydroxybenzamide in $(CD_3)_2SO$ at 298 K.

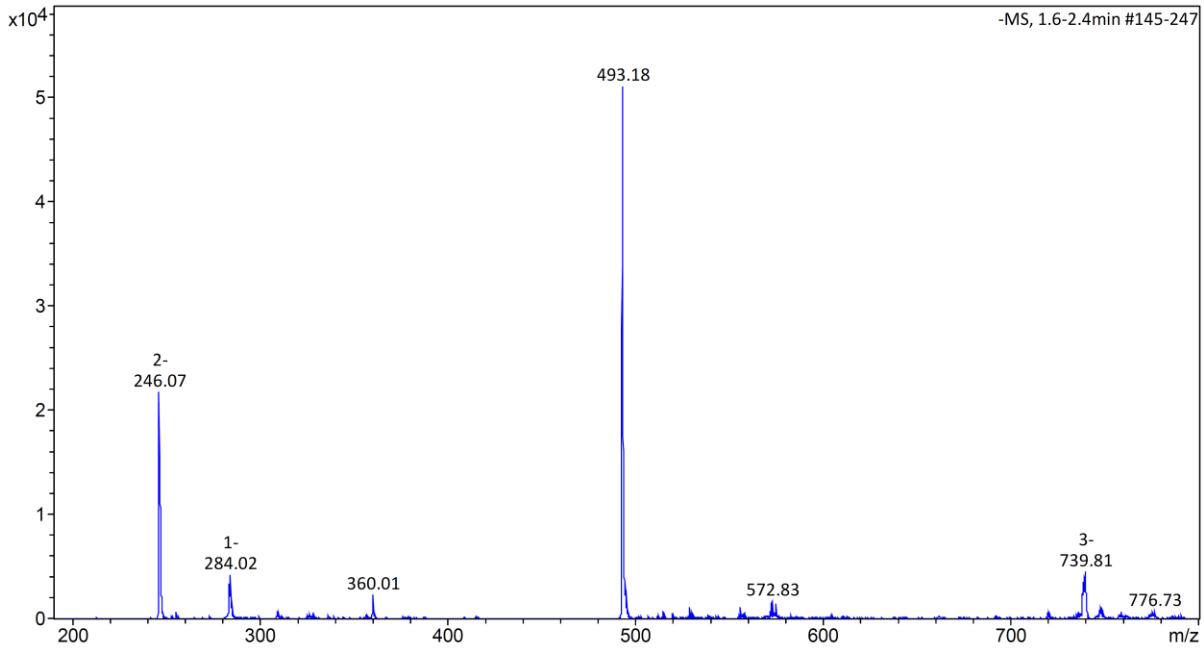

Figure 23. LR-MS (ESI$^+$) of N-(4-fluorophenyl)-2,5-dihydroxybenzamide.

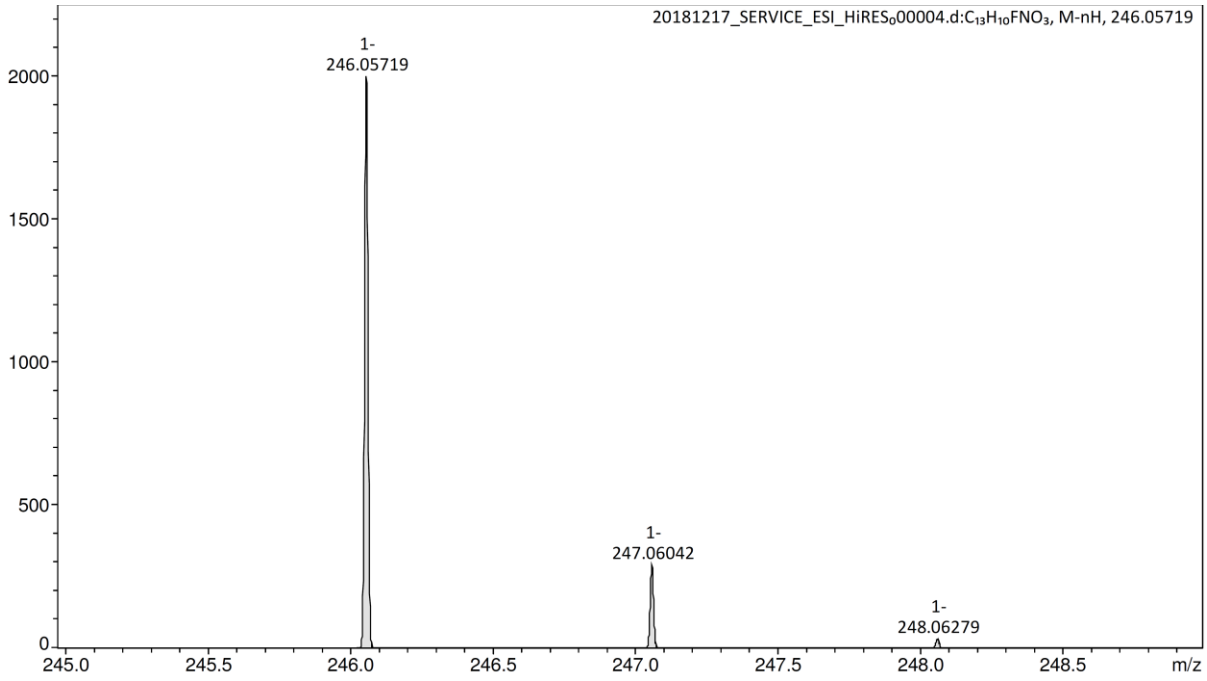

Figure 24. HR-MS (ESI$^+$) of N-(4-fluorophenyl)-2,5-dihydroxybenzamide.

N-(3,5-bis(trifluoromethyl)phenyl)-2,5-dihydroxybenzamide

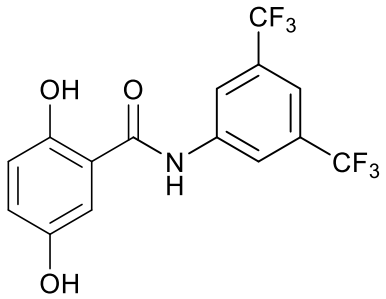

N-(3,5-bis(trifluoromethyl)phenyl)-2,5-dimethoxybenzamide (0.515 g, 1.31 mmol) was dissolved as much as possible in dry DCM (6 mL), and the solution was cooled to 0 °C under a N_2 atmosphere. Subsequently, BBr_3 (1.658 g, 6.62 mmol) in 1M DCM solution (6.6 mL) was added dropwise. The clear solution immediately changed to yellow in colour and the temperature sustained at 0 °C for 1 hour. The solution was then allowed to warm to room temperature and stirred for another 5 hours. Following this, the solution was poured into a conical flask and deionised water (20 mL) was poured in to elicit the formation of a green precipitate, which turned white after being in water for 15 minutes. In addition, deionised water was also added to the original rbf to collect any residue which was also stirred in deionised water for 15 minutes. Next, the precipitate was filtered using a Büchner funnel and the solid washed with hexane (3 x 30 mL). The solid was collected from the filter paper and dried under vacuum to afford a whitish-brown solid (0.395 g, 1.508 mmol, 83%).

^{1}H NMR (500 MHz, DMSO-*d*$_6$) δ ppm 10.82 (1 H, s), 10.68 (1 H, s), 9.16 (1 H, s), 8.45 (2 H, s), 7.80 (1 H, s), 7.29 (1 H, d, J 2.5), 6.91 (1 H, dd, J 8.8, 2.8), 6.85 (1 H, d, J 8.8); **^{13}C{^{1}H} NMR** (101 MHz, DMSO-*d*$_6$) δ ppm 167.0 (s), 150.7 (s), 150.3 (s), 140.9 (s), 131.2 (q, J 32.8), 123.7 (q, J 272.7), 122.0 (s), 120.7 (q[poorly defined], J 3.3), 118.6 (s), 118.4 (s), 117.0 (s), 115.1 (s).

LR-MS (ESI$^-$) *m/z* 363.85 [M - H]$^-$; **HR-MS** (ESI$^+$) calcd for $C_{15}H_9F_6NO_3$ [M+Na]$^+$: 388.03843, found *m/z* 388.03788

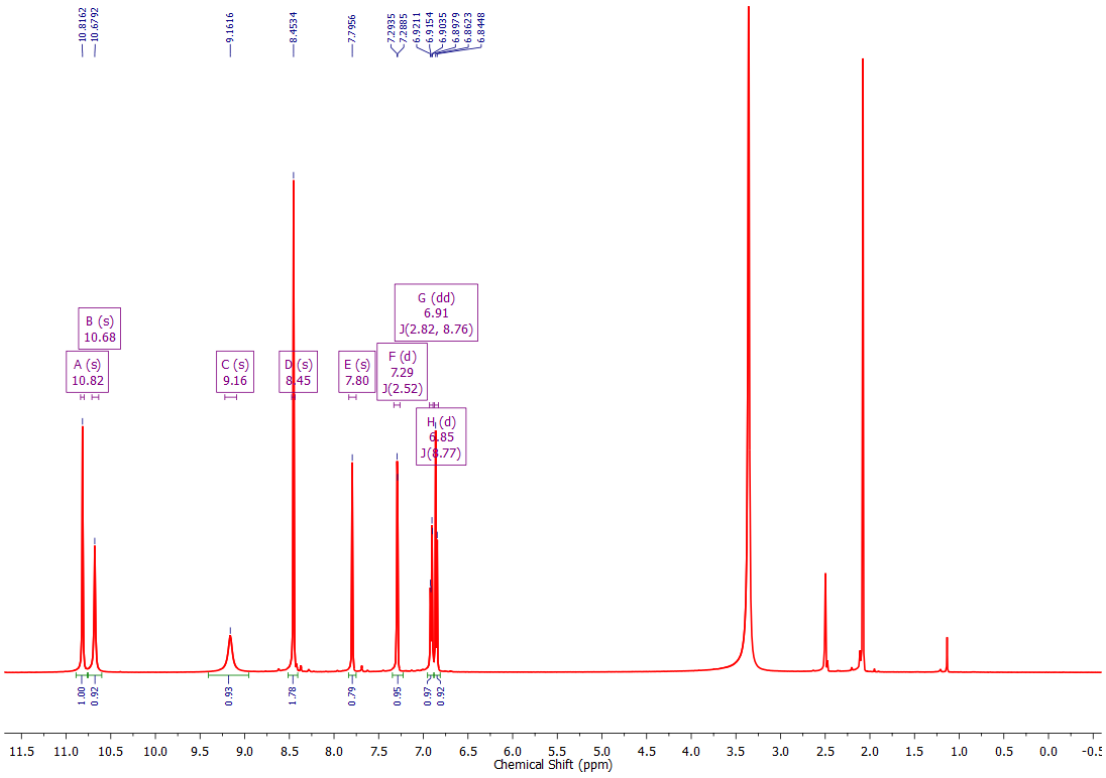

Figure 25. ^{1}H NMR (500 MHz) spectrum of N-(3,5-bis(trifluoromethyl)phenyl)-2,5-dimethoxybenzamide in $(CD_3)_2SO$ at 298 K.

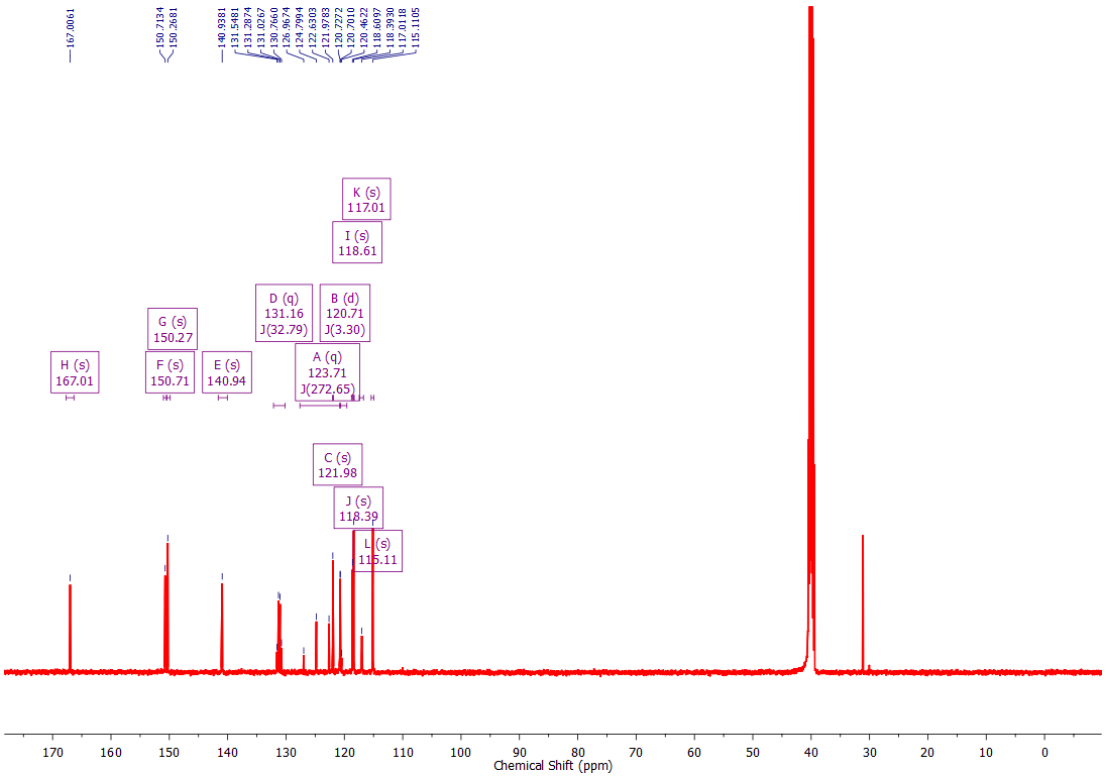

Figure 26. $^{13}C\{^{1}H\}$ NMR (101 MHz) spectrum of N-(3,5-bis(trifluoromethyl)phenyl)-2,5-dimethoxybenzamide in $(CD_3)_2SO$ at 298 K.

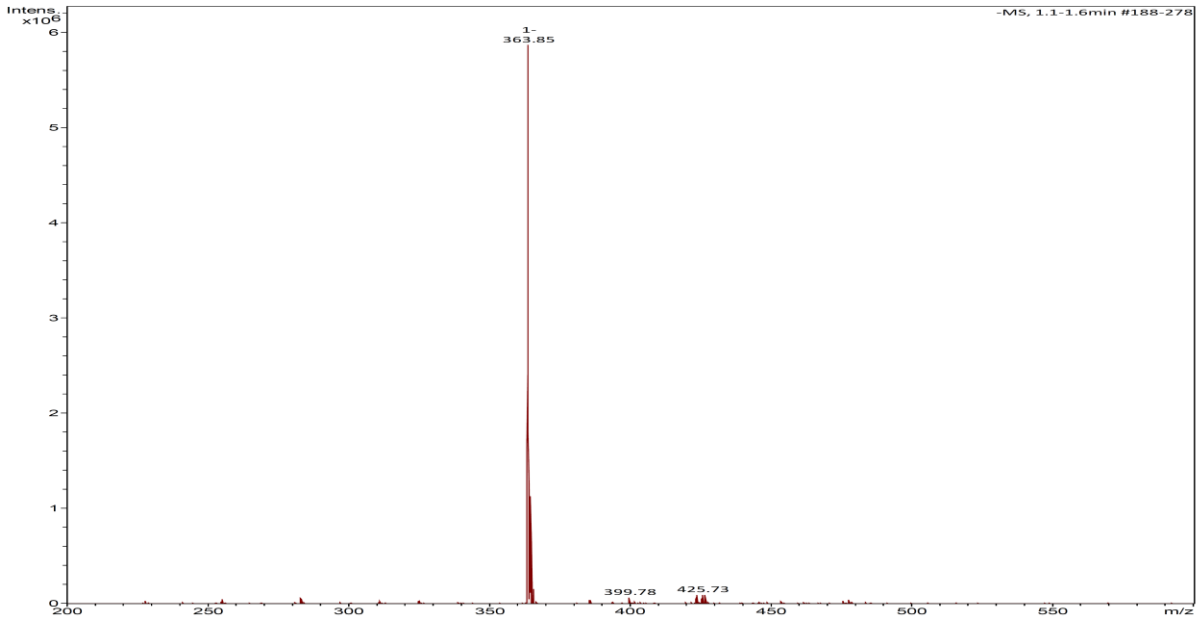

Figure 27. LR-MS (ESI^-) of N-(3,5-bis(trifluoromethyl)phenyl)-2,5-dimethoxybenzamide.

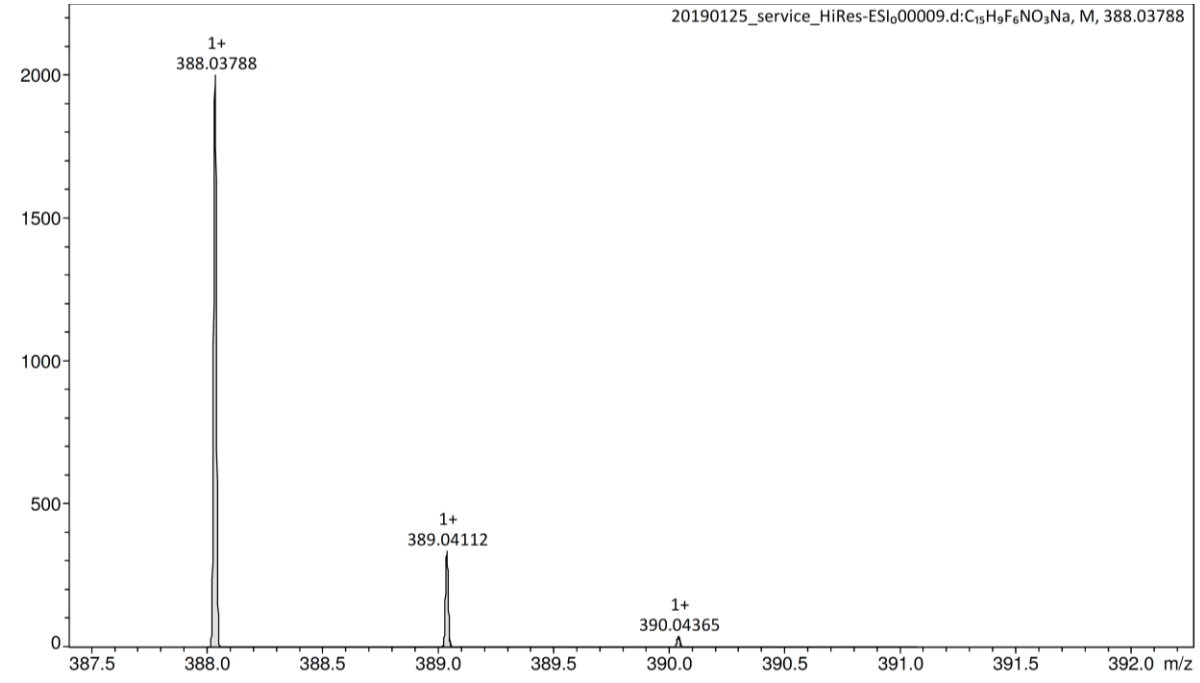

Figure 28. HR-MS (ESI^+) of N-(3,5-bis(trifluoromethyl)phenyl)-2,5-dimethoxybenzamide.

3,6-dioxo-*N*-phenylcyclohexa-1,4-diene-1-carboxamide

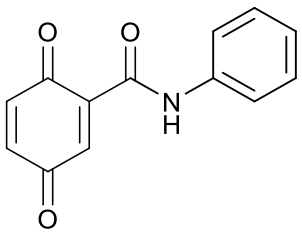

2,5-dimethoxy-N-phenylbenzamide (0.080 g, 0.35 mmol) and Mg_2SO_4 (0.235 g, 1.95 mmol) were suspended in DCM (16 ml). To this suspension was added Ag_2O (0.145 g, 0.63 mmol) and the reaction was left to stir for 2 hours, which turned to orange in colour. The reaction was tracked *via* TLC using a 50% EtOAc/Hex solvent mixture. Having reached completion, the solution was filtered through celite and the solvent removed on a rotary evaporator to leave a bright orange solid (0.067 g, 0.3 mmol, 85%).

^{1}H NMR (400 MHz, $CDCl_3$) δ ppm 10.29 (1 H, s), 7.78 (1 H, s), 7.69 (2 H, d, J 7.8), 7.38 (2 H, t, J 7.9, 7.4), 7.18 (1 H, t, J 7.4), 6.89 (2 H, s); **^{13}C{^{1}H} NMR** (101 MHz, $CDCl_3$-d)) δ ppm 188.7, 187.1, 158.5, 139.9, 137.2, 137.1, 134.8, 129.2, 125.4, 120.7.

LR-MS (APCI) *m/z* 228.01 $[M+H]^+$; **HR-MS** (APCI) calcd for $C_{13}H_8NO_3$ $[M+H]^+$: 228.05824, found *m/z* 228.06552.

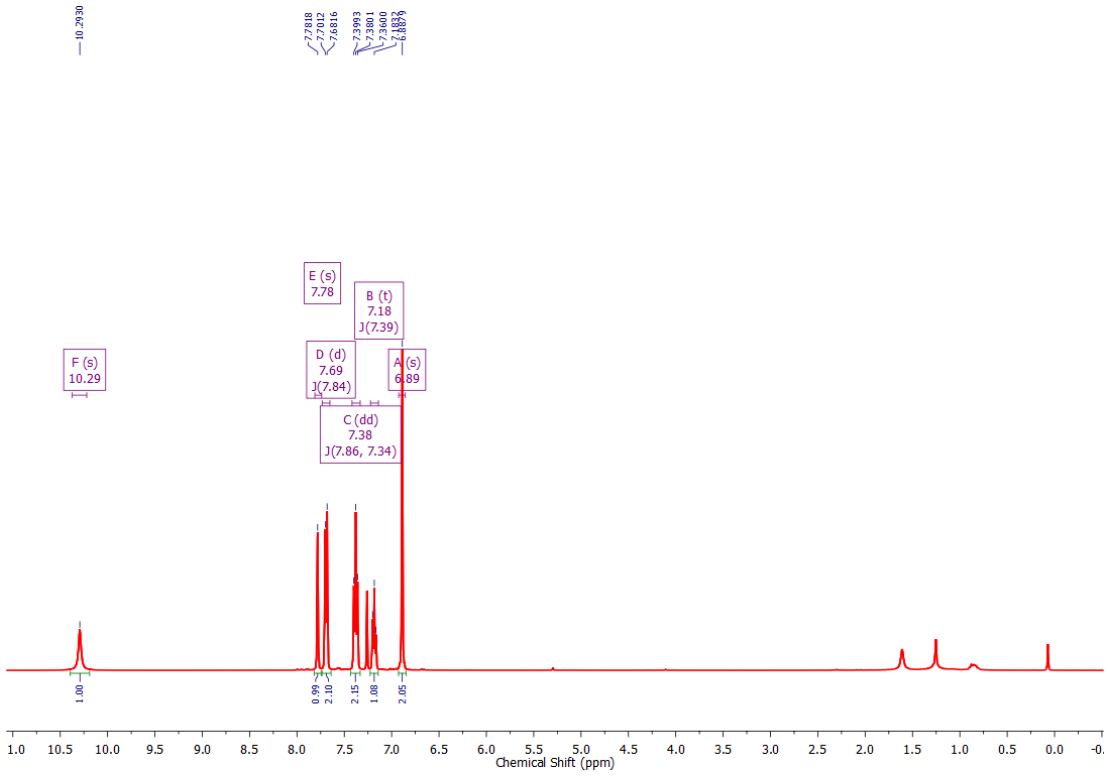

Figure 29. ^{1}H NMR (400 MHz) spectrum of 3,6-dioxo-*N*-phenylcyclohexa-1,4-diene-1-carboxamide in $CDCl_3$ at 298 K.

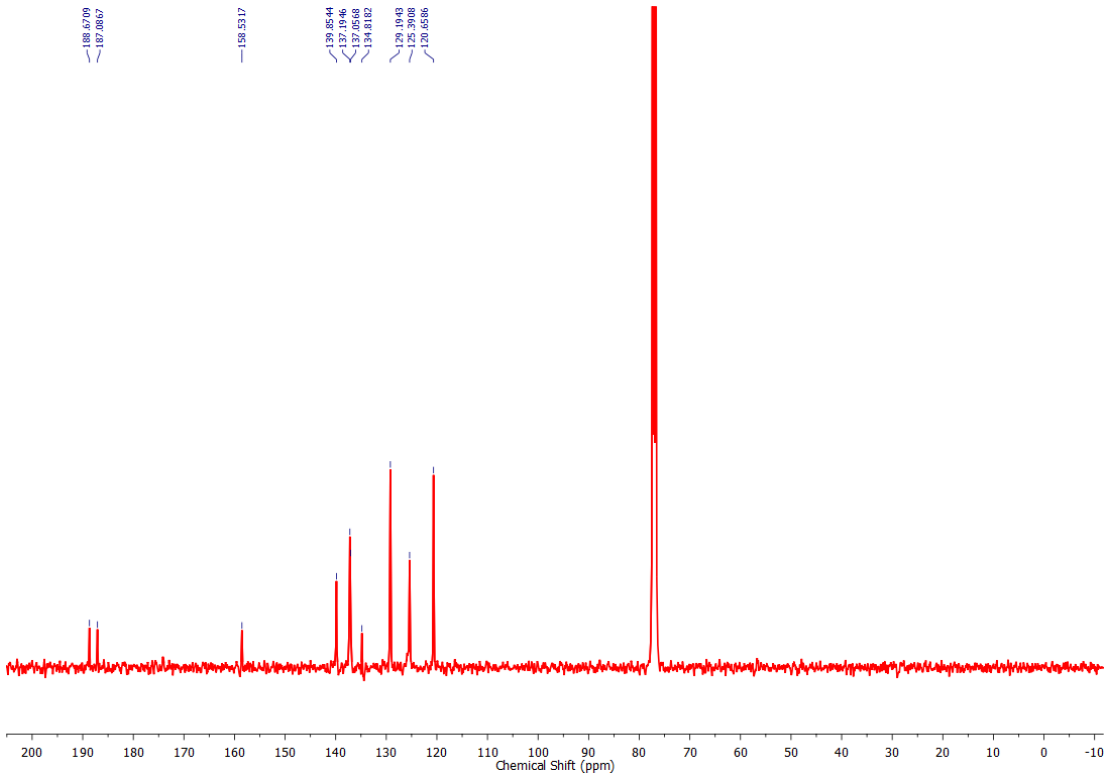

Figure 30. ^{13}C{^{1}H} NMR (101 MHz) spectrum of 3,6-dioxo-*N*-phenylcyclohexa-1,4-diene-1-carboxamide in $CDCl_3$ at 298 K.

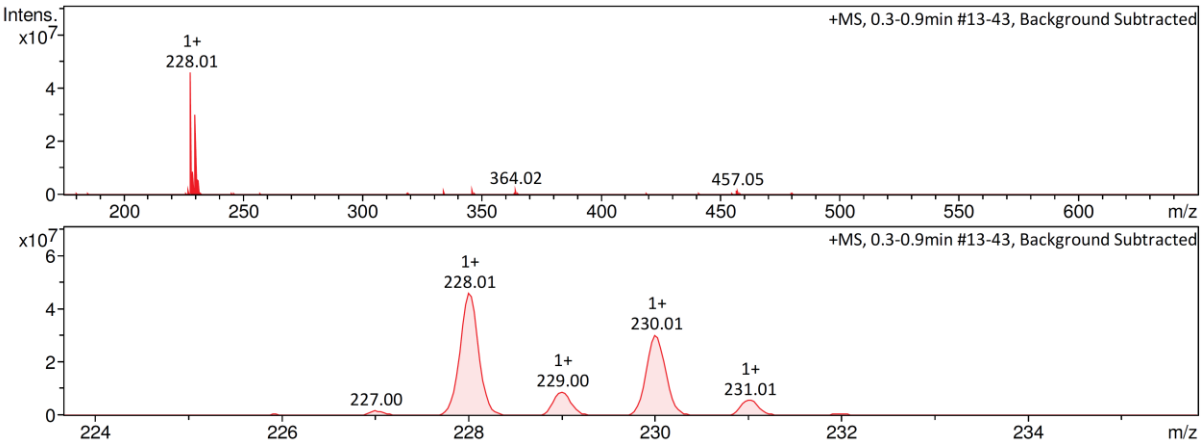

Figure 31. LR-MS (APCI) of 3,6-dioxo-*N*-phenylcyclohexa-1,4-diene-1-carboxamide.

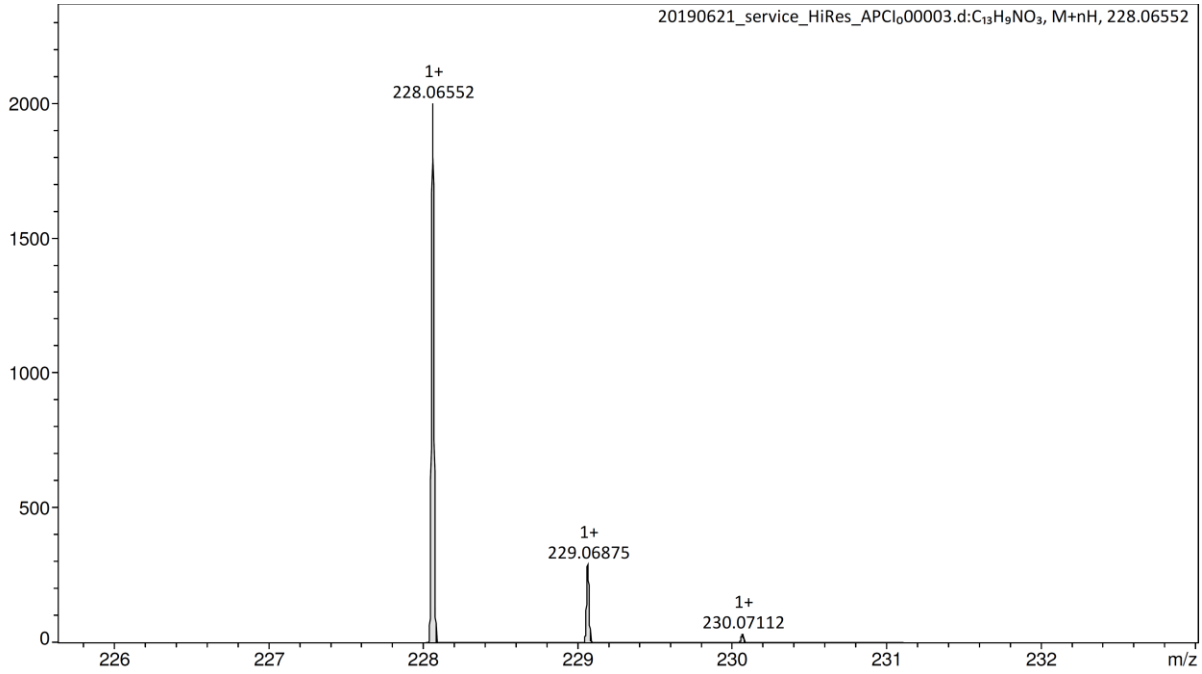

Figure 32. HR-MS (APCI) of 3,6-dioxo-*N*-phenylcyclohexa-1,4-diene-1-carboxamide.

3,6-dioxo-N-(p-tolyl)cyclohexa-1,4-diene-1-carboxamide

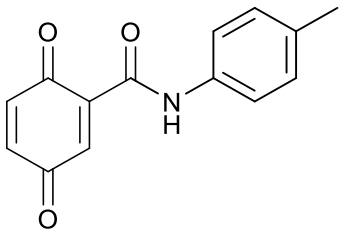

2,5-dihydroxy-N-(p-tolyl)benzamide (0.060 g, 0.25 mmol) and Mg_2SO_4 (0.400 g, 2.90 mmol) were suspended in DCM (16 ml). To this suspension was added Ag_2O (0.340 g, 1.48 mmol) and the reaction was left to stir overnight. The day after, the reaction mixture had turned orange in colour and was filtered through celite. The solvent of the subsequent solution was removed on a rotary evaporator to leave a bright red solid (0.031 g, 0.13 mmol, 52%).

^{1}H NMR (400 MHz, $CDCl_3$) δ ppm 10.23 (1 H, s), 7.76 (1 H, s), 7.57 (2 H, d, J 8.4), 7.17 (2 H, d, J 8.2), 6.87 (2 H, s), 2.34 (3 H, s). **^{13}C{^{1}H} NMR** (101 MHz, $CDCl_3$) δ ppm 188.7, 187.1, 158.4, 139.7, 137.2, 137.0, 135.2, 134.9, 134.8, 129.7, 120.6, 21.0.

LR-MS (APCI) *m/z* 242.05 $[M+H]^+$; **HR-MS** (APCI) calcd for $C_{13}H_8NO_3$ [M]: 241.07389, found *m/z* 241.07433.

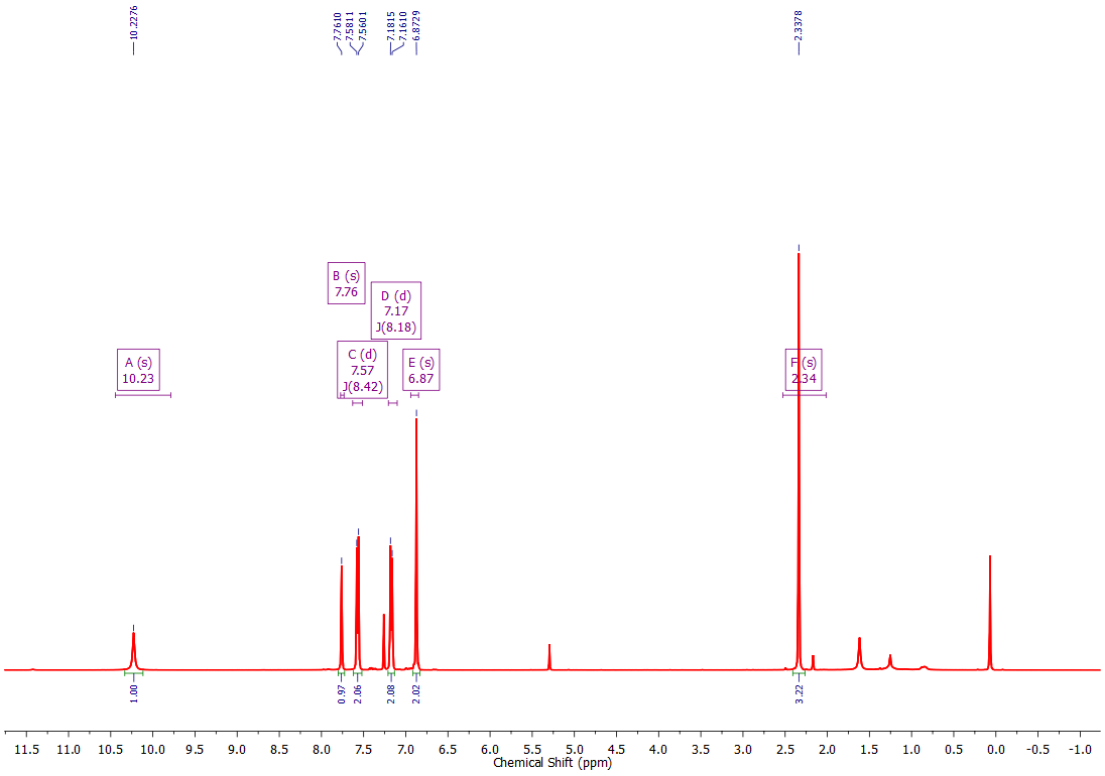

Figure 33. ^{1}H NMR (400 MHz) spectrum of 3,6-dioxo-N-(p-tolyl)cyclohexa-1,4-diene-1-carboxamide in $CDCl_3$ at 298 K.

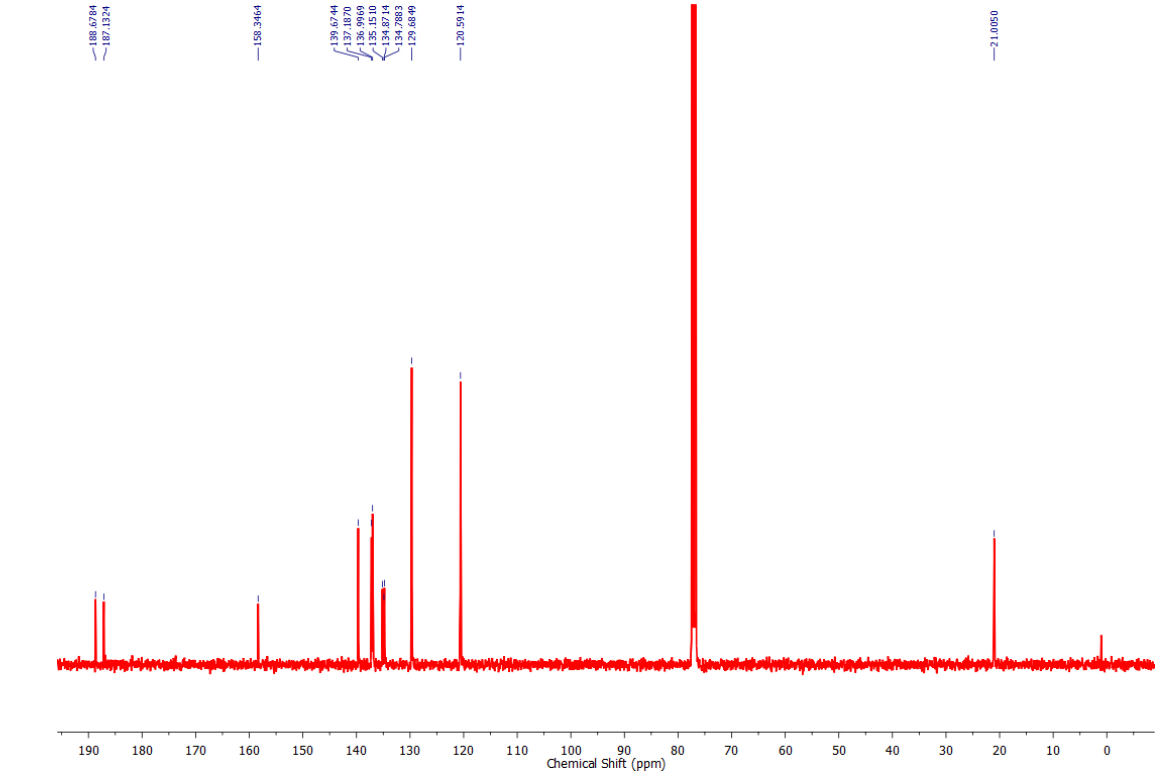

Figure 34. $^{13}C\{^{1}H\}$ NMR (101 MHz) spectrum of 3,6-dioxo-N-(p-tolyl)cyclohexa-1,4-diene-1-carboxamide in $CDCl_3$ at 298 K.

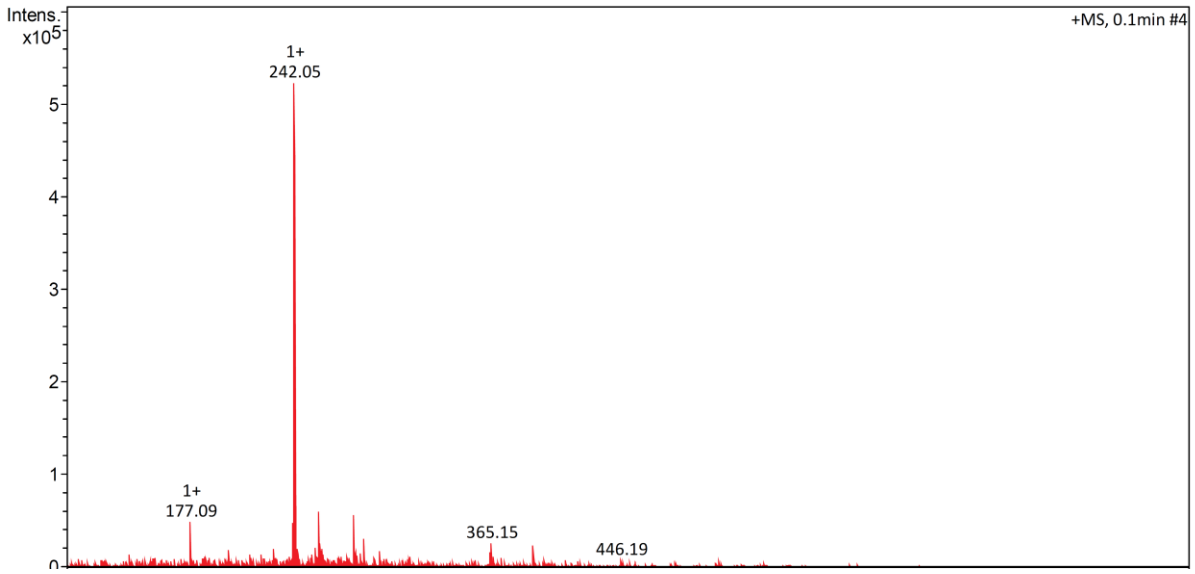

Figure 35. LR-MS (APCI) of 3,6-dioxo-N-(p-tolyl)cyclohexa-1,4-diene-1-carboxamide.

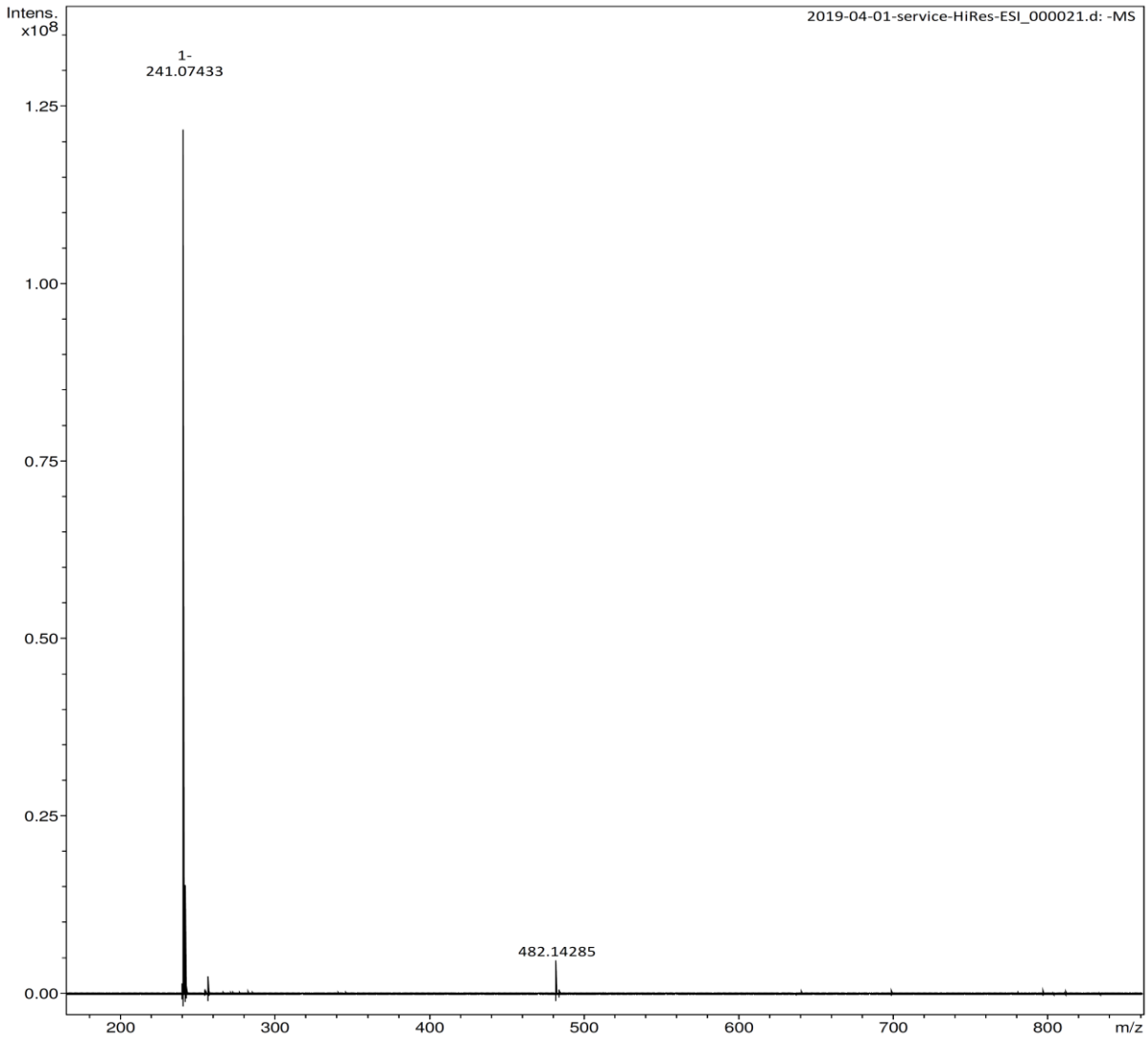

Figure 36. HR-MS (APCI) of 3,6-dioxo-N-(p-tolyl)cyclohexa-1,4-diene-1-carboxamide.

N-(4-fluorophenyl)-3,6-dioxocyclohexa-1,4-diene-1-carboxamide

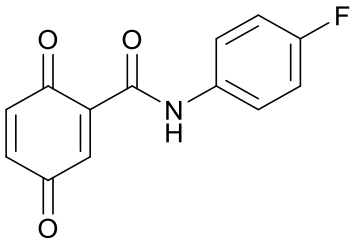

N-(4-fluorophenyl)-2,5-dihydroxybenzamide (0.045 g, 0.18 mmol) and Mg_2SO_4 (0.176 g, 1.46 mmol) were suspended in DCM (12 ml). To this suspension was added Ag_2O (0.201 g, 0.86 mmol) and the reaction was left to stir overnight. The day after, the reaction mixture had turned orange in colour and was filtered through celite. The solvent of the subsequent solution was removed on a rotary evaporator to leave a red solid (0.039 g, 0.15 mmol, 84%).

^{1}H NMR (400 MHz, DMSO-d_6) δ ppm 10.29 (1 H, s), 7.78 (1 H, d, J 1.2), 7.67 (2 H, dd, J 9.0, 4.8), 7.07 (2 H, t, J 8.6), 6.90 (2 H, s); **^{13}C{^{1}H} NMR** (101 MHz, $CDCL_3$) δ ppm 188.7 (s), 187.0 (s), 158.5 (s), 138.5 (d, J 279.3), 137.2 (s), 134.7 (s), 133.4 (s), 122.4 (d, J 7.9), 120.0 (s), 115.9 (d, J 22.5).

LR-MS (APCI) *m/z* 245.09 [M]; **HR-MS** (ESI^-) calcd for $C_{13}H_8FNO$ [M]: 245.04882, found *m/z* 245.0930.

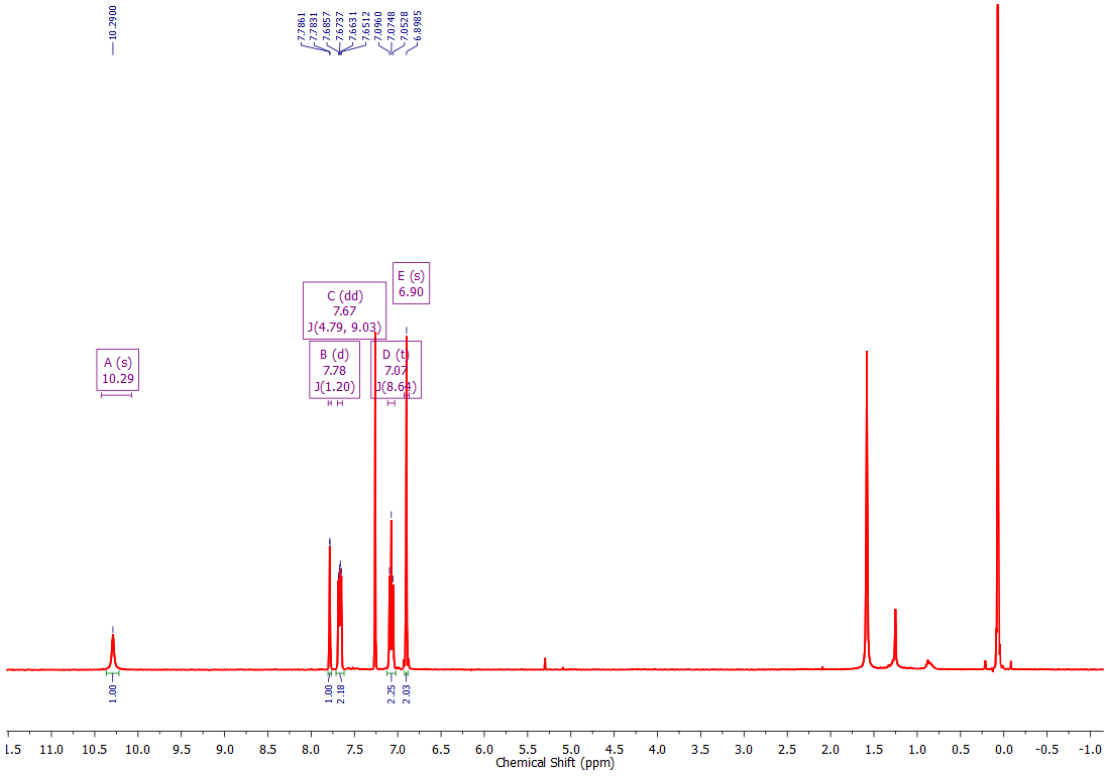

Figure 37. ^{1}H NMR (400 MHz) spectrum of *N*-(4-fluorophenyl)-3,6-dioxocyclohexa-1,4-diene-1-carboxamide in $CDCl_3$ at 298 K.

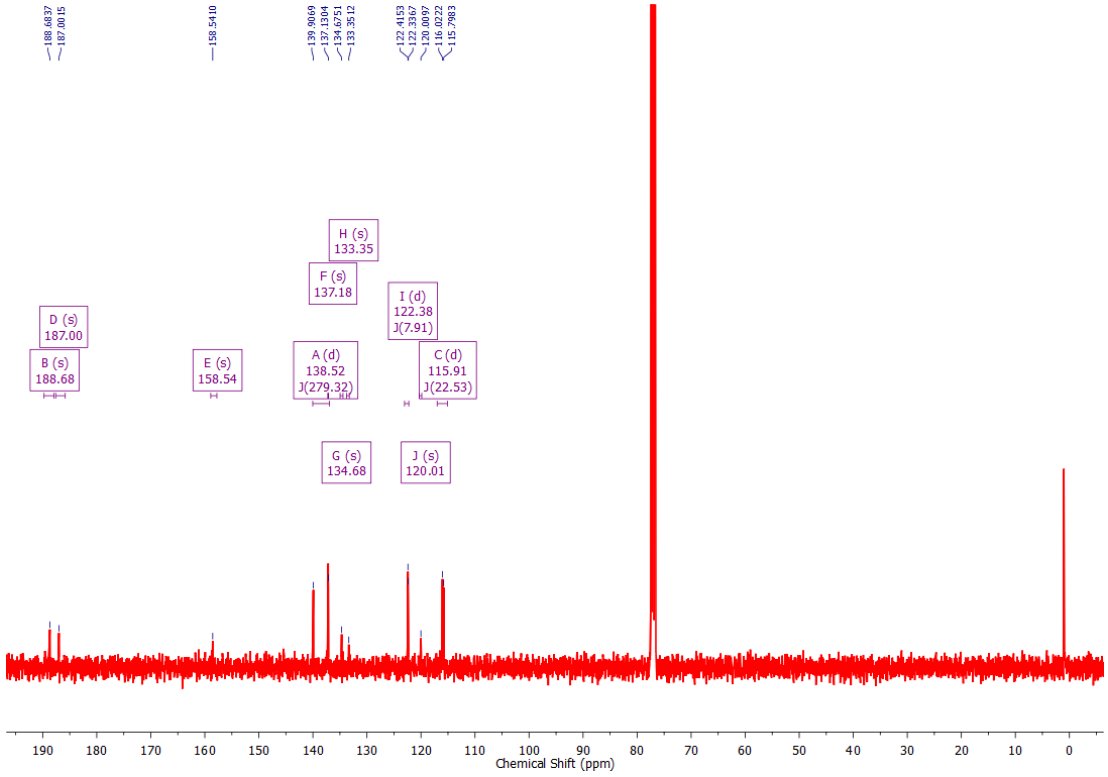

Figure 38. ^{13}C{^{1}H} NMR (101 MHz) spectrum of N-(4-fluorophenyl)-3,6-dioxocyclohexa-1,4-diene-1-carboxamide in $CDCl_3$ at 298 K.

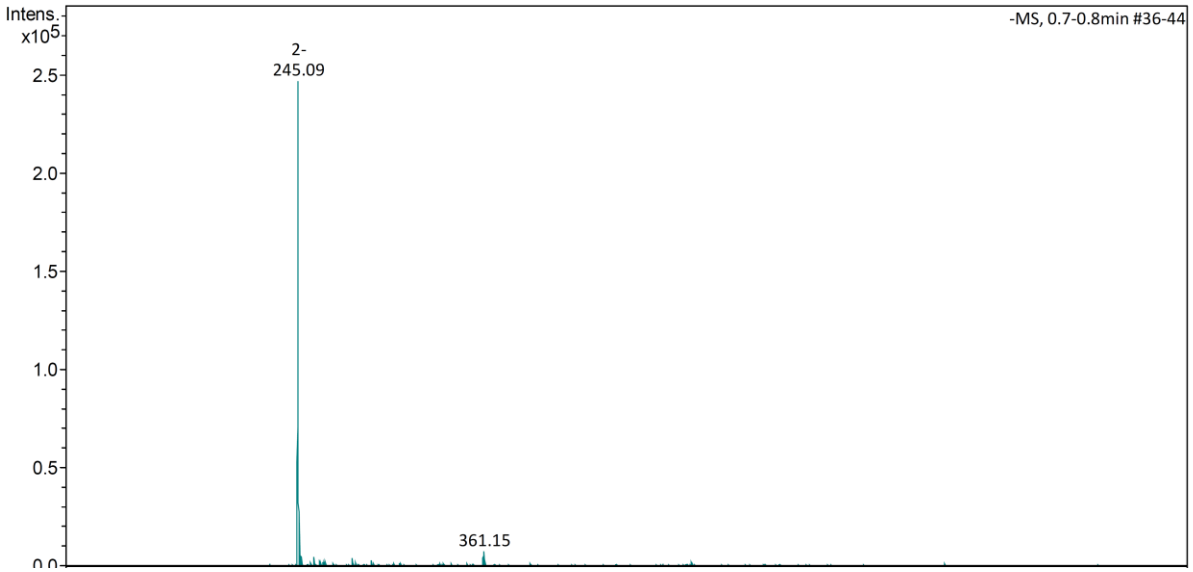

Figure 39. LR-MS (APCI) of *N*-(4-fluorophenyl)-3,6-dioxocyclohexa-1,4-diene-1-carboxamide.

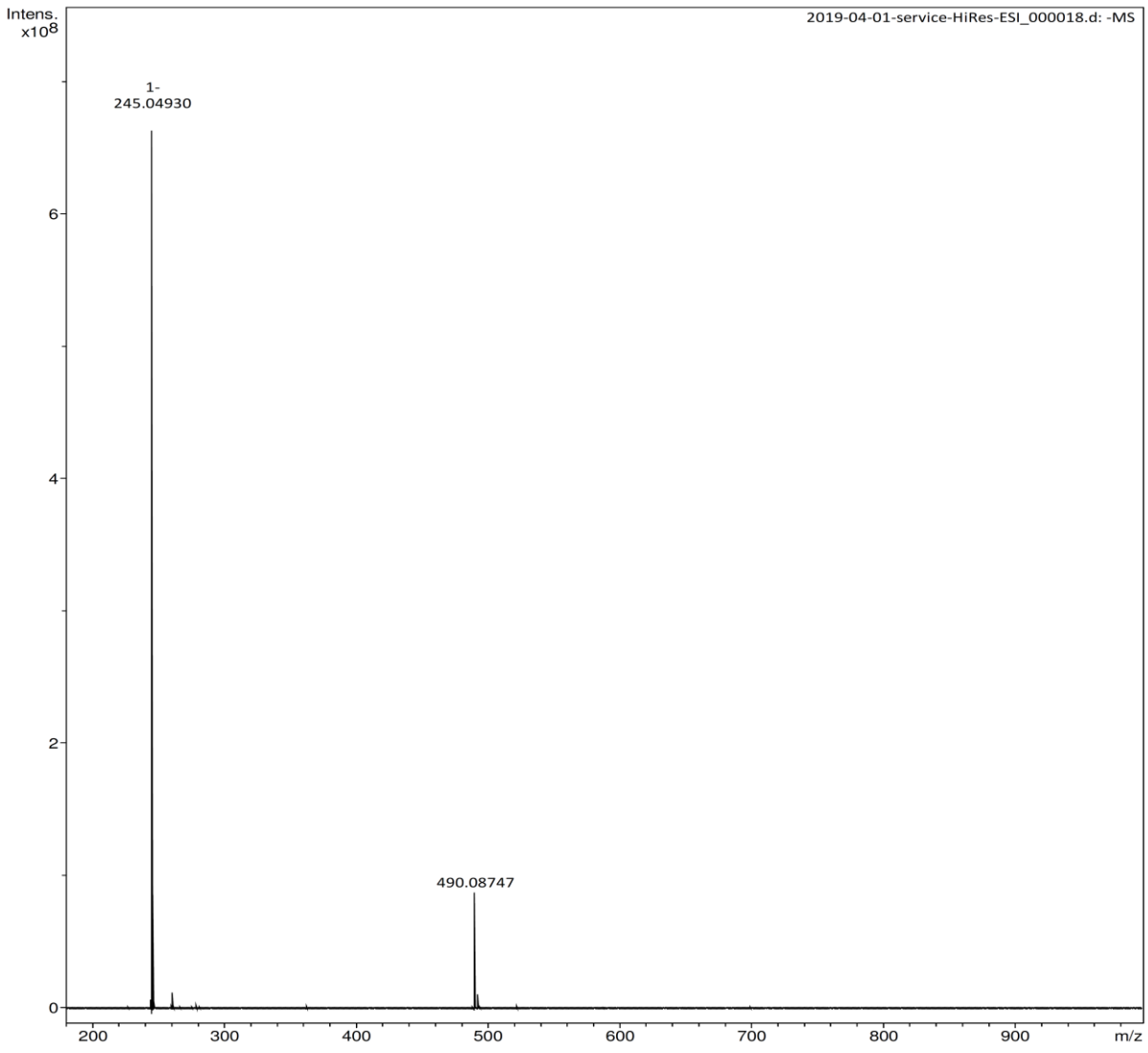

Figure 40. HR-MS (APCI) of *N*-(4-fluorophenyl)-3,6-dioxocyclohexa-1,4-diene-1-carboxamide.

N-(3,5-bis(trifluoromethyl)phenyl)-3,6-dioxocyclohexa-1,4-diene-1-carboxamide

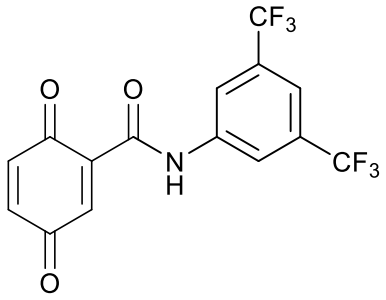

N-(3,5-bis(trifluoromethyl)phenyl)-2,5-dihydroxybenzamide (0.042 g, 0.12 mmol) and Mg_2SO_4 (0.200 g, 1.66 mmol) were suspended in DCM (12 ml). To this suspension was added Ag_2O (0.200 g, 0.86 mmol) and the reaction was left to stir overnight. The day after, the reaction mixture had turned orange in colour and was filtered through celite. The solvent of the subsequent solution was removed on a rotary evaporator to leave a bright red solid (0.040 g, 0.11 mmol, 96%).

^{1}H NMR (400 MHz, $CDCl_3$) δ ppm 10.67 (1 H, s), 8.20 (2 H, s), 7.79 (1 H, m), 7.68 (1 H, s), 6.95 (2 H, d, J 1.1); **^{13}C{^{1}H} NMR** (101 MHz, $CDCl_3$) δ ppm 188.7 (s), 186.7 (s), 159.4 (s), 140.7 (s), 138.7 (s), 137.5 (s), 137.2 (s), 134.0 (s), 132.7 (q, J 33.8), 123.1 (q, J 272.8), 120.5 (d, J 3.0), 118.7 (s).

LR-MS (APCI) *m/z* 364.03 $[M + H]^+$; **HR-MS** (APCI) calcd for $C_{15}H_7F_6NO_3$ [M]:363.21542, found *m/z* 363.03330.

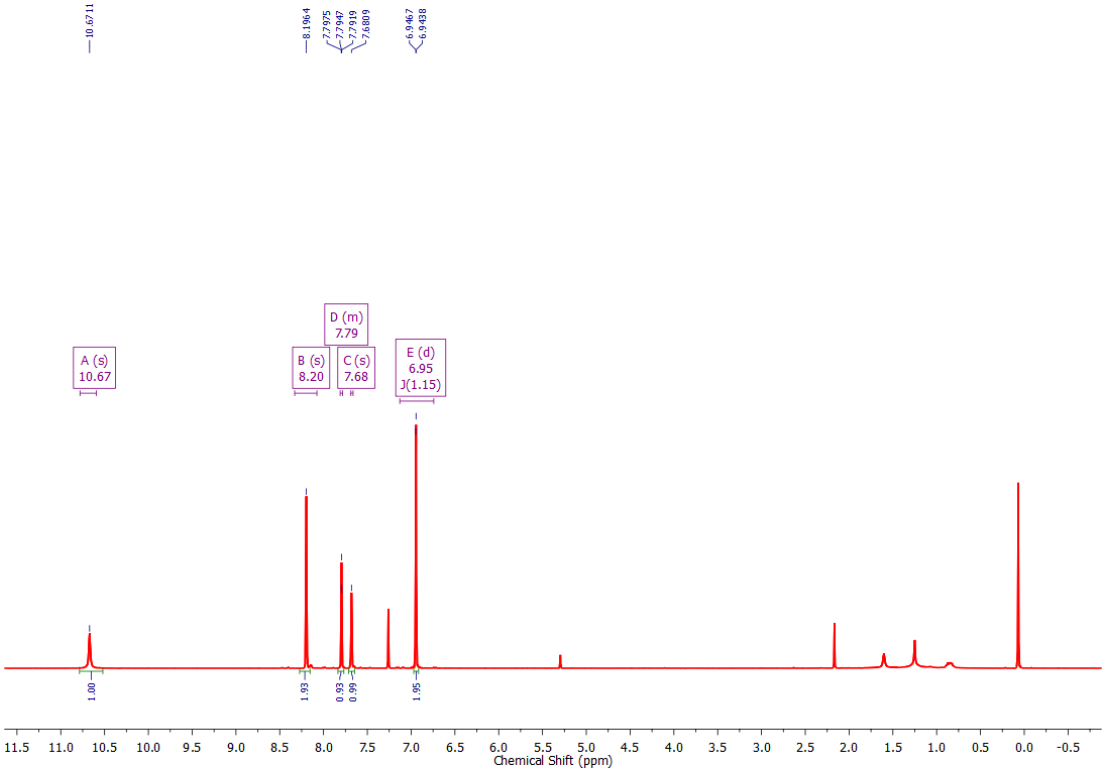

Figure 41. ^{1}H NMR (400 MHz) spectrum of N-(3,5-bis(trifluoromethyl)phenyl)-3,6-dioxocyclohexa-1,4-diene-1-carboxamide in $CDCl_3$ at 298 K.

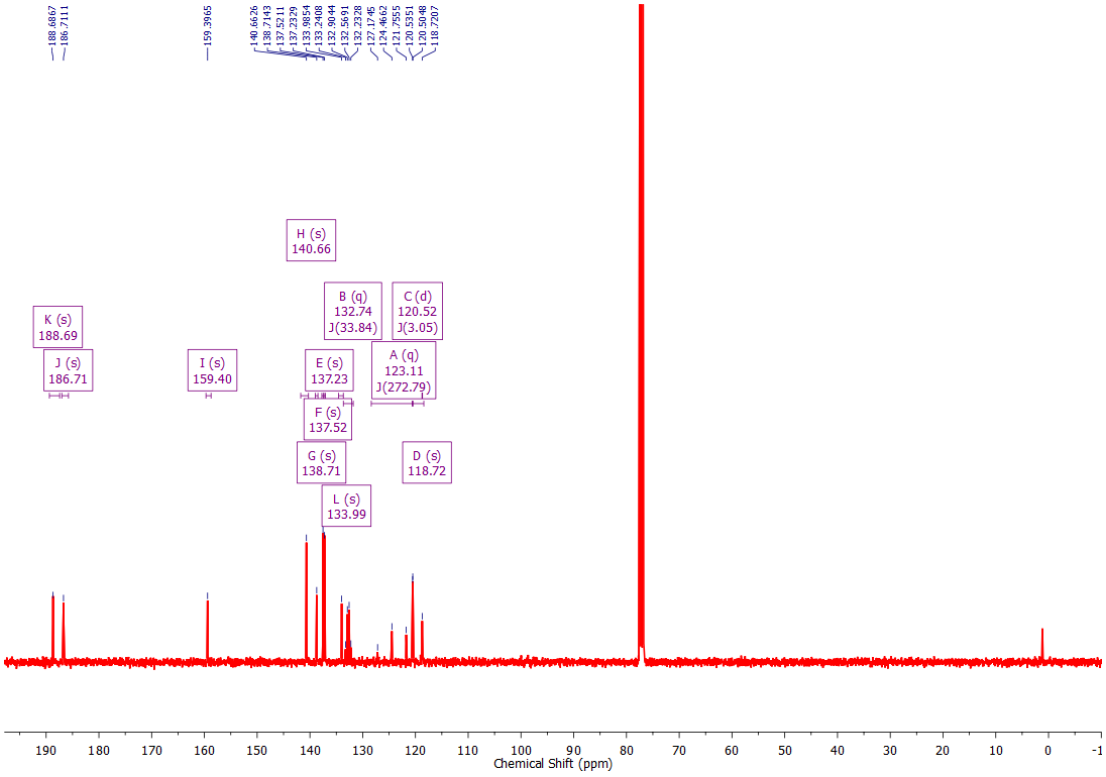

Figure 42. $^{13}C\{^{1}H\}$ NMR (101 MHz) spectrum of N-(3,5-bis(trifluoromethyl)phenyl)-3,6-dioxocyclohexa-1,4-diene-1-carboxamide in $CDCl_3$ at 298 K.

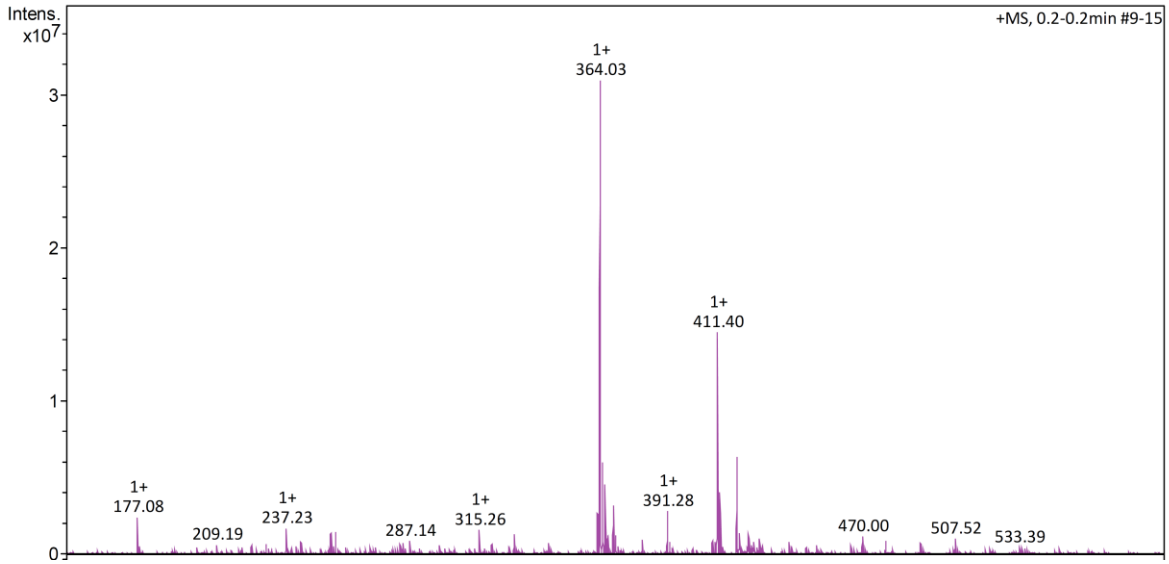

Figure 43. LR-MS (APCI) of N-(3,5-bis(trifluoromethyl)phenyl)-3,6-dioxocyclohexa-1,4-diene-1-carboxamide.

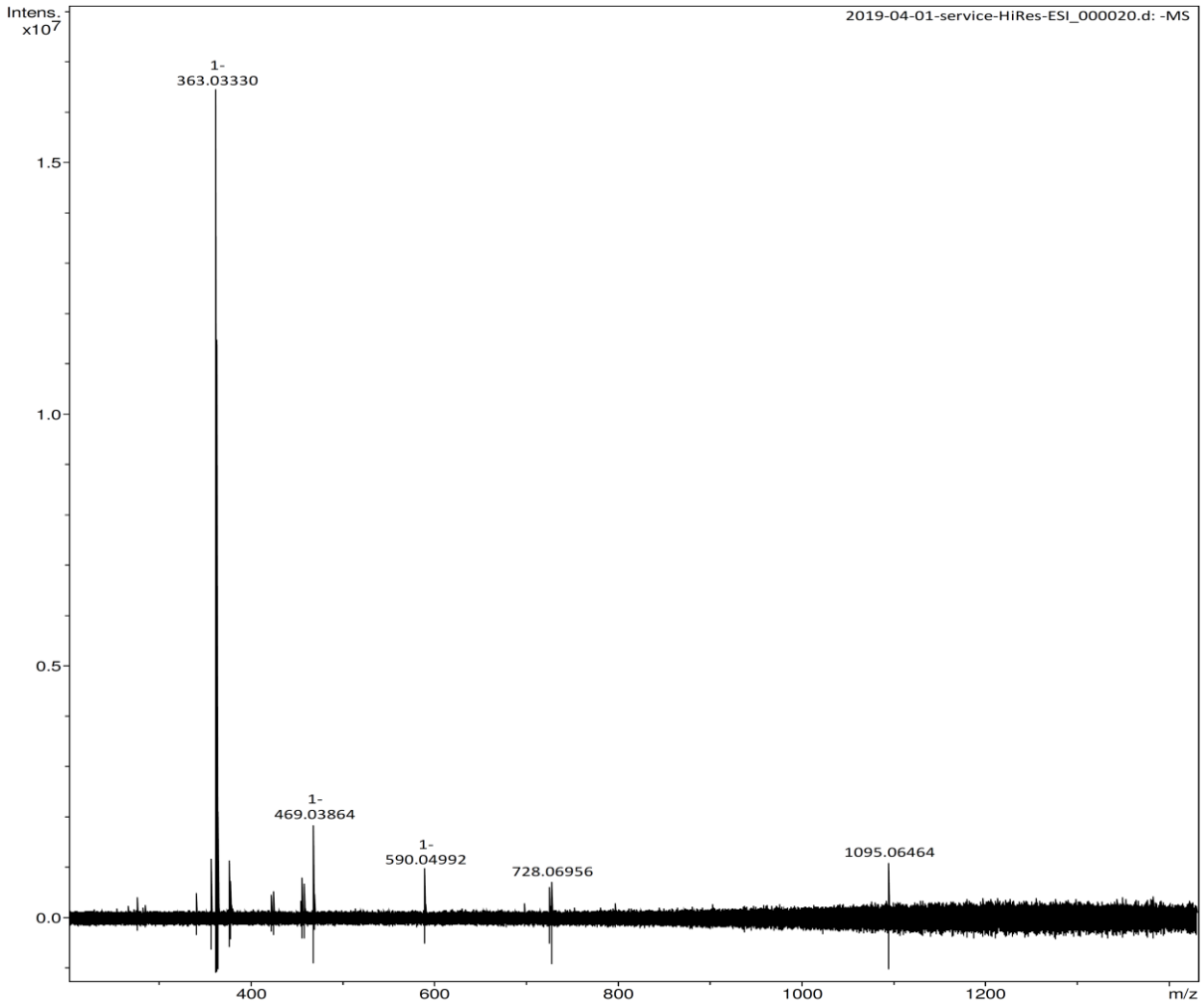

Figure 44. HR-MS (APCI) of N-(3,5-bis(trifluoromethyl)phenyl)-3,6-dioxocyclohexa-1,4-diene-1-carboxamide.

2. Crystal Structures

Single crystals were obtained from slow evaporation from a saturated acetonitrile solution containing the respective free receptors only. A suitable crystal was selected and [in a film of paratone on a micromount] on a SuperNova, Dual, Cu at home/near, Atlas diffractometer. The crystal was kept at 100(2) K during data collection. Using Olex2 [1], the structure was solved with the olex2.solve [2] structure solution program using Charge Flipping and refined with the ShelXL [3] refinement package using Least Squares minimisation.

1. Dolomanov, O.V., Bourhis, L.J., Gildea, R.J, Howard, J.A.K. & Puschmann, H. (2009), J. Appl. Cryst. 42, 339-341.

2. Bourhis, L.J., Dolomanov, O.V., Gildea, R.J., Howard, J.A.K., Puschmann, H. (2015). Acta Cryst. A71, 59-75.

3. Sheldrick, G.M. (2015). Acta Cryst. C71, 3-8.

2.1Crystal Data for *N*-(4-fluorophenyl)-2,5-dimethoxybenzamide:

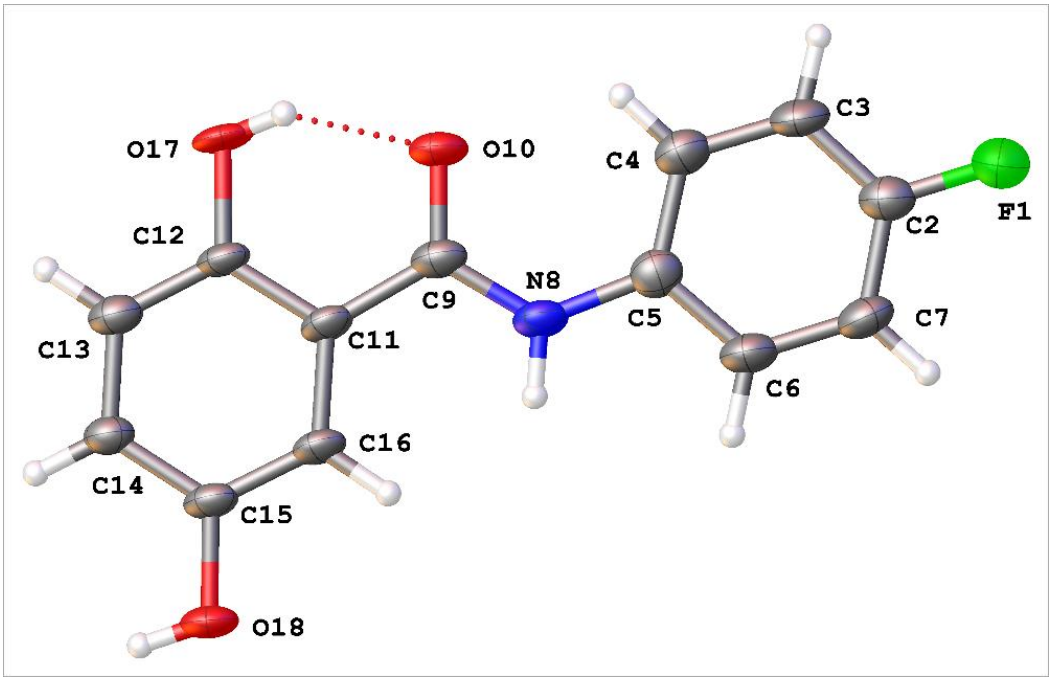

Table 2.1.1 Crystal data and structure refinement for *N*-(4-fluorophenyl)-2,5-dimethoxybenzamide.

Identification code	pag19_s1731
Empirical formula	$C_{13}H_{10}FNO_3$
Formula weight	247.22
Temperature/K	100(2)
Crystal system	tetragonal
Space group	$I4_1/a$
a/Å	13.4738(10)
b/Å	13.4738(10)
c/Å	23.638(2)
α/°	90
β/°	90
γ/°	90
Volume/Å^3	4291.3(7)
Z	16
ρ_{calc}g/cm^3	1.531
μ/mm^{-1}	0.121
F(000)	2048.0
Crystal size/mm^3	0.195 × 0.166 × 0.158
Radiation	MoKα (λ = 0.71073)
2Θ range for data collection/°	3.48 to 55.326
Index ranges	$-12 \leq h \leq 12$, $0 \leq k \leq 17$, $-30 \leq l \leq 30$
Reflections collected	2498
Independent reflections	2498 [R_{int} = ?, R_{sigma} = 0.0725]
Data/restraints/parameters	2498/429/331
Goodness-of-fit on F^2	1.093
Final R indexes [I>=2σ (I)]	R_1 = 0.1039, wR_2 = 0.2745
Final R indexes [all data]	R_1 = 0.1394, wR_2 = 0.3040
Largest diff. peak/hole / e Å^{-3}	0.63/-0.35

Table 2.1.2 Fractional Atomic Coordinates ($\times 10^4$) and Equivalent Isotropic Displacement Parameters ($Å^2 \times 10^3$) for *N*-(4-fluorophenyl)-2,5-dimethoxybenzamide. U_{eq} is defined as 1/3 of of the trace of the orthogonalised U_{IJ} tensor.

Atom	*x*	*y*	*z*	U(eq)
F1	4412(3)	3767(3)	4679.7(15)	51.4(10)
O10	9077(3)	3640(3)	4130.1(15)	42.3(11)
O17	10875(3)	3800(3)	3892.8(14)	41.8(11)
O18	11721(3)	3810(3)	6177.5(15)	41.4(10)
N8	8487(4)	3699(4)	5024(2)	35.6(11)
C2	5411(5)	3737(5)	4749(3)	39.3(13)
C3	6019(5)	3707(5)	4291(2)	41.8(14)
C4	7046(5)	3675(5)	4355(2)	40.4(13)
C5	7449(5)	3697(6)	4907(3)	35.2(13)
C6	6800(6)	3730(20)	5365(3)	41.2(16)
C7	5775(6)	3745(9)	5294(3)	40.9(15)
C9	9244(4)	3689(4)	4650(2)	34.2(11)
C11	10282(4)	3737(4)	4863(2)	31.0(11)
C12	11053(4)	3786(4)	4469(2)	31.9(12)
C13	12038(5)	3820(4)	4641(2)	35.4(12)
C14	12277(4)	3835(4)	5206(2)	32.1(11)
C15	11523(5)	3792(4)	5604(2)	32.8(12)
C16	10533(5)	3742(4)	5440(2)	31.6(12)
F1A	18139(18)	3680(18)	4740(14)	58(6)
O10A	13510(20)	3960(20)	4154(8)	52(6)
O17A	11690(20)	3980(20)	3902(8)	43(6)
O18A	10790(20)	3680(20)	6164(9)	55(7)
N8A	14099(15)	3750(20)	5055(10)	40(5)
C2A	17140(20)	3700(50)	4801(16)	51(6)
C3A	16540(20)	3730(40)	4342(14)	52(6)
C4A	15520(20)	3780(30)	4414(14)	50(6)
C5A	15142(17)	3730(30)	4975(14)	48(5)
C6A	15770(20)	3770(60)	5438(14)	49(6)
C7A	16800(20)	3750(120)	5355(16)	50(7)
C9A	13352(15)	3820(30)	4669(9)	40(5)
C11A	12293(16)	3830(30)	4871(10)	38(5)
C12A	11529(18)	3830(30)	4471(9)	37(5)
C13A	10529(19)	3820(30)	4630(12)	36(5)
C14A	10280(20)	3720(30)	5183(12)	37(5)
C15A	11010(20)	3780(30)	5593(9)	39(5)
C16A	12000(20)	3780(30)	5437(10)	37(5)

Table 2.1.3 Anisotropic Displacement Parameters ($Å^2 \times 10^3$) for *N*-(4-fluorophenyl)-2,5-dimethoxybenzamide. The Anisotropic displacement factor exponent takes the form: $-2\pi^2[h^2a^{*2}U_{11}+2hka^*b^*U_{12}+\ldots]$.

Atom	U_{11}	U_{22}	U_{33}	U_{23}	U_{13}	U_{12}
F1	46(2)	72(3)	36.6(19)	-1.5(18)	-3.3(15)	-0.7(18)
O10	49(2)	61(3)	17.4(16)	6.5(16)	-4.0(15)	-2(2)
O17	54(3)	61(3)	10.6(15)	7.4(16)	2.0(15)	0(2)
O18	47(2)	62(3)	15.1(16)	3.7(16)	-3.1(15)	0(2)
N8	43(3)	44(3)	20(2)	6.5(19)	-0.4(18)	-1(2)
C2	45(3)	44(3)	28(3)	0(3)	-2(2)	0(3)
C3	52(4)	54(4)	20(2)	-1(2)	-1(2)	0(3)
C4	45(3)	47(3)	29(3)	5(2)	4(2)	-1(3)
C5	39(3)	33(3)	33(3)	4(2)	2(2)	-1(3)
C6	48(3)	53(4)	22(3)	3(3)	0(2)	-1(3)
C7	48(3)	52(4)	23(3)	0(3)	7(2)	1(3)
C9	46(3)	36(3)	20(2)	4.7(19)	0.6(19)	3(2)
C11	40(3)	35(3)	18(2)	7(2)	5.0(19)	2(2)
C12	42(3)	38(3)	15(2)	4.4(19)	3(2)	3(3)
C13	44(3)	40(3)	22(2)	2(2)	2(2)	2(3)
C14	37(3)	38(3)	21(2)	2(2)	0(2)	2(2)
C15	44(3)	38(3)	17(2)	4.9(19)	1(2)	5(3)
C16	42(3)	36(3)	16(2)	6(2)	2.8(19)	1(2)
F1A	52(11)	38(12)	84(16)	-7(12)	16(10)	-6(9)
O10A	78(15)	48(13)	30(8)	2(9)	14(8)	-7(12)
O17A	51(13)	60(14)	19(8)	-1(8)	1(8)	-4(12)
O18A	76(16)	61(14)	27(9)	16(10)	10(9)	14(13)
N8A	59(9)	34(9)	26(8)	-3(7)	12(7)	-19(8)
C2A	54(11)	42(12)	57(12)	-9(10)	16(9)	-13(10)
C3A	55(11)	48(12)	53(12)	-5(10)	17(9)	-17(11)
C4A	56(11)	47(11)	48(11)	-5(10)	18(9)	-19(10)
C5A	58(9)	40(10)	44(10)	-4(9)	12(8)	-21(8)
C6A	55(10)	41(12)	51(11)	-6(11)	11(8)	-20(10)
C7A	55(11)	40(13)	55(12)	-8(11)	12(9)	-17(11)
C9A	59(9)	34(9)	27(7)	-4(7)	9(6)	-13(8)
C11A	54(9)	37(9)	23(8)	-2(8)	3(6)	-10(8)
C12A	50(10)	39(10)	21(8)	-5(7)	5(7)	-11(9)
C13A	50(10)	36(10)	20(9)	-9(9)	6(7)	-10(9)
C14A	46(10)	42(11)	23(9)	-2(9)	5(7)	-8(9)
C15A	49(11)	43(10)	24(8)	2(8)	2(7)	-6(9)
C16A	50(10)	40(10)	22(8)	0(8)	-1(7)	-8(9)

Table 2.1.4 Bond Lengths for *N*-(4-fluorophenyl)-2,5-dimethoxybenzamide.

Atom	Atom	Length/Å	Atom	Atom	Length/Å
F1	C2	1.357(7)	F1A	C2A	1.36(2)
O10	C9	1.252(6)	O10A	C9A	1.252(18)
O17	C12	1.383(6)	O17A	C12A	1.381(18)
O18	C15	1.381(6)	O18A	C15A	1.386(18)
N8	C5	1.425(8)	N8A	C5A	1.417(19)
N8	C9	1.349(7)	N8A	C9A	1.362(18)
C2	C3	1.359(9)	C2A	C3A	1.35(2)
C2	C7	1.378(8)	C2A	C7A	1.39(2)
C3	C4	1.393(10)	C3A	C4A	1.39(2)
C4	C5	1.412(8)	C4A	C5A	1.42(2)
C5	C6	1.393(9)	C5A	C6A	1.39(2)
C6	C7	1.392(9)	C6A	C7A	1.398(19)
C9	C11	1.489(8)	C9A	C11A	1.504(19)
C11	C12	1.396(7)	C11A	C12A	1.397(18)
C11	C16	1.406(7)	C11A	C16A	1.395(19)
C12	C13	1.390(9)	C12A	C13A	1.40(2)
C13	C14	1.374(7)	C13A	C14A	1.358(19)
C14	C15	1.386(8)	C14A	C15A	1.385(19)
C15	C16	1.391(9)	C15A	C16A	1.39(2)

Table 2.1.5 Bond Angles for *N*-(4-fluorophenyl)-2,5-dimethoxybenzamide.

Atom	Atom	Atom	Angle/°	Atom	Atom	Atom	Angle/°
C9	N8	C5	128.0(5)	C9A	N8A	C5A	130(2)
F1	C2	C3	120.1(6)	F1A	C2A	C7A	115(2)
F1	C2	C7	117.8(6)	C3A	C2A	F1A	120(2)
C3	C2	C7	122.1(6)	C3A	C2A	C7A	124(2)
C2	C3	C4	120.8(5)	C2A	C3A	C4A	120(2)
C3	C4	C5	118.9(5)	C3A	C4A	C5A	118(2)
C4	C5	N8	123.8(6)	N8A	C5A	C4A	118(2)
C6	C5	N8	117.7(5)	C6A	C5A	N8A	120(2)
C6	C5	C4	118.5(6)	C6A	C5A	C4A	121(2)
C7	C6	C5	122.0(7)	C5A	C6A	C7A	120(3)
C2	C7	C6	117.7(6)	C2A	C7A	C6A	117(3)
O10	C9	N8	120.5(5)	O10A	C9A	N8A	122(2)
O10	C9	C11	120.2(5)	O10A	C9A	C11A	118(2)
N8	C9	C11	119.3(5)	N8A	C9A	C11A	119.3(17)
C12	C11	C9	118.4(5)	C12A	C11A	C9A	119.0(18)
C12	C11	C16	118.0(5)	C16A	C11A	C9A	124.8(19)
C16	C11	C9	123.6(5)	C16A	C11A	C12A	116.1(17)
O17	C12	C11	121.9(5)	O17A	C12A	C11A	123(2)
O17	C12	C13	116.9(5)	O17A	C12A	C13A	115(2)
C13	C12	C11	121.1(5)	C11A	C12A	C13A	121.9(18)
C14	C13	C12	120.6(5)	C14A	C13A	C12A	120(2)
C13	C14	C15	119.2(5)	C13A	C14A	C15A	119(2)
O18	C15	C14	121.7(5)	O18A	C15A	C16A	117(2)
O18	C15	C16	117.3(5)	C14A	C15A	O18A	122(2)
C14	C15	C16	121.0(5)	C14A	C15A	C16A	120.1(19)
C15	C16	C11	120.0(5)	C15A	C16A	C11A	122(2)

Table 2.1.6 Hydrogen Bonds for *N*-(4-fluorophenyl)-2,5-dimethoxybenzamide.

D	H	A	d(D-H)/Å	d(H-A)/Å	d(D-A)/Å	D-H-A/°
O17	H17	O10	0.84	1.81	2.496(6)	137.4
O18	H18	O17[1]	0.84	1.97	2.778(6)	160.8
N8	H8	O18[2]	0.88	2.33	3.162(6)	158.8
O17A	H17A	O10A	0.84	1.79	2.52(4)	144.5
O18A	H18A	O18A[2]	0.84	1.92	2.75(5)	166.4
N8A	H8A	O17A[1]	0.88	2.48	3.33(3)	161.9

[1]7/4-Y,-3/4+X,1/4+Z; [2]5/4-Y,-3/4+X,5/4-Z

Table 2.1.7 Torsion Angles for *N*-(4-fluorophenyl)-2,5-dimethoxybenzamide.

A	B	C	D	Angle/°	A	B	C	D	Angle/°
F1	C2	C3	C4	-180.0(6)	F1A	C2A	C3A	C4A	-178(5)
F1	C2	C7	C6	-179.1(14)	F1A	C2A	C7A	C6A	180(9)
O10	C9	C11	C12	3.7(8)	O10A	C9A	C11A	C12A	11(6)
O10	C9	C11	C16	-176.7(5)	O10A	C9A	C11A	C16A	-173(4)
O17	C12	C13	C14	178.3(5)	O17A	C12A	C13A	C14A	-177(4)
O18	C15	C16	C11	179.0(5)	O18A	C15A	C16A	C11A	177(4)
N8	C5	C6	C7	179.0(16)	N8A	C5A	C6A	C7A	-180(9)
N8	C9	C11	C12	-176.2(5)	N8A	C9A	C11A	C12A	-176(4)
N8	C9	C11	C16	3.4(8)	N8A	C9A	C11A	C16A	0(6)
C2	C3	C4	C5	-1.4(10)	C2A	C3A	C4A	C5A	-4(8)
C3	C2	C7	C6	0.4(18)	C3A	C2A	C7A	C6A	5(18)
C3	C4	C5	N8	-178.0(6)	C3A	C4A	C5A	N8A	-179(4)
C3	C4	C5	C6	1.3(16)	C3A	C4A	C5A	C6A	9(8)
C4	C5	C6	C7	0(3)	C4A	C5A	C6A	C7A	-8(12)
C5	N8	C9	O10	-2.5(9)	C5A	N8A	C9A	O10A	-7(6)
C5	N8	C9	C11	177.4(6)	C5A	N8A	C9A	C11A	180(4)
C5	C6	C7	C2	-1(3)	C5A	C6A	C7A	C2A	1(17)
C7	C2	C3	C4	0.6(11)	C7A	C2A	C3A	C4A	-3(12)
C9	N8	C5	C4	0.5(11)	C9A	N8A	C5A	C4A	1(6)
C9	N8	C5	C6	-178.8(14)	C9A	N8A	C5A	C6A	173(5)
C9	C11	C12	O17	0.7(8)	C9A	C11A	C12A	O17A	-11(6)
C9	C11	C12	C13	-179.2(5)	C9A	C11A	C12A	C13A	179(4)
C9	C11	C16	C15	-179.8(5)	C9A	C11A	C16A	C15A	-179(4)
C11	C12	C13	C14	-1.8(9)	C11A	C12A	C13A	C14A	-6(7)
C12	C11	C16	C15	-0.2(8)	C12A	C11A	C16A	C15A	-3(7)
C12	C13	C14	C15	1.5(9)	C12A	C13A	C14A	C15A	10(6)
C13	C14	C15	O18	-179.6(5)	C13A	C14A	C15A	O18A	-180(4)
C13	C14	C15	C16	-0.6(9)	C13A	C14A	C15A	C16A	-10(7)
C14	C15	C16	C11	-0.1(9)	C14A	C15A	C16A	C11A	7(7)
C16	C11	C12	O17	-179.0(5)	C16A	C11A	C12A	O17A	173(4)
C16	C11	C12	C13	1.1(9)	C16A	C11A	C12A	C13A	3(7)

Table 2.1.8 Hydrogen Atom Coordinates (Å×10^4) and Isotropic Displacement Parameters (Å^2×10^3) for *N*-(4-fluorophenyl)-2,5-dimethoxybenzamide.

Atom	***x***	***y***	***z***	**U(eq)**
H17	10310.35	3562.51	3827.15	63
H18	12337.32	3822.12	6229.22	62
H8	8653.77	3708.39	5383.4	43
H3	5739.44	3708.22	3921.56	50
H4	7467.85	3639.39	4033.93	48
H6	7065.42	3740.09	5737.12	49
H7	5340.57	3761.85	5610.6	49
H13	12551.45	3833.32	4365.41	42
H14	12951.04	3874.82	5322.12	39
H16	10025.28	3711.92	5718.88	38
H17A	12302.21	4059.81	3844.03	65
H18A	10176.28	3665.68	6209.27	82
H8A	13904.6	3722.37	5409.51	47
H3A	16818.99	3726.82	3972.89	62
H4A	15085.06	3851.05	4099.54	60
H6A	15509.61	3816.72	5809.47	59
H7A	17249.05	3765.74	5664.54	60
H13A	10027.03	3883.34	4350.66	43
H14A	9603.78	3609.75	5288.16	45
H16A	12496.33	3751.06	5722.66	45

Table 2.1.9 Atomic Occupancy for *N*-(4-fluorophenyl)-2,5-dimethoxybenzamide.

Atom	***Occupancy***	**Atom**	***Occupancy***	**Atom**	***Occupancy***
F1	0.861(6)	O10	0.861(6)	O17	0.861(6)
H17	0.861(6)	O18	0.861(6)	H18	0.861(6)
N8	0.861(6)	H8	0.861(6)	C2	0.861(6)
C3	0.861(6)	H3	0.861(6)	C4	0.861(6)
H4	0.861(6)	C5	0.861(6)	C6	0.861(6)
H6	0.861(6)	C7	0.861(6)	H7	0.861(6)
C9	0.861(6)	C11	0.861(6)	C12	0.861(6)
C13	0.861(6)	H13	0.861(6)	C14	0.861(6)
H14	0.861(6)	C15	0.861(6)	C16	0.861(6)
H16	0.861(6)	F1A	0.139(6)	O10A	0.139(6)
O17A	0.139(6)	H17A	0.139(6)	O18A	0.139(6)
H18A	0.139(6)	N8A	0.139(6)	H8A	0.139(6)
C2A	0.139(6)	C3A	0.139(6)	H3A	0.139(6)
C4A	0.139(6)	H4A	0.139(6)	C5A	0.139(6)
C6A	0.139(6)	H6A	0.139(6)	C7A	0.139(6)
H7A	0.139(6)	C9A	0.139(6)	C11A	0.139(6)
C12A	0.139(6)	C13A	0.139(6)	H13A	0.139(6)
C14A	0.139(6)	H14A	0.139(6)	C15A	0.139(6)
C16A	0.139(6)	H16A	0.139(6)		

Crystal structure determination of *N*-(4-fluorophenyl)-2,5-dimethoxybenzamide

Crystal Data for $C_{13}H_{10}FNO_3$ (*M* =247.22 g/mol): tetragonal, space group $I4_1/a$ (no. 88), *a* = 13.4738(10) Å, *c* = 23.638(2) Å, *V* = 4291.3(7) $Å^3$, *Z* = 16, *T* = 100(2) K, μ(MoKα) = 0.121 mm^{-1}, *Dcalc* = 1.531 g/cm^3, 2498 reflections measured ($3.48° \leq 2\Theta \leq 55.326°$), 2498 unique ($R_{int}$ = ?, R_{sigma} = 0.0725) which were used in all calculations. The final R_1 was 0.1039 ($I > 2\sigma(I)$) and wR_2 was 0.3040 (all data).

Refinement model description

Number of restraints - 429, number of constraints - unknown.

Details:

1. Twinned data refinement
 Scales: 0.943(3)
 0.057(3)
2. Fixed Uiso
 At 1.2 times of:
  All C(H) groups, All N(H) groups
 At 1.5 times of:
  All O(H) groups
3. Uiso/Uaniso restraints and constraints
F1A ≈ O10A ≈ O17A ≈ O18A ≈ N8A ≈ C2A ≈ C3A ≈ C4A
≈ C5A ≈ C6A ≈ C7A ≈ C9A ≈ C11A ≈ C12A ≈ C13A ≈
C14A ≈ C15A ≈ C16A: within 2A with sigma of 0.01 and sigma for terminal
atoms of 0.02
4. Rigid body (RIGU) restrains
 All non-hydrogen atoms
 with sigma for 1-2 distances of 0.004 and sigma for 1-3 distances of 0.004
5. Same fragment restrains
{F1, O10, O17, O18, N8, C2, C3, C4, C5, C6, C7, C9, C11, C12, C13, C14,
C15,
C16} sigma for 1-2: 0.02, 1-3: 0.04
as
{F1A, O10A, O17A, O18A, N8A, C2A, C3A, C4A, C5A, C6A, C7A, C9A, C11A, C12A,
C13A, C14A, C15A, C16A}
6. Others

Sof(F1A)=Sof(O10A)=Sof(O17A)=Sof(H17A)=Sof(O18A)=Sof(H18A)=Sof(N8A)=Sof(H8A
)=
 Sof(C2A)=Sof(C3A)=Sof(H3A)=Sof(C4A)=Sof(H4A)=Sof(C5A)=Sof(C6A)=Sof(H6A)=

Sof(C7A)=Sof(H7A)=Sof(C9A)=Sof(C11A)=Sof(C12A)=Sof(C13A)=Sof(H13A)=Sof(C14A
)=
 Sof(H14A)=Sof(C15A)=Sof(C16A)=Sof(H16A)=1-FVAR(1)

Sof(F1)=Sof(O10)=Sof(O17)=Sof(H17)=Sof(O18)=Sof(H18)=Sof(N8)=Sof(H8)=Sof(C2
)=
 Sof(C3)=Sof(H3)=Sof(C4)=Sof(H4)=Sof(C5)=Sof(C6)=Sof(H6)=Sof(C7)=Sof(H7)=
 Sof(C9)=Sof(C11)=Sof(C12)=Sof(C13)=Sof(H13)=Sof(C14)=Sof(H14)=Sof(C15)=
 Sof(C16)=Sof(H16)=FVAR(1)
7.a Aromatic/amide H refined with riding coordinates:
 N8(H8), C3(H3), C4(H4), C6(H6), C7(H7), C13(H13), C14(H14), C16(H16),
 N8A(H8A), C3A(H3A), C4A(H4A), C6A(H6A), C7A(H7A), C13A(H13A), C14A(H14A),
 C16A(H16A)
7.b Idealised tetrahedral OH refined as rotating group:
 O17(H17), O18(H18), O17A(H17A), O18A(H18A)

2.2 Crystal data for *N*-(3,5-bis(trifluoromethyl)phenyl)-2,5-dimethoxybenzamide

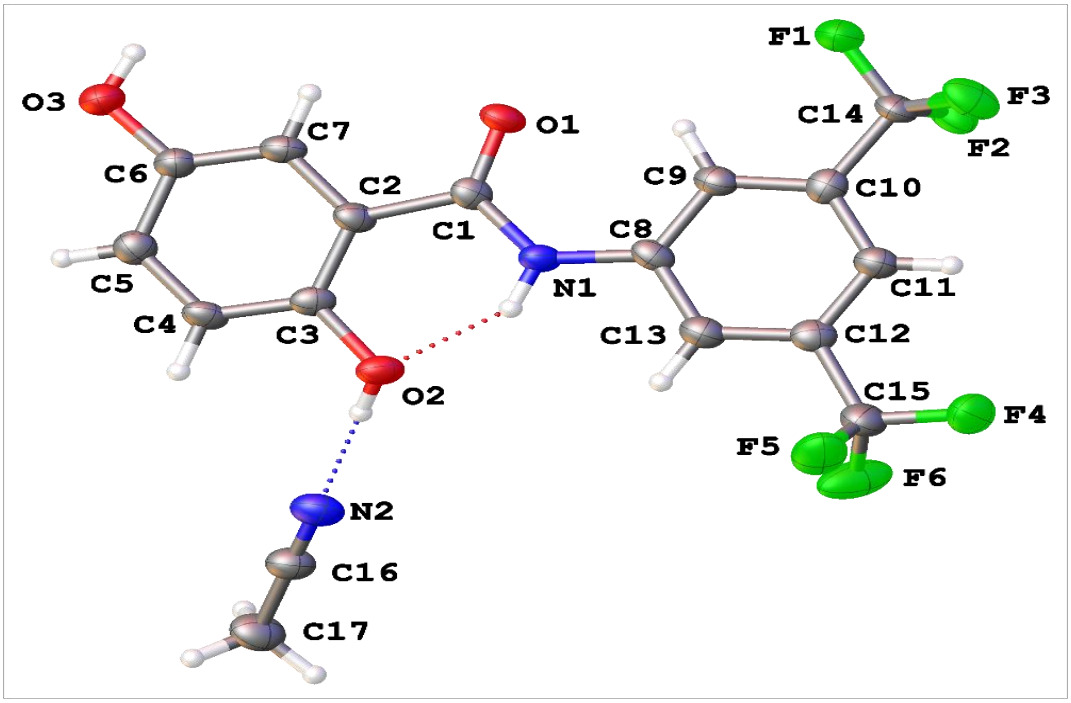

Table 2.2.1 Crystal data and structure refinement for *N*-(3,5-bis(trifluoromethyl)phenyl)-2,5-dimethoxybenzamide.

Identification code	pag19_s1730
Empirical formula	$C_{17}H_{12}F_6N_2O_3$
Formula weight	406.29
Temperature/K	100(2)
Crystal system	monoclinic
Space group	$P2_1/c$
a/Å	11.9740(16)
b/Å	4.8398(5)
c/Å	29.092(3)
α/°	90
β/°	91.105(11)
γ/°	90
Volume/Å^3	1685.6(3)
Z	4
ρ_{calc}g/cm^3	1.601
μ/mm^{-1}	1.372
F(000)	824.0
Crystal size/mm^3	0.147 × 0.031 × 0.01
Radiation	CuKα (λ = 1.54184)
2Θ range for data collection/°	7.384 to 145.802
Index ranges	$-14 \leq h \leq 14$, $-5 \leq k \leq 5$, $0 \leq l \leq 35$
Reflections collected	3231
Independent reflections	3231 [R_{int} = ?, R_{sigma} = 0.0938]
Data/restraints/parameters	3231/3/264
Goodness-of-fit on F^2	1.173
Final R indexes [I>=2σ (I)]	R_1 = 0.1123, wR_2 = 0.3501
Final R indexes [all data]	R_1 = 0.1432, wR_2 = 0.3707
Largest diff. peak/hole / e Å^{-3}	0.55/-0.52

Table 2.2.2 Fractional Atomic Coordinates ($\times 10^4$) and Equivalent Isotropic Displacement Parameters ($Å^2 \times 10^3$) for *N*-(3,5-bis(trifluoromethyl)phenyl)-2,5-dimethoxybenzamide. U_{eq} is defined as 1/3 of of the trace of the orthogonalised U_{IJ} tensor.

Atom	*x*	*y*	*z*	U(eq)
F1	11285(4)	11755(12)	4013.4(16)	43.9(13)
F2	10927(4)	11406(11)	4729.3(15)	41.0(12)
F3	10704(4)	15294(10)	4388.3(18)	43.2(12)
F4	6841(4)	15505(12)	4934.8(17)	46.9(13)
F5	5736(5)	14674(14)	4370.6(18)	54.9(15)
F6	5967(6)	11613(12)	4904(2)	66.3(19)
O1	9375(4)	6004(11)	3154.6(17)	30.0(12)
O2	5954(4)	4105(12)	3220.6(18)	30.3(12)
O3	8592(5)	-1319(13)	1965.5(19)	37.1(13)
N1	7715(5)	7071(13)	3474(2)	25.1(13)
C1	8352(6)	5623(14)	3178(2)	23.6(14)
C2	7767(6)	3529(15)	2885(2)	24.9(14)
C3	6642(6)	2751(15)	2918(2)	24.0(14)
C4	6201(6)	691(15)	2640(2)	26.0(15)
C5	6864(6)	-677(17)	2326(2)	29.3(16)
C6	7990(6)	75(16)	2288(2)	25.5(15)
C7	8426(6)	2143(16)	2563(2)	27.5(15)
C8	8049(6)	9076(15)	3797(2)	24.5(14)
C9	9154(6)	9880(16)	3881(2)	26.5(15)
C10	9380(6)	11823(16)	4219(2)	27.1(15)
C11	8537(6)	13026(16)	4473(2)	27.7(15)
C12	7444(6)	12251(15)	4383(2)	27.1(15)
C13	7195(6)	10275(16)	4051(2)	28.3(15)
C14	10568(6)	12580(17)	4332(2)	28.3(15)
C15	6504(7)	13484(18)	4647(3)	34.7(17)
N2	4428(5)	251(15)	3574(2)	35.5(15)
C16	3845(7)	-1375(18)	3713(3)	33.8(17)
C17	3105(8)	-3454(19)	3892(3)	42(2)

Table 2.2.3 Anisotropic Displacement Parameters ($Å^2 \times 10^3$) for *N*-(3,5-bis(trifluoromethyl)phenyl)-2,5-dimethoxybenzamide. The Anisotropic displacement factor exponent takes the form: $-2\pi^2[h^2a^{*2}U_{11}+2hka^*b^*U_{12}+\ldots]$.

Atom	U_{11}	U_{22}	U_{33}	U_{23}	U_{13}	U_{12}
F1	26(2)	58(3)	47(3)	-14(2)	7.2(19)	-8(2)
F2	41(3)	44(3)	37(2)	9(2)	-7.2(19)	-15(2)
F3	34(3)	30(3)	66(3)	2(2)	-4(2)	-9(2)
F4	43(3)	47(3)	51(3)	-19(2)	7(2)	1(2)
F5	38(3)	69(4)	57(3)	-19(3)	-2(2)	20(3)
F6	71(4)	37(3)	93(4)	-3(3)	52(3)	-2(3)
O1	18(2)	31(3)	40(3)	-4(2)	3.1(19)	-6(2)
O2	23(3)	30(3)	38(3)	-3(2)	10(2)	0(2)
O3	29(3)	45(4)	38(3)	-12(3)	8(2)	-2(3)
N1	18(3)	27(3)	30(3)	-3(2)	5(2)	1(2)
C1	23(3)	18(3)	30(3)	2(3)	0(3)	0(3)
C2	21(3)	22(3)	32(3)	0(3)	2(3)	-4(3)
C3	20(3)	22(3)	30(3)	3(3)	4(2)	4(3)
C4	16(3)	25(4)	37(4)	1(3)	1(3)	1(3)
C5	29(4)	27(4)	31(3)	0(3)	0(3)	1(3)
C6	19(3)	29(4)	29(3)	-2(3)	2(2)	3(3)
C7	21(3)	30(4)	32(3)	2(3)	5(3)	1(3)
C8	19(3)	22(4)	32(3)	5(3)	-1(3)	-3(3)
C9	22(3)	30(4)	28(3)	3(3)	2(3)	-4(3)
C10	31(4)	26(4)	24(3)	2(3)	1(3)	0(3)
C11	24(4)	26(4)	32(3)	1(3)	2(3)	-2(3)
C12	27(4)	23(4)	31(3)	4(3)	5(3)	-1(3)
C13	24(3)	29(4)	32(3)	2(3)	1(3)	-3(3)
C14	21(3)	31(4)	33(4)	-2(3)	4(3)	-6(3)
C15	29(4)	34(4)	41(4)	-4(3)	6(3)	-5(3)
N2	24(3)	37(4)	46(4)	4(3)	4(3)	-1(3)
C16	27(4)	38(5)	37(4)	3(3)	5(3)	3(3)
C17	37(4)	34(5)	56(5)	1(4)	7(4)	-10(4)

Table 2.2.4 Bond Lengths for *N*-(3,5-bis(trifluoromethyl)phenyl)-2,5-dimethoxybenzamide.

Atom	Atom	Length/Å	Atom	Atom	Length/Å
F1	C14	1.337(9)	C3	C4	1.383(11)
F2	C14	1.350(9)	C4	C5	1.388(10)
F3	C14	1.333(10)	C5	C6	1.403(10)
F4	C15	1.344(10)	C6	C7	1.379(11)
F5	C15	1.341(10)	C8	C9	1.397(10)
F6	C15	1.346(10)	C8	C13	1.400(10)
O1	C1	1.243(9)	C9	C10	1.385(11)
O2	C3	1.382(8)	C10	C11	1.389(10)
O3	C6	1.371(9)	C10	C14	1.500(10)
N1	C1	1.356(9)	C11	C12	1.382(10)
N1	C8	1.403(9)	C12	C13	1.387(11)
C1	C2	1.491(10)	C12	C15	1.499(10)
C2	C3	1.403(10)	N2	C16	1.132(11)
C2	C7	1.407(10)	C16	C17	1.444(12)

Table 2.2.5 Bond Angles for *N*-(3,5-bis(trifluoromethyl)phenyl)-2,5-dimethoxybenzamide.

Atom	Atom	Atom	Angle/°	Atom	Atom	Atom	Angle/°
C1	N1	C8	128.8(6)	C9	C10	C14	119.6(7)
O1	C1	N1	121.7(6)	C11	C10	C14	118.5(7)
O1	C1	C2	121.5(6)	C12	C11	C10	118.8(7)
N1	C1	C2	116.8(6)	C11	C12	C13	120.6(7)
C3	C2	C1	125.7(6)	C11	C12	C15	120.9(7)
C3	C2	C7	118.0(7)	C13	C12	C15	118.6(7)
C7	C2	C1	116.2(6)	C12	C13	C8	120.3(7)
O2	C3	C2	120.1(7)	F1	C14	F2	105.7(6)
O2	C3	C4	119.3(6)	F1	C14	C10	113.2(6)
C4	C3	C2	120.6(6)	F2	C14	C10	111.7(6)
C3	C4	C5	120.8(7)	F3	C14	F1	107.5(6)
C4	C5	C6	119.4(7)	F3	C14	F2	105.9(6)
O3	C6	C5	116.5(7)	F3	C14	C10	112.4(7)
O3	C6	C7	123.8(6)	F4	C15	F6	106.5(6)
C7	C6	C5	119.7(7)	F4	C15	C12	113.0(7)
C6	C7	C2	121.4(7)	F5	C15	F4	104.8(7)
C9	C8	N1	124.5(6)	F5	C15	F6	107.0(7)
C9	C8	C13	119.5(7)	F5	C15	C12	112.1(6)
C13	C8	N1	116.1(6)	F6	C15	C12	112.9(7)
C10	C9	C8	119.0(7)	N2	C16	C17	179.7(10)
C9	C10	C11	121.9(7)				

Table 2.2.6 Hydrogen Bonds for *N*-(3,5-bis(trifluoromethyl)phenyl)-2,5-dimethoxybenzamide.

D	H	A	d(D-H)/Å	d(H-A)/Å	d(D-A)/Å	D-H-A/°
O2	H2	N2	0.84(2)	1.99(3)	2.818(9)	168(11)
O3	H3	O1[1]	0.84(2)	1.91(4)	2.711(8)	161(11)
N1	H1	O2	0.88(2)	1.89(6)	2.645(8)	143(8)

[1]2-X,-1/2+Y,1/2-Z

Table 2.2.7 Torsion Angles for *N*-(3,5-bis(trifluoromethyl)phenyl)-2,5-dimethoxybenzamide.

A	B	C	D	Angle/°	A	B	C	D	Angle/°
O1	C1	C2	C3	173.2(7)	C8	C9	C10	C11	-1.0(11)
O1	C1	C2	C7	-3.8(10)	C8	C9	C10	C14	176.4(7)
O2	C3	C4	C5	178.8(6)	C9	C8	C13	C12	0.3(11)
O3	C6	C7	C2	179.3(7)	C9	C10	C11	C12	0.0(11)
N1	C1	C2	C3	-6.2(10)	C9	C10	C14	F1	15.2(10)
N1	C1	C2	C7	176.8(6)	C9	C10	C14	F2	-103.9(8)
N1	C8	C9	C10	-177.9(7)	C9	C10	C14	F3	137.2(7)
N1	C8	C13	C12	179.1(7)	C10	C11	C12	C13	1.1(11)
C1	N1	C8	C9	-2.5(11)	C10	C11	C12	C15	179.9(7)
C1	N1	C8	C13	178.7(7)	C11	C10	C14	F1	-167.4(7)
C1	C2	C3	O2	4.9(11)	C11	C10	C14	F2	73.5(9)
C1	C2	C3	C4	-177.2(7)	C11	C10	C14	F3	-45.4(9)
C1	C2	C7	C6	177.0(7)	C11	C12	C13	C8	-1.2(11)
C2	C3	C4	C5	0.9(11)	C11	C12	C15	F4	5.5(11)
C3	C2	C7	C6	-0.2(11)	C11	C12	C15	F5	123.6(8)
C3	C4	C5	C6	-1.0(11)	C11	C12	C15	F6	-115.5(8)
C4	C5	C6	O3	-178.8(7)	C13	C8	C9	C10	0.8(10)
C4	C5	C6	C7	0.5(11)	C13	C12	C15	F4	-175.6(7)
C5	C6	C7	C2	0.1(11)	C13	C12	C15	F5	-57.5(10)
C7	C2	C3	O2	-178.2(6)	C13	C12	C15	F6	63.4(10)
C7	C2	C3	C4	-0.3(10)	C14	C10	C11	C12	-177.3(7)
C8	N1	C1	O1	-1.7(11)	C15	C12	C13	C8	179.9(7)
C8	N1	C1	C2	177.7(6)					

Table 2.2.8 Hydrogen Atom Coordinates (Å×10^4) and Isotropic Displacement Parameters (Å^2×10^3) for *N*-(3,5-bis(trifluoromethyl)phenyl)-2,5-dimethoxybenzamide.

Atom	*x*	*y*	*z*	U(eq)
H2	5450(60)	3160(190)	3340(30)	46
H3	9200(50)	-500(200)	1990(40)	56
H1	7000(20)	6680(190)	3460(30)	30
H4	5435.86	206.99	2663.17	31
H5	6557.61	-2109.56	2139.48	35
H7	9189.04	2643.5	2534.57	33
H9	9742.43	9103.88	3708.21	32
H11	8709.57	14357.5	4703.2	33
H13	6441.48	9731.76	3996.84	34
H17A	2527.28	-3895.54	3660.36	63
H17B	2752.91	-2753.75	4169.98	63
H17C	3533.8	-5124.83	3967.04	63

Crystal structure determination of [pag19_s1730]

Crystal Data for $C_{17}H_{12}F_6N_2O_3$ (*M* =406.29 g/mol): monoclinic, space group $P2_1/c$ (no. 14), *a* = 11.9740(16) Å, *b* = 4.8398(5) Å, *c* = 29.092(3) Å, *β* = 91.105(11)°, *V* = 1685.6(3) Å^3, *Z* = 4, *T* = 100(2) K, μ(CuKα) = 1.372 mm^{-1}, *Dcalc* = 1.601 g/cm^3, 3231 reflections measured (7.384° ≤ 2Θ ≤ 145.802°), 3231 unique (R_{int} = ?, R_{sigma} = 0.0938) which were used in all calculations. The final R_1 was 0.1123 (I > 2σ(I)) and wR_2 was 0.3707 (all data).

Refinement model description

Number of restraints - 3, number of constraints - unknown.

Details:

```
1. Twinned data refinement
 Scales: 0.694
 0.306
2. Fixed Uiso
 At 1.2 times of:
  All C(H) groups, All N(H) groups
 At 1.5 times of:
  All C(H,H,H) groups, All O(H) groups
3. Restrained distances
 N1-H1
 0.88 with sigma of 0.02
 O2-H2 = O3-H3
 0.84 with sigma of 0.02
4.a Aromatic/amide H refined with riding coordinates:
 C4(H4), C5(H5), C7(H7), C9(H9), C11(H11), C13(H13)
4.b Idealised Me refined as rotating group:
 C17(H17A,H17B,H17C)
```

3. ^{1}H NMR Titration Anion Binding Studies

Equipment and Sample Preparation

^{1}H NMR titrations were performed on a Bruker Avance DPX 400 spectrometer. For NMR titrations with chloride, a constant host concentration was maintained (~ 5.0 mM) by using the host solution to dissolve the guest to make the guest stock solution. Over the course of the titration Hamiltonian Microlitre syringes were used to add aliquots of the guest stock solution to the NMR sample of the host solution.

The anions were added as the tetrabutylammonium (TBA) salts after being dried under high vacuum (< 1.0 mmHg) for 24 h. Stock solutions of the host were prepared in a CD_3CN / 1% DMSO-d_6 solution, or a pure CD_3CN solution. The solvent used is noted in the information for each titration. The host stock solutions (500 μL) were transferred to an air-tight screw-cap NMR sample tube (5 mm ID) and the same host stock solution was used to prepare the standard guest titrant solution containing 20-100 mM of the TBA-anion salts. This ensured a constant concentration of the host for the duration of the titration experiment.

Titration Procedure

Over the course of the titration small aliquots (2-100 μL) of the standard guest solution were added to the host solution (~ 500 μL) in the NMR tube. For each titration 15-20 data points were collected and at the end of the titration approximately 50 equivalents of the guest anion salt were present. Upon each addition of the standard guest solution the samples were thoroughly shaken in the NMR tube and then allowed to equilibrate for up to 2 minutes inside the NMR probe before the spectra were taken. Throughout each titration experiment all parameters of the NMR spectrometer remained constant.

Titration Data Fitting

In all cases the proton resonances were monitored for changes in chemical shift. Where possible two or more resonances were followed, allowing several data sets to use in determination of the association constant (K_a). Global fitting takes into account all data sets at the same time and improves the quality of the nonlinear curve fitting. The supramolecular.org web applet was used to fit the titration data to either a 1:1 binding model or 2:1 binding model. A 2:1 model was preferred when the covariance of fit (cov_{fit}) was greater than 5 times better than for the 1:1 model.

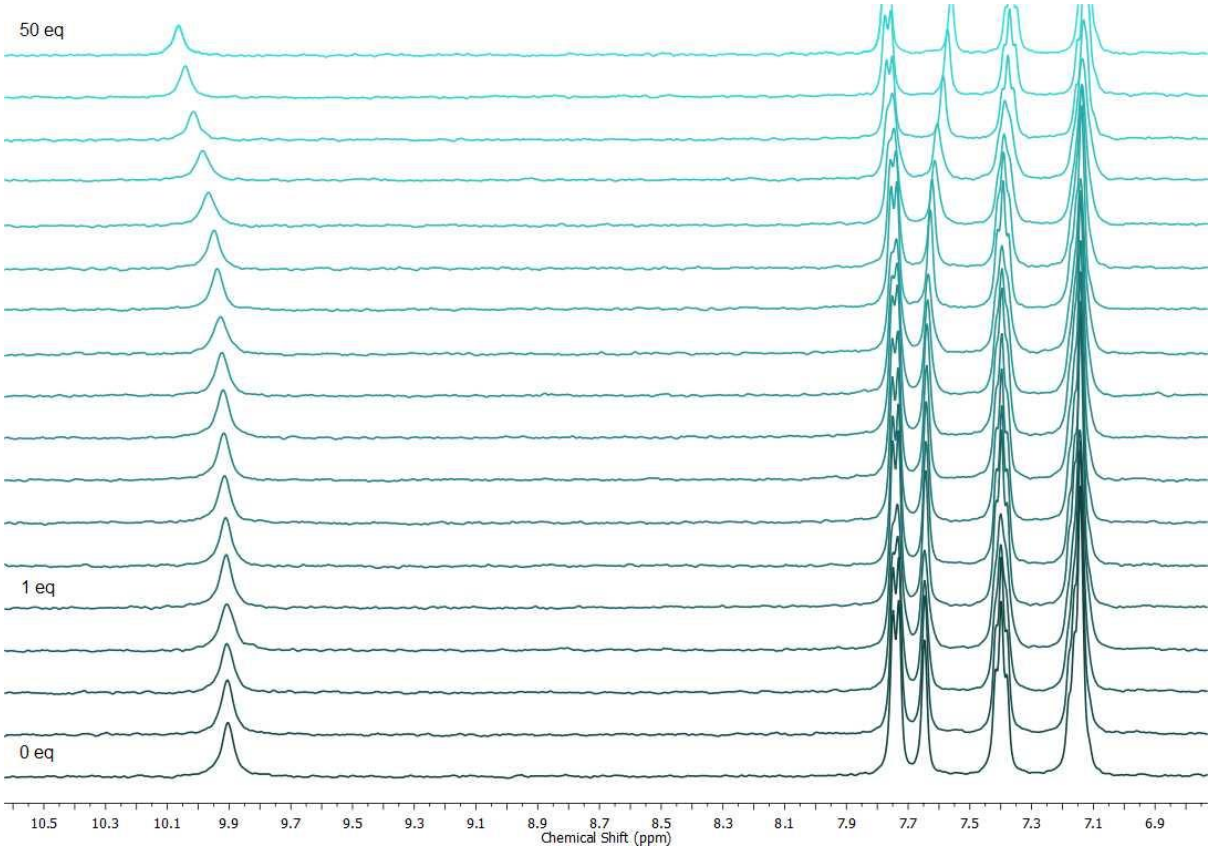

Figure 45. ^{1}H NMR titration spectra as a stack plot for 2,5-dimethoxy-N-phenylbenzamide (5 mM) + TBACl in CD_3CN-d_3 / 1% DMSO-d_6 at 298 K.

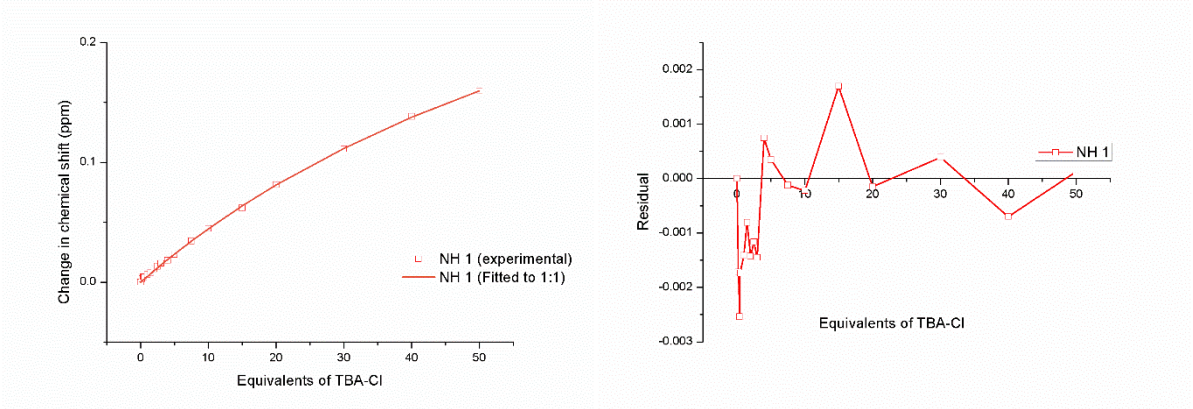

Figure 46. Fitted binding isotherm of 2,5-dimethoxy-N-phenylbenzamide + TBACl showing the change in chemical shift of the NH proton fitted to the 1:1 binding model (left). K_a = 2.18 M^{-1} Residual plot showing the random error obtained from the binding isotherm fitting (right). Covariance of fit (cov_{fit}) = 4.57 x 10^{-4}. Link to Bindfit fitting: http://app.supramolecular.org/bindfit/view/a3a8083e-2d82-4ce7-8eb8-8c326a21b893.

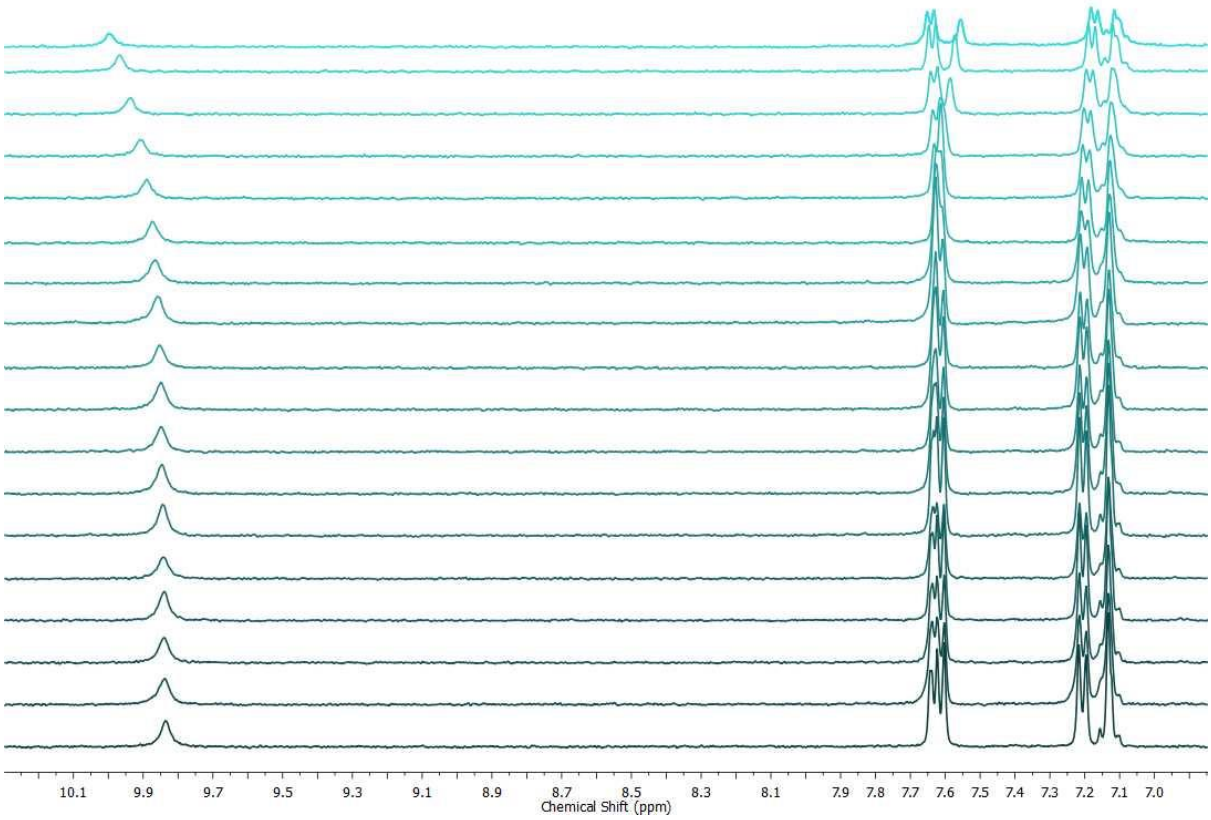

Figure 47. ^{1}H NMR titration spectra as a stack plot for 2,5-dimethoxy-N-(p-tolyl)benzamide (5 mM) + TBACl in CD_3CN-d_3 /1% DMSO-d_6 at 298 K.

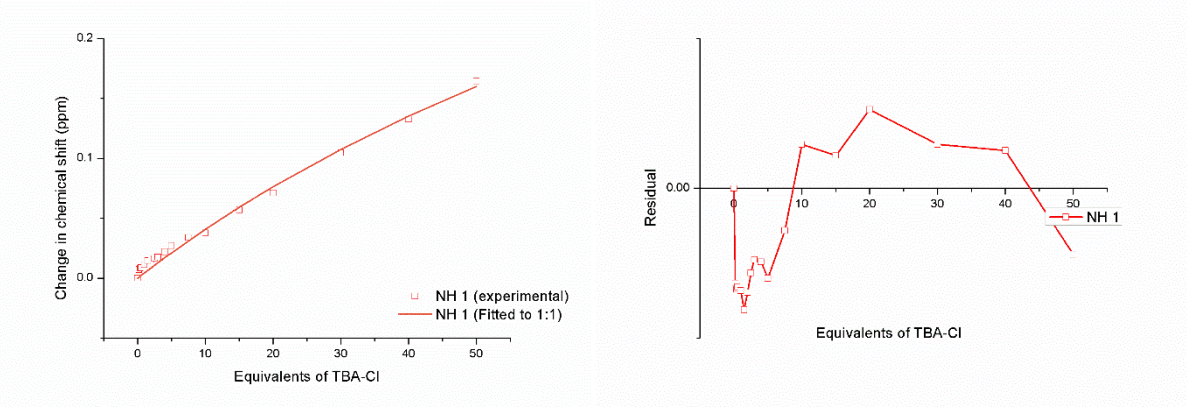

Figure 48. Fitted binding isotherm of 2,5-dimethoxy-N-(p-tolyl)benzamide + TBACl showing the change in chemical shift of the NH proton fitted to the 1:1 binding model (left). K_a = 1.48 M^{-1} Residual plot showing the random error obtained from the binding isotherm fitting (right). Covariance of fit (cov_{fit}) = 5.34 x 10^{-3}. Link to Bindfit fitting: http://app.supramolecular.org/bindfit/view/6f20ff00-a6c8-4bd6-9451-accc783b3fb0.

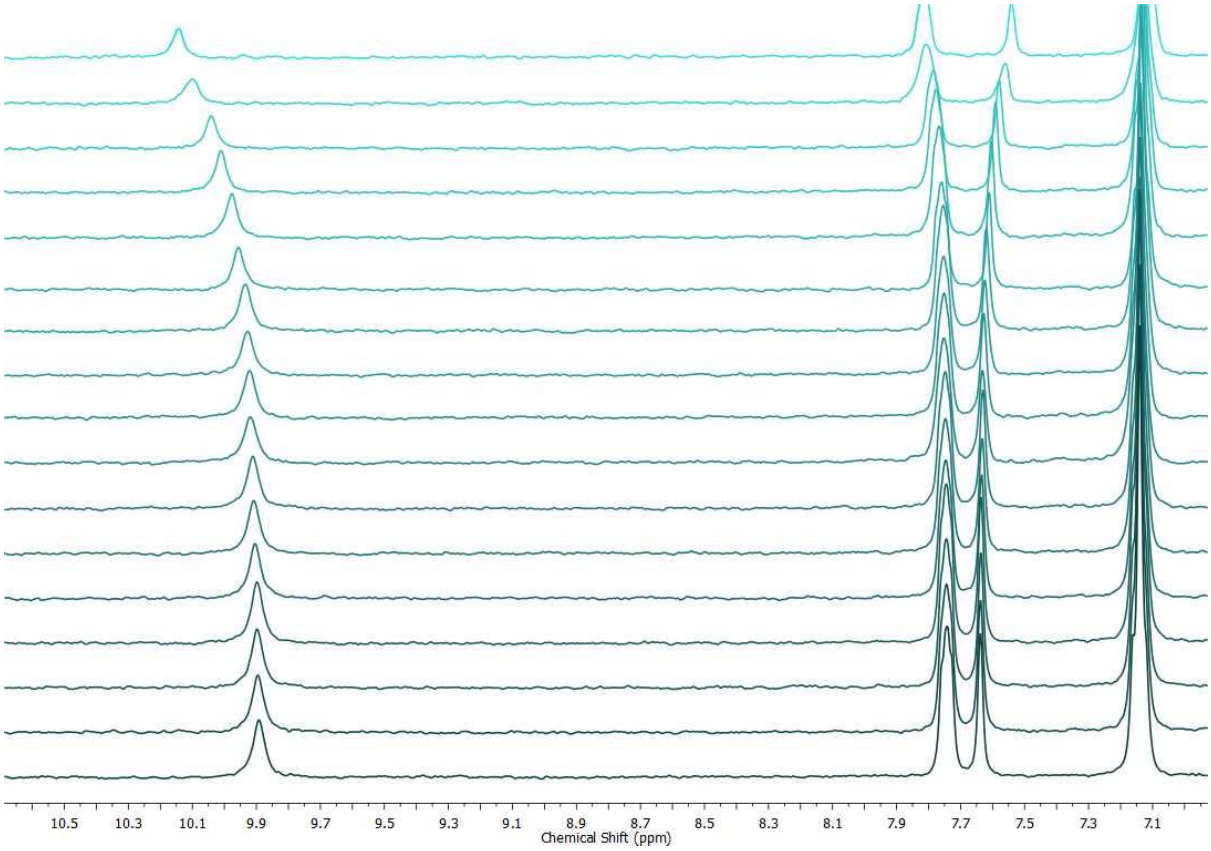

Figure 49. ^{1}H NMR titration spectra as a stack plot for *N*-(4-fluorophenyl)-2,5-dimethoxybenzamide (5 mM) + TBACl in CD_3CN-d_3 /1% DMSO-d_6 at 298 K.

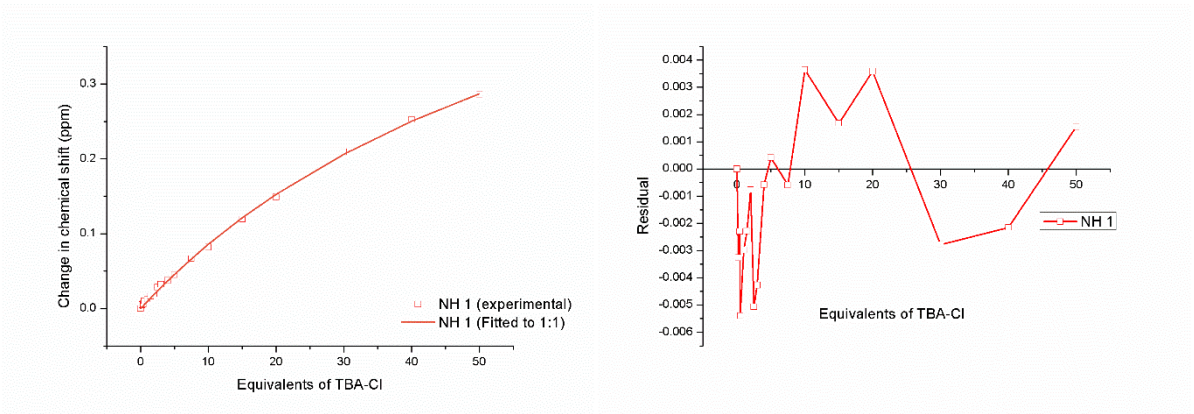

Figure 50. Fitted binding isotherm of N-(4-fluorophenyl)-2,5-dimethoxybenzamide + TBACl showing the change in chemical shift of the NH proton fitted to the 1:1 binding model (left). K_a = 2.92 M^{-1} Residual plot showing the random error obtained from the binding isotherm fitting (right). Covariance of fit (cov_{fit}) = 8.91 x 10^{-4}. Link to Bindfit fitting: http://app.supramolecular.org/bindfit/view/5bfbd64f-7e92-4de1-8492-aa930d7321dc.

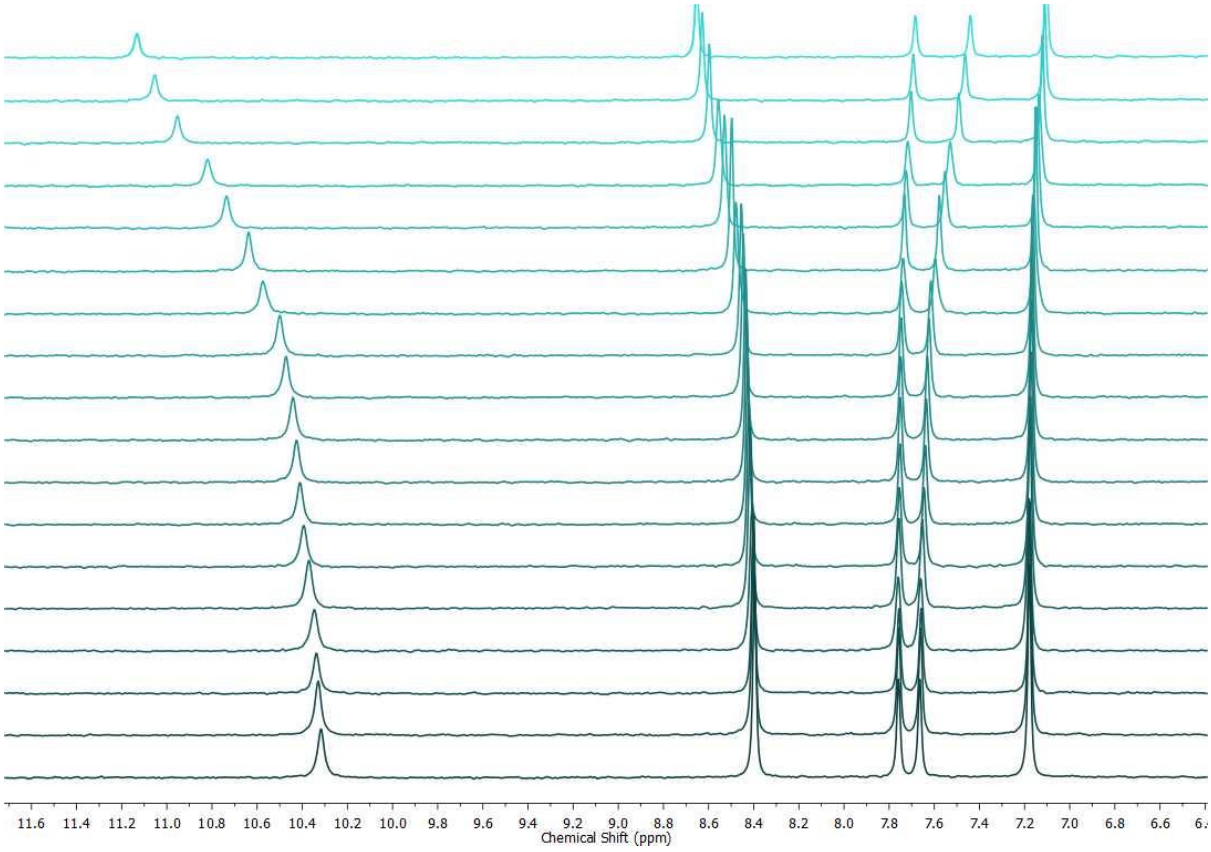

Figure 51. ^{1}H NMR titration spectra as a stack plot for *N*-(3,5-bis(trifluoromethyl)phenyl)-2,5-dimethoxybenzamide (5 mM) + TBACl in CD_3CN-d_3 /1% DMSO-d_6 at 298 K.

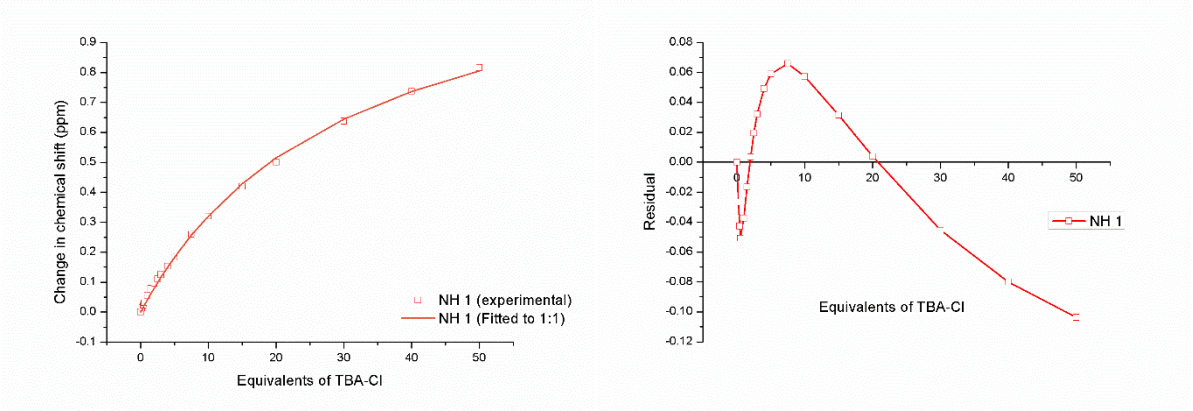

Figure 52. Fitted binding isotherm of *N*-(3,5-bis(trifluoromethyl)phenyl)-2,5-dimethoxybenzamide + TBACl showing the change in chemical shift of the NH proton fitted to the 1:1 binding model (left). K_a = 6.69 M^{-1} Residual plot showing the random error obtained from the binding isotherm fitting (right). Covariance of fit (cov_{fit}) = 1.16 x 10^{-3}. Link to Bindfit fitting: http://app.supramolecular.org/bindfit/view/e6081634-e1d0-49a8-a641-7e7c69fd6d15.

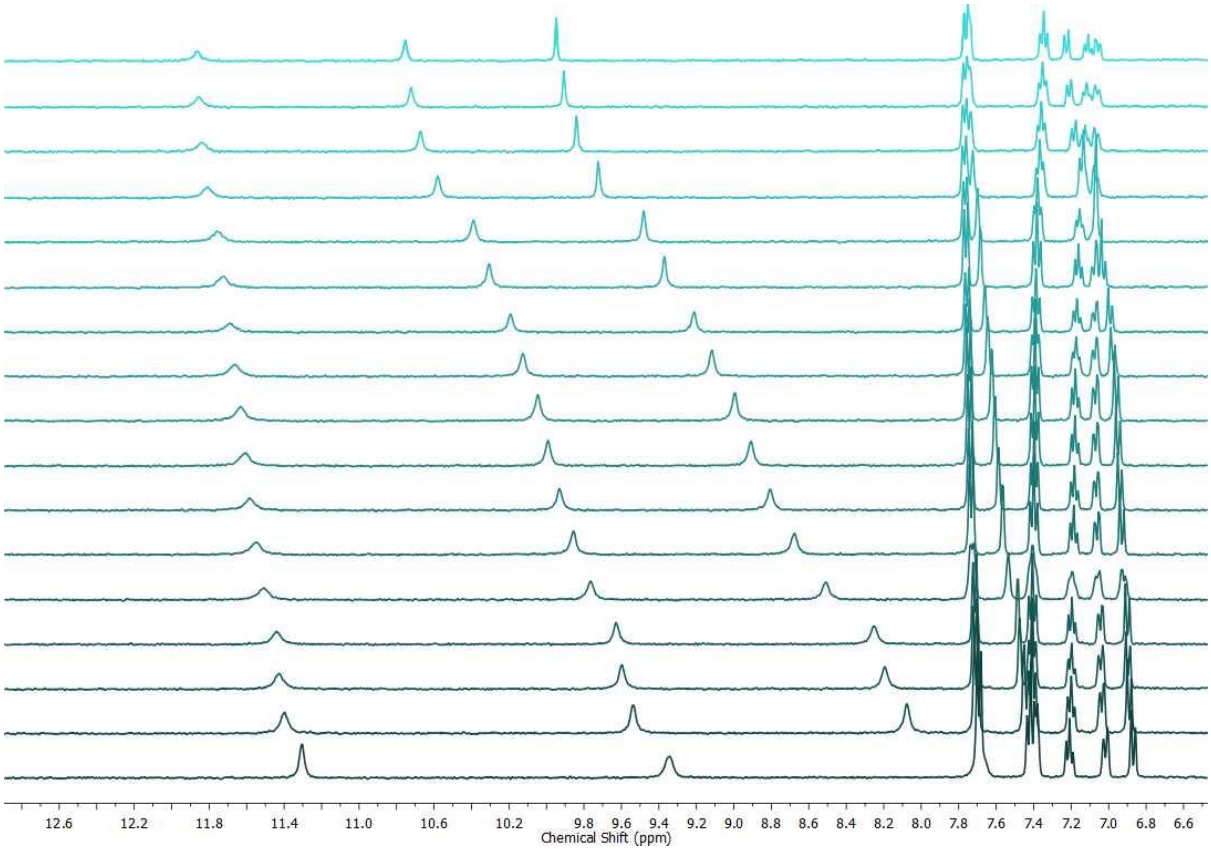

Figure 53. ^{1}H NMR titration spectra as a stack plot for 2,5-dihydroxy-*N*-phenylbenzamide (5 mM) + TBACl in CD_3CN-d_3 /1% DMSO-d_6 at 298 K.

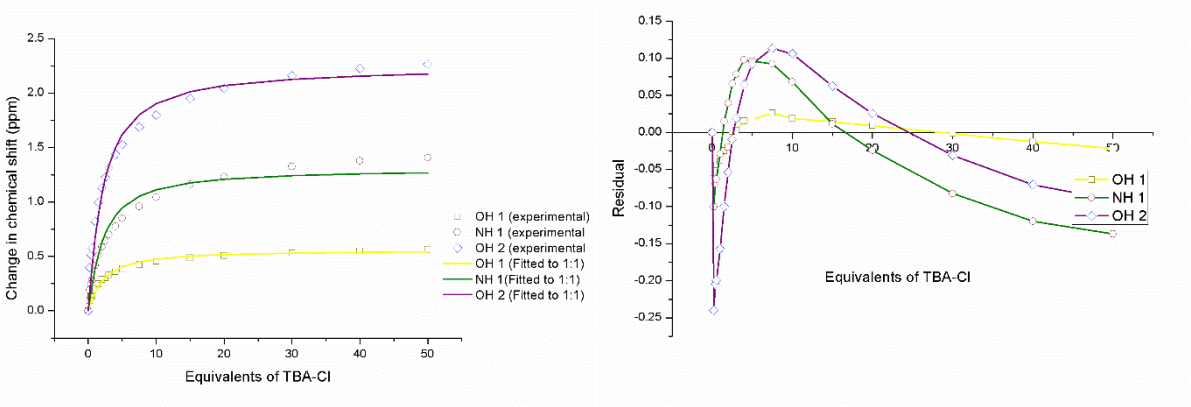

Figure 54. Fitted binding isotherm of 2,5-dihydroxy-*N*-phenylbenzamide + TBACl showing the change in chemical shift of the OH and NH protons fitted to the 1:1 binding model (left). K_a = 124.85 M^{-1} Residual plot showing the random error obtained from the binding isotherm fitting (right). Covariance of fit (cov_{fit}) = 1.61 x 10^{-2}. Link to Bindfit fitting: http://app.supramolecular.org/bindfit/view/8ebd8323-a206-43ad-9482-c8a6625e0288.

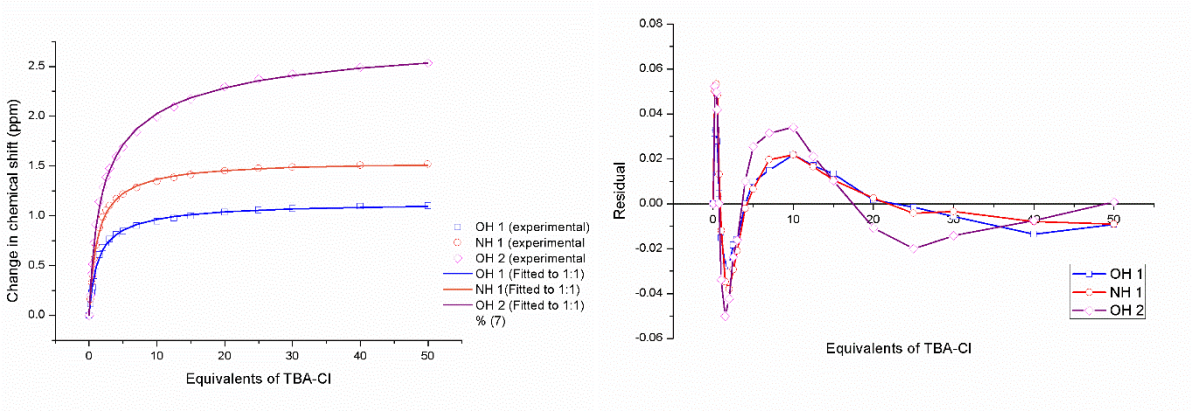

Figure 55. Fitted binding isotherm of 2,5-dihydroxy-*N*-phenylbenzamide + TBACl showing the change in chemical shift of the OH and NH protons fitted to the 2:1 binding model (left) K_{11} = 112.96 M^{-1}, K_{12} = 679.5 M^{-1}. Residual plot showing the random error obtained from the binding isotherm fitting (right). Covariance of fit (cov_{fit}) = 1.23 x 10^{-3}. Link to Bindfit fitting: http://app.supramolecular.org/bindfit/view/6b35f570-2a30-4e86-bc62-e13bdf396c6d.

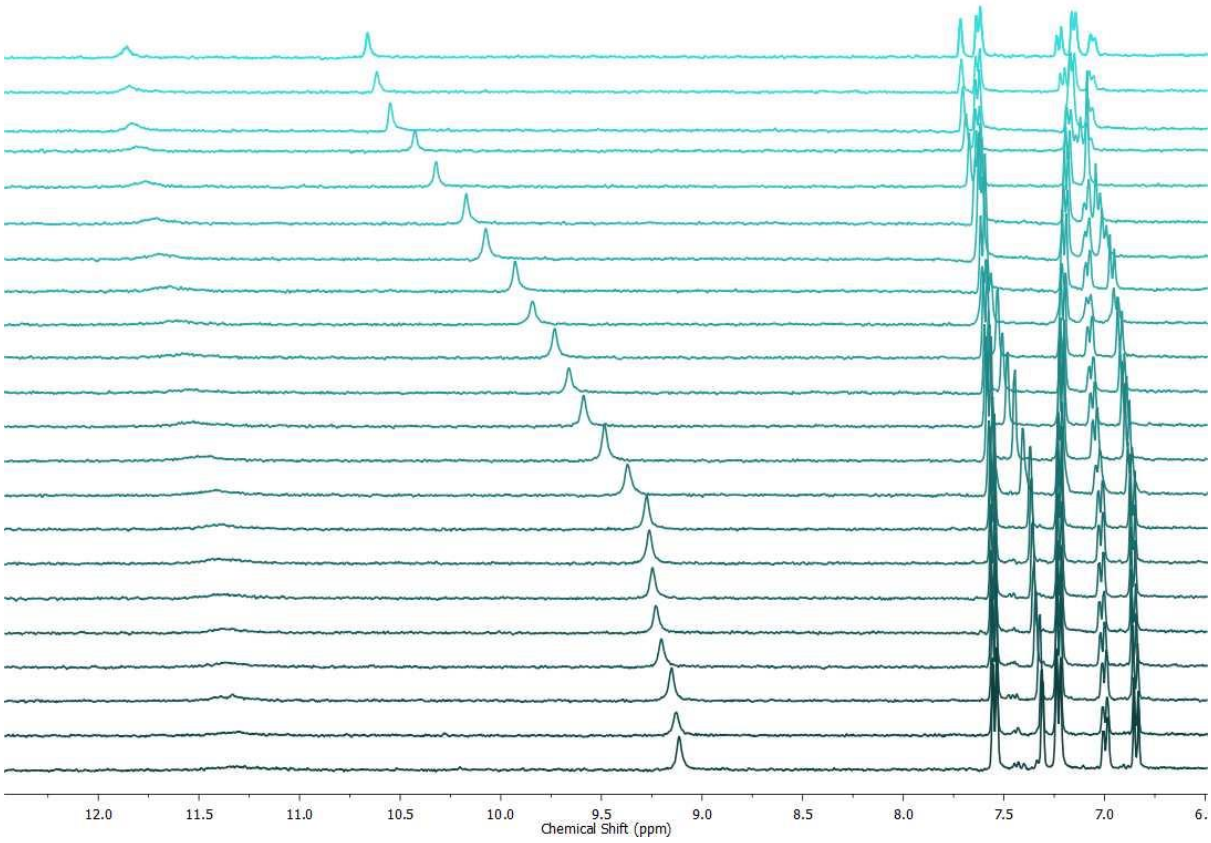

Figure 56. ^{1}H NMR titration spectra as a stack plot for 2,5-dihydroxy-N-(p-tolyl)benzamide (5 mM) + TBACl in CD_3CN-d_3 /1% DMSO-d_6 at 298 K.

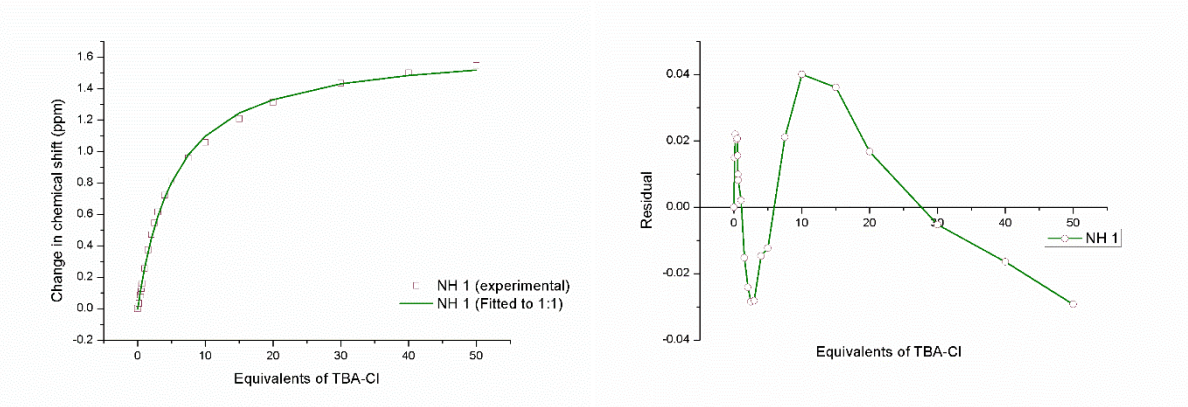

Figure 57. Fitted binding isotherm of *N*-(4-fluorophenyl)-2,5-dihydroxybenzamide + TBACl showing the change in chemical shift of the OH and NH protons fitted to the 1:1 binding model (left) K_a = 41.47 M^{-1}. Residual plot showing the random error obtained from the binding isotherm fitting (right). Covariance of fit (cov_{fit}) = 1.56 x 10^{-3}. Link to Bindfit fitting: http://app.supramolecular.org/bindfit/view/d28e7bd7-dbf9-4532-851d-7a81ca565211.

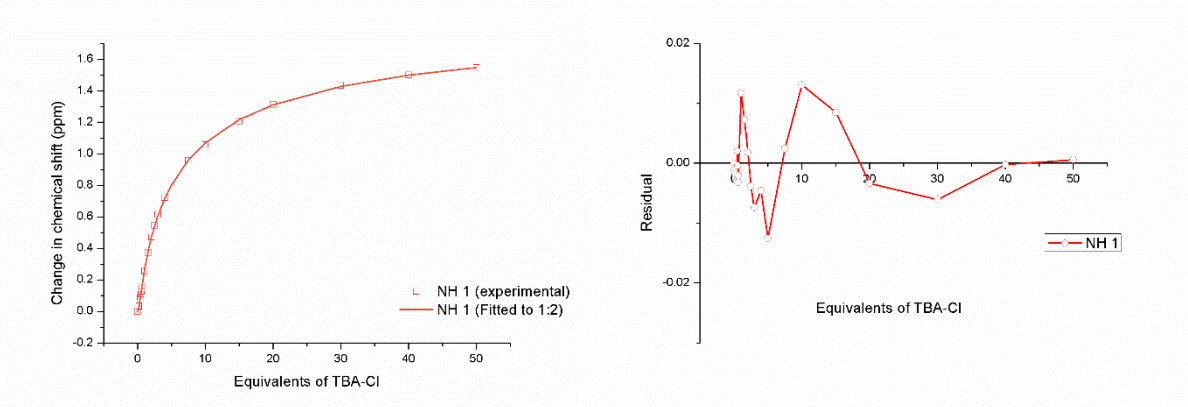

Figure 58. Fitted binding isotherm of 2,5-dihydroxy-N-(p-tolyl)benzamide + TBACl showing the change in chemical shift of the NH protons fitted to the 2:1 binding model (left) K_{11} = 191.36 M^{-1}, K_{12} = 665.6 M^{-1}.Residual plot showing the random error obtained from the binding isotherm fitting (right). Covariance of fit (cov_{fit}) = 1.28 x 10^{-4}. Link to Bindfit fitting: http://app.supramolecular.org/bindfit/view/7a990a8d-730c-4de2-b904-2821f4114c32.

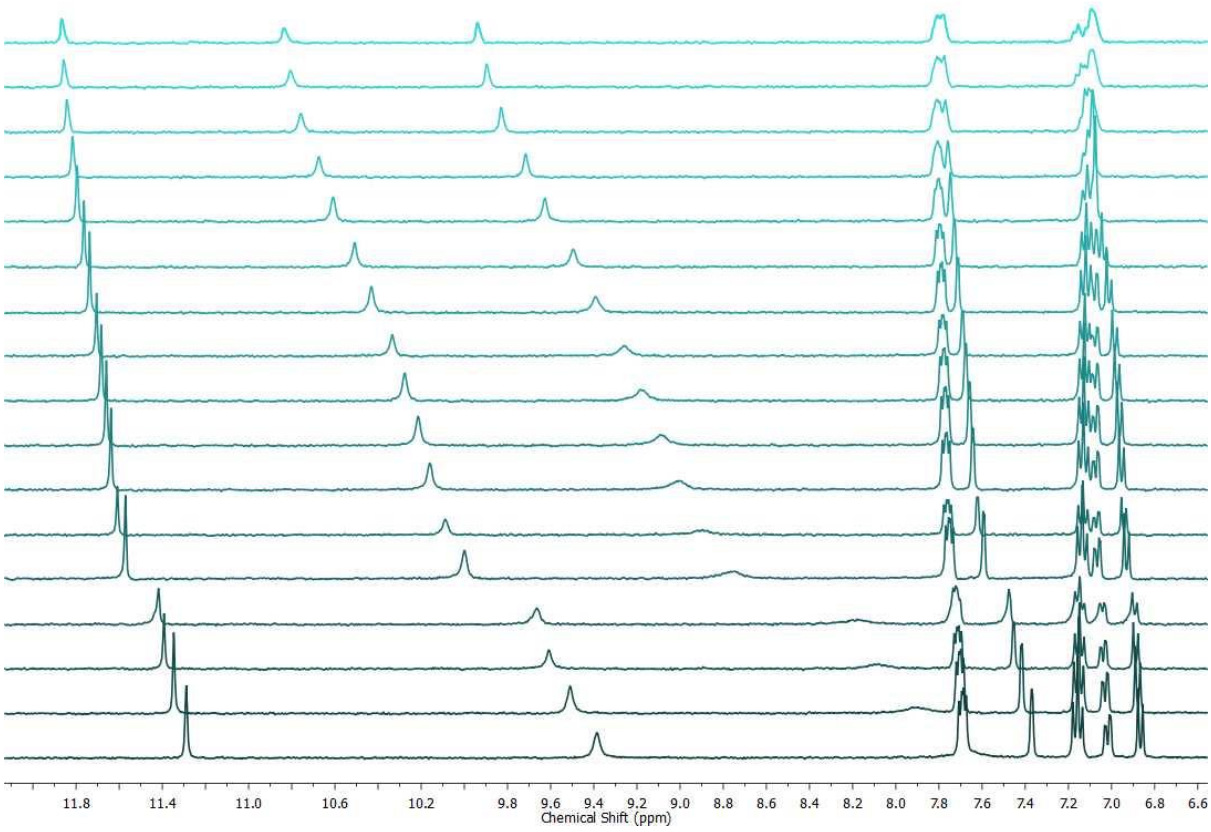

Figure 59. ^{1}H NMR titration spectra as a stack plot for *N*-(4-fluorophenyl)-2,5-dihydroxybenzamide (5 mM) + TBACl in CD_3CN-d_3 /1% DMSO-d_6 at 298 K.

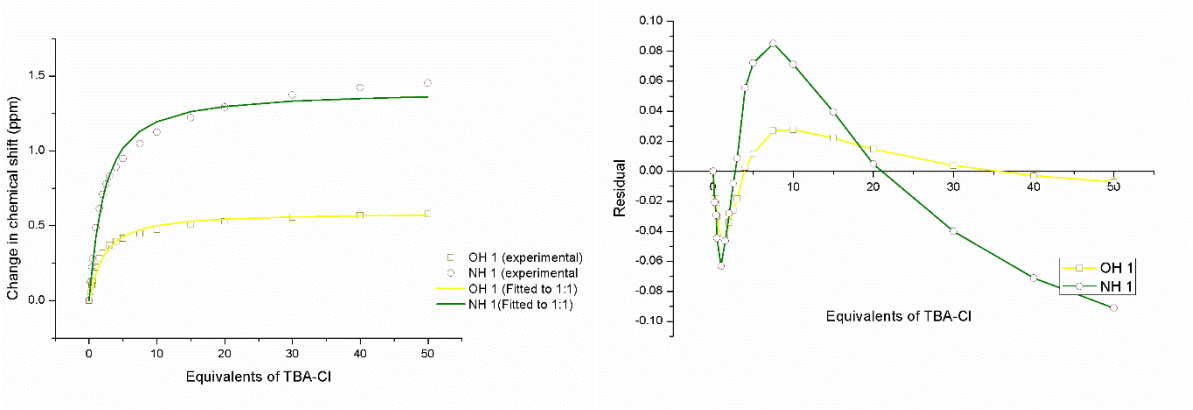

Figure 60. Fitted binding isotherm of *N*-(4-fluorophenyl)-2,5-dihydroxybenzamide + TBACl showing the change in chemical shift of the OH and NH protons fitted to the 1:1 binding model (left) K_a = 125.55 M^{-1}. Residual plot showing the random error obtained from the binding isotherm fitting (right). Covariance of fit (cov_{fit}) = 9.07 x 10^{-3}. Link to Bindfit fitting: http://app.supramolecular.org/bindfit/view/d1dfa649-4fa8-4dc9-9486-54fa7b6dc005.

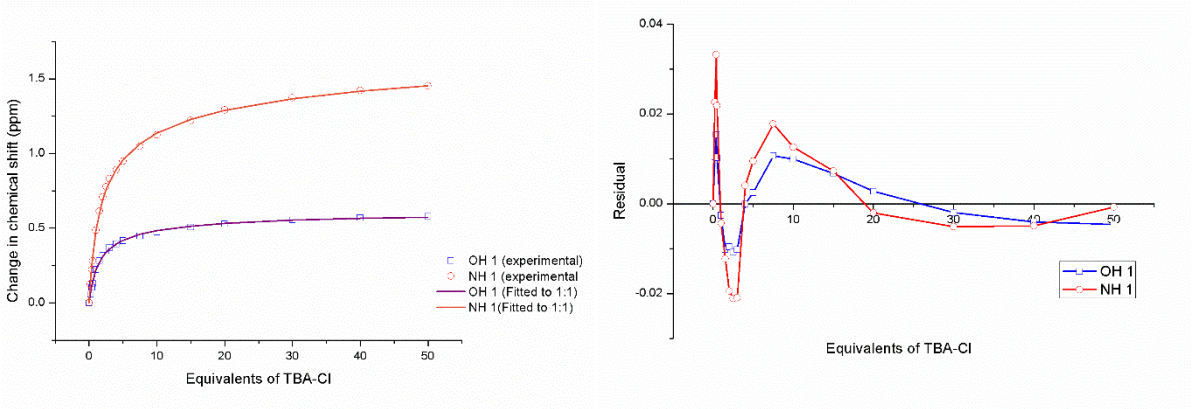

Figure 61. Fitted binding isotherm of *N*-(4-fluorophenyl)-2,5-dihydroxybenzamide + TBACl showing the change in chemical shift of the downfield OH and NH protons fitted to the 2:1 binding model (left) K_{11} = 30.76 M^{-1}, K_{12} = 517.79 M^{-1}.Residual plot showing the random error obtained from the binding isotherm fitting (right). Covariance of fit (cov_{fit}) = 8.61 x 10^{-4}. Link to Bindfit fitting: http://app.supramolecular.org/bindfit/view/1ebd9451-9a97-44e0-b04a-f0da4ec9da66.

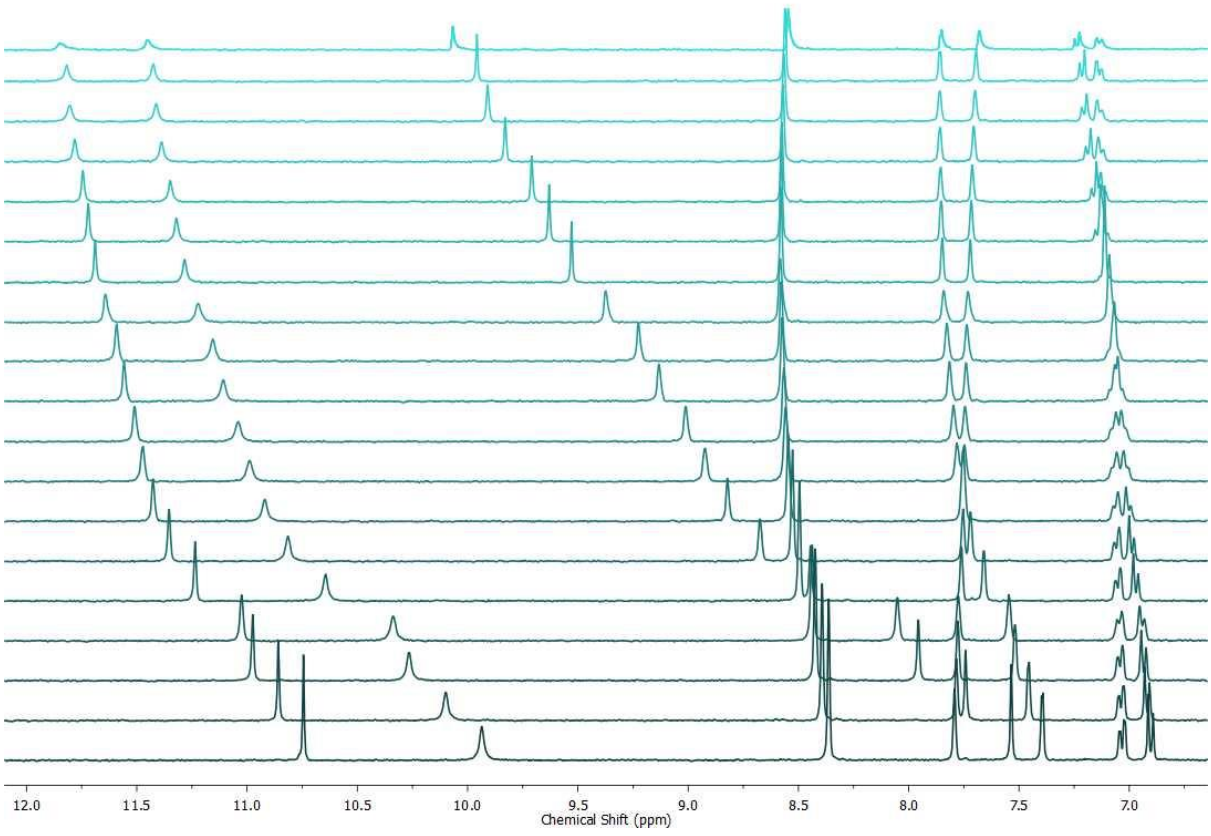

Figure 62. ^{1}H NMR titration spectra as a stack plot for *N*-(3,5-bis(trifluoromethyl)phenyl)-2,5-dihydroxybenzamide (5 mM) + TBACl in CD_3CN-d_3 /1% DMSO-d_6 at 298 K.

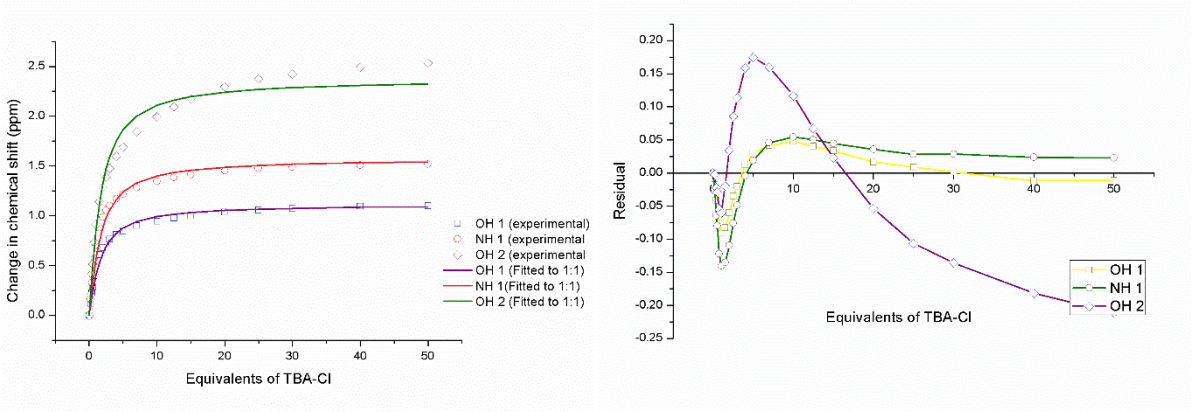

Figure 63. Fitted binding isotherm of *N*-(3,5-bis(trifluoromethyl)phenyl)-2,5-dihydroxybenzamide + TBACl showing the change in chemical shift of the OH and NH protons fitted to the 1:1 binding model (left). K_a = 173.50 M^{-1}. Residual plot showing the random error obtained from the binding isotherm fitting (right). Covariance of fit (cov_{fit}) = 1.41 x 10^{-2}. Link to Bindfit fitting: http://app.supramolecular.org/bindfit/view/3c5571ea-697b-415b-a44c-eef7bc4a492d.

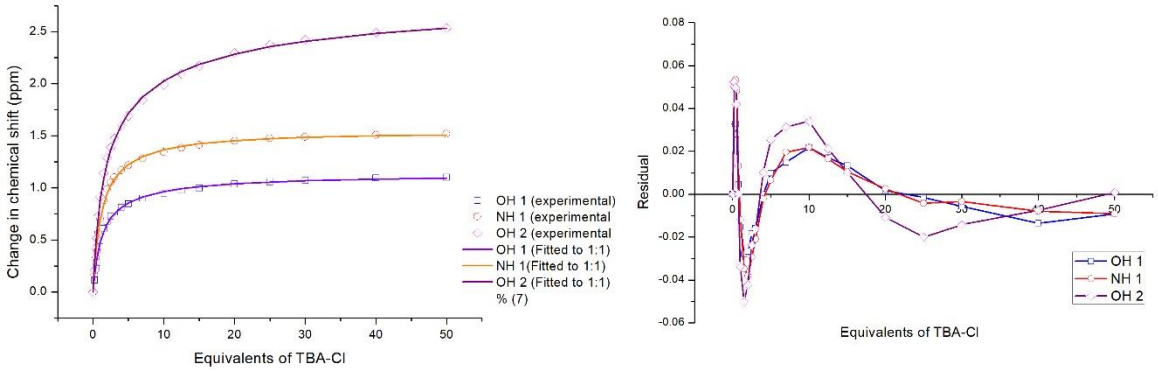

Figure 64. Fitted binding isotherm of *N*-(3,5-bis(trifluoromethyl)phenyl)-2,5-dihydroxybenzamide + TBACl showing the change in chemical shift of the OH and NH protons fitted to the 2:1 binding model (left) K_{11} = 54.44 M^{-1}, K_{12} = 336.49 M^{-1}. Residual plot showing the random error obtained from the binding isotherm fitting (right). Covariance of fit (cov_{fit}) = 1.42 x 10^{-3}. Link to Bindfit fitting: http://app.supramolecular.org/bindfit/view/b5da4bd0-0c39-48e6-b0d6-7ca3dc5d4c32.

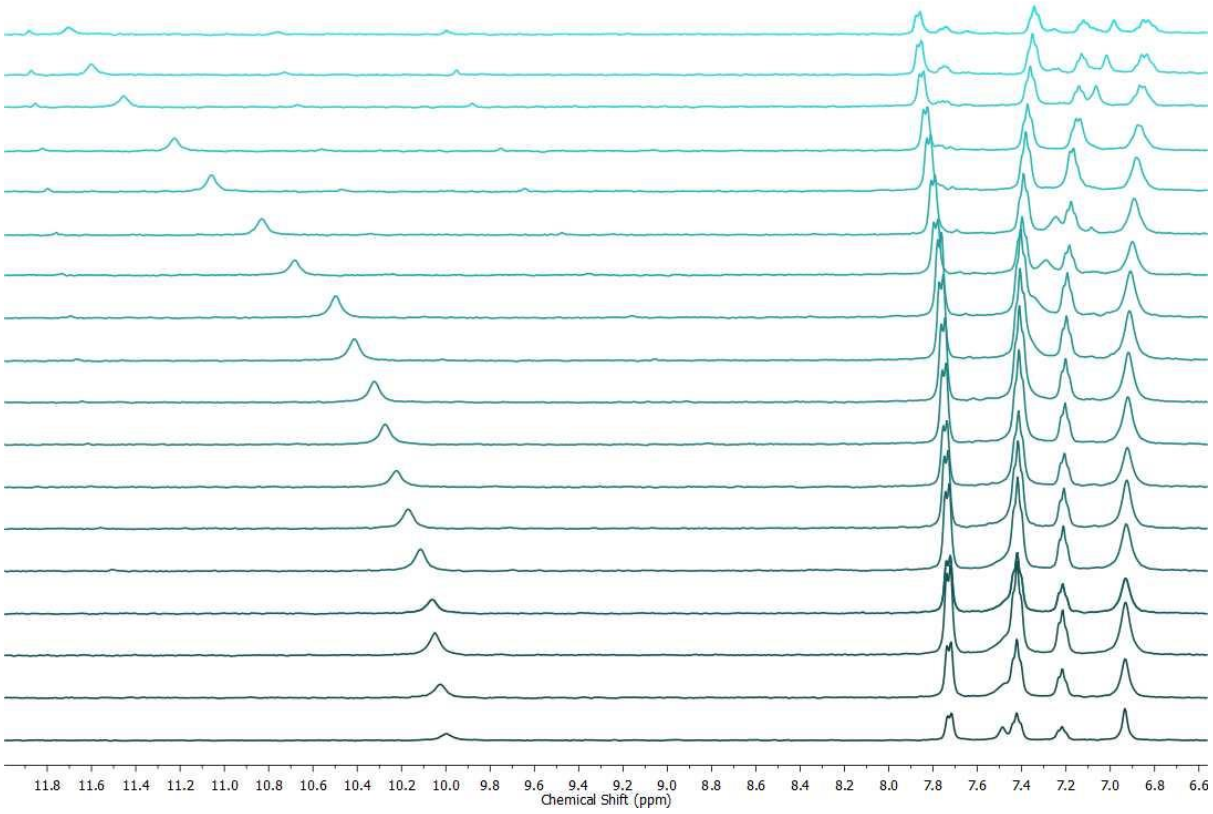

Figure 65. ^{1}H NMR titration spectra as a stack plot for 3,6-dioxo-*N*-phenylcyclohexa-1,4-diene-1-carboxamide (5 mM) + TBACl in CD_3CN-d_3 /1% DMSO-d_6 at 298 K.

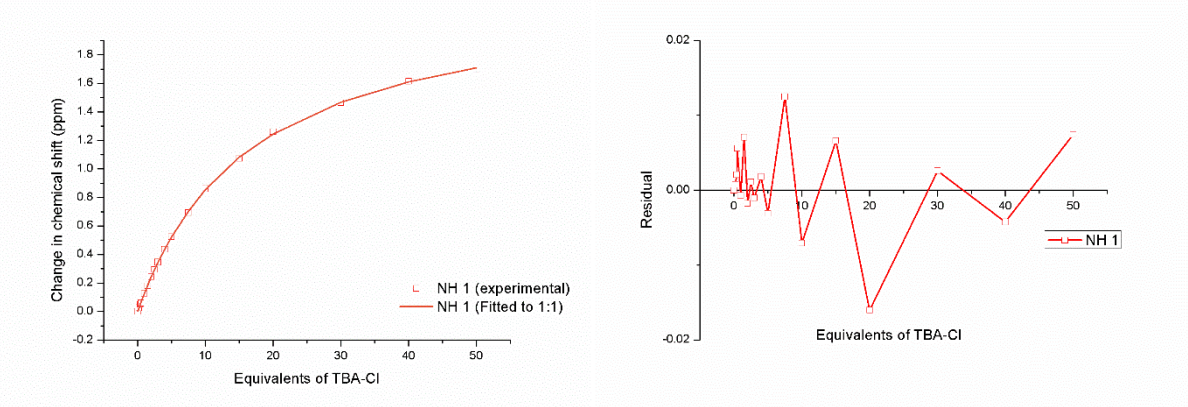

Figure 66. Fitted binding isotherm of 3,6-dioxo-*N*-phenylcyclohexa-1,4-diene-1-carboxamide + TBACl showing the change in chemical shift of the NH proton fitted to the 1:1 binding model (left). K_a = 12.57 M^{-1} Residual plot showing the random error obtained from the binding isotherm fitting (right). Covariance of fit (cov_{fit}) = 1.19 x 10^{-4}. Link to Bindfit: http://app.supramolecular.org/bindfit/view/c47caa71-aa70-4477-8ff5-a03f89cf0970.

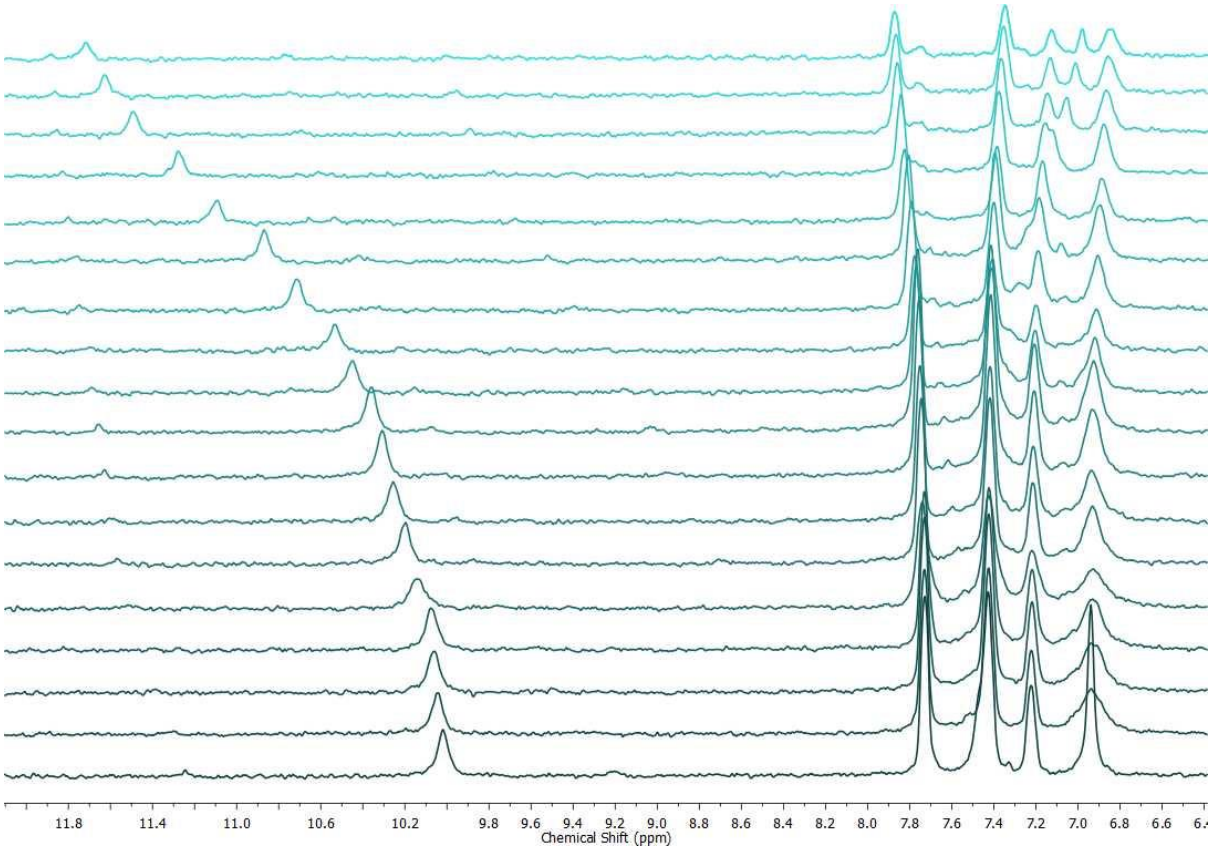

Figure 67. ^{1}H NMR titration spectra as a stack plot for 3,6-dioxo-*N*-phenylcyclohexa-1,4-diene-1-carboxamide (5 mM) + TBACl in pure CD_3CN-d_3 at 298 K.

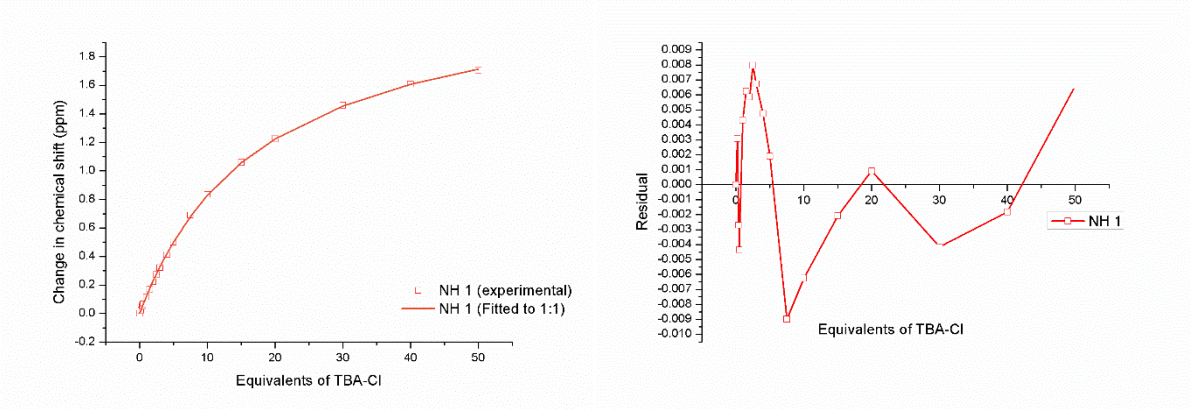

Figure 68. Fitted binding isotherm of 3,6-dioxo-*N*-phenylcyclohexa-1,4-diene-1-carboxamide + TBACl in pure acetonitrile, showing the change in chemical shift of the NH proton fitted to the 1:1 binding model (left). K_a = 11.2 M^{-1} Residual plot showing the random error obtained from the binding isotherm fitting (right). Covariance of fit (cov_{fit}) = 7.59 x 10^{-5}. Link to Bindfit fitting: http://app.supramolecular.org/bindfit/view/0e8c07c2-f323-421f-9064-7fd84b33b6ee.

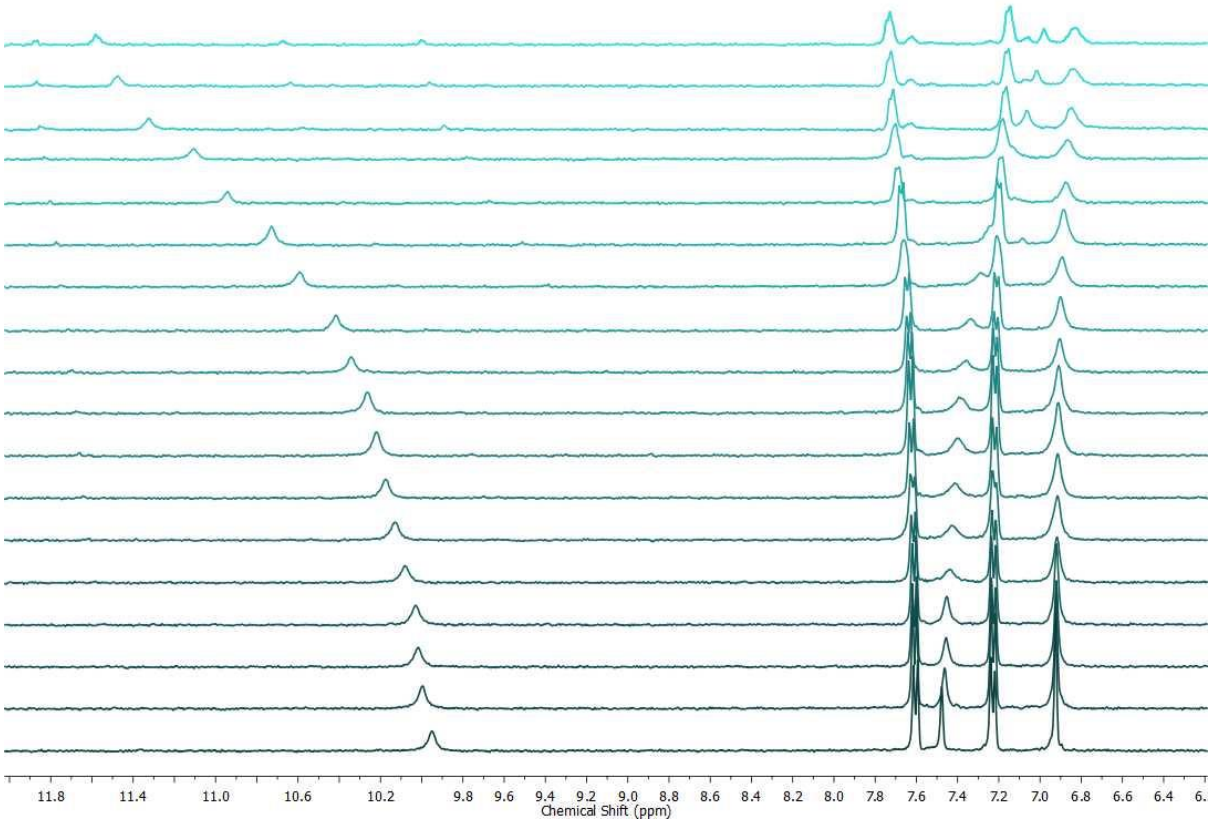

Figure 69. ^{1}H NMR titration spectra as a stack plot for 3,6-dioxo-N-(p-tolyl)cyclohexa-1,4-diene-1-carboxamide (5 mM) + TBACl in CD_3CN-d_3 at 298 K.

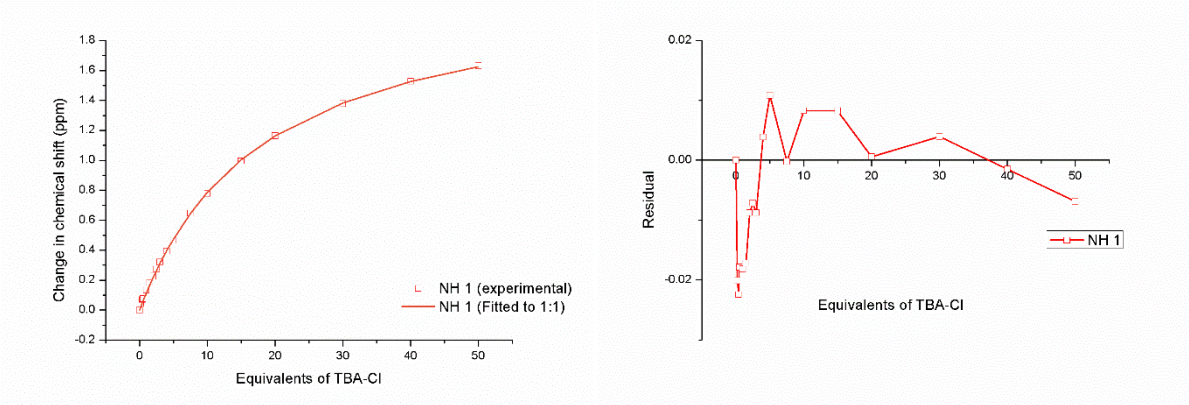

Figure 70. Fitted binding isotherm of 3,6-dioxo-N-(p-tolyl)cyclohexa-1,4-diene-1-carboxamide + TBACl showing the change in chemical shift of the NH proton fitted to the 1:1 binding model (left). K_a = 11.39 M^{-1} Residual plot showing the random error obtained from the binding isotherm fitting (right). Covariance of fit (cov_{fit}) = 3.79 x 10^{-4}. Link to Bindfit fitting: http://app.supramolecular.org/bindfit/view/702ba05b-af22-41f8-92d3-03851c9bbfa4.

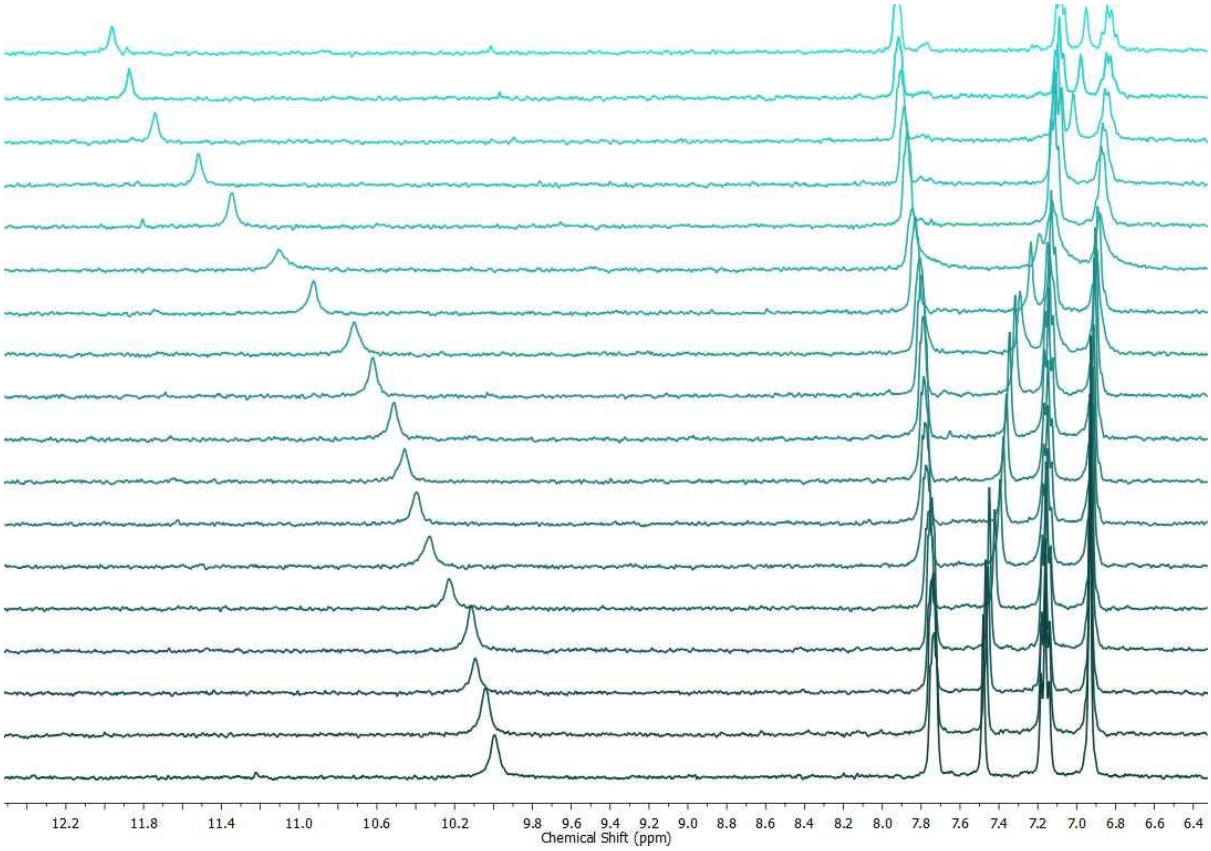

Figure 71. ^{1}H NMR titration spectra as a stack plot for *N*-(4-fluorophenyl)-3,6-dioxocyclohexa-1,4-diene-1-carboxamide (5mM) + TBACl in CD_3CN-d_3 at 298 K.

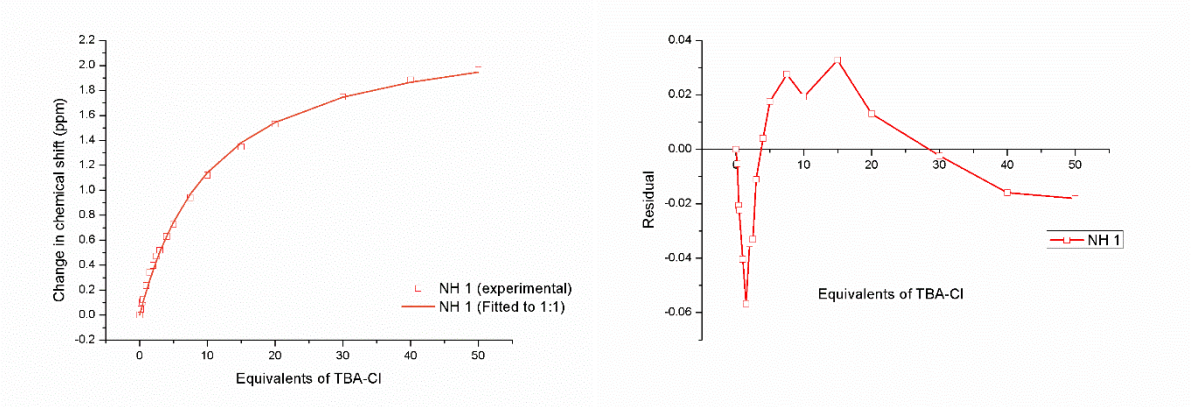

Figure 72. Fitted binding isotherm of *N*-(4-fluorophenyl)-3,6-dioxocyclohexa-1,4-diene-1-carboxamide + TBACl, showing the change in chemical shift of the NH proton fitted to the 1:1 binding model (left). K_a = 19.64 M^{-1} Residual plot showing the random error obtained from the binding isotherm fitting (right). Covariance of fit (cov_{fit}) = 1.39 x 10^{-3}. Link to Bindfit fitting: http://app.supramolecular.org/bindfit/view/c1e8a021-5a3e-449d-9029-c877be8af61f.

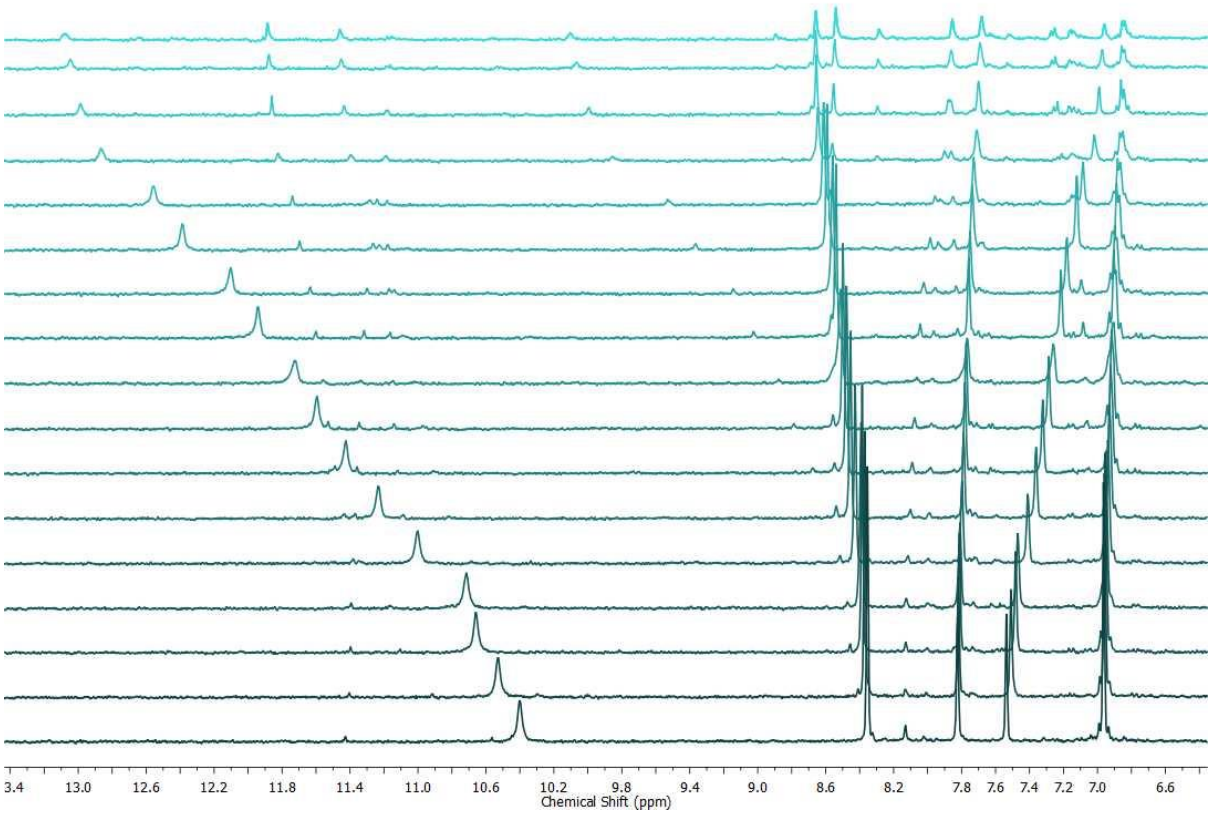

Figure 73. ^{1}H NMR titration spectra as a stack plot for *N*-(3,5-bis(trifluoromethyl)phenyl)-3,6-dioxocyclohexa-1,4-diene-1-carboxamide (5mM) + TBACl in CD_3CN-d_3 at 298 K.

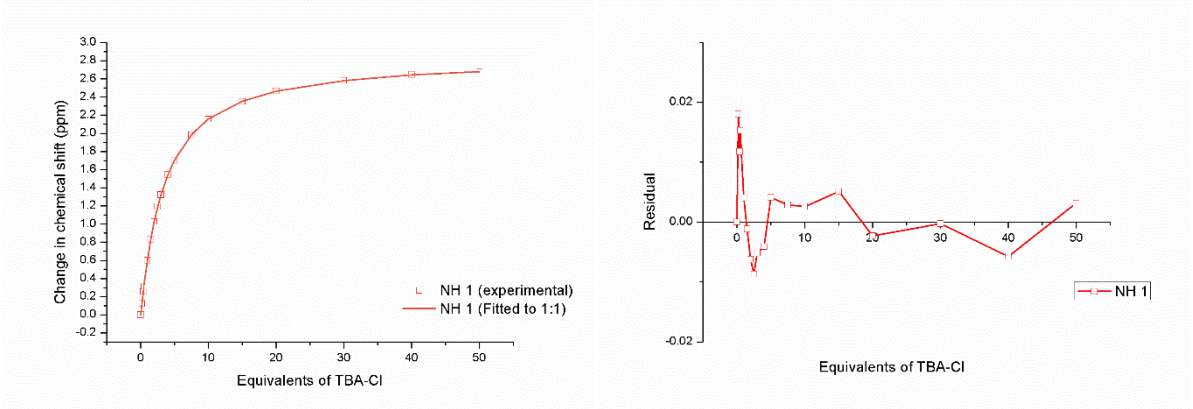

Figure 74. Fitted binding isotherm of *N*-(3,5-bis(trifluoromethyl)phenyl)-3,6-dioxocyclohexa-1,4-diene-1-carboxamide + TBACl showing the change in chemical shift of NH proton fitted to the 1:1 binding model (left). K_a = 68.05 M^{-1} Residual plot showing the random error obtained from the binding isotherm fitting (right). Covariance of fit (cov_{fit}) = 8.60 x 10^{-4}. Link to Bindfit fitting: http://app.supramolecular.org/bindfit/view/e26132bd-3fcb-428f-a064-18bd69f38557.

4. Electrochemical Studies

Equipment and Procedure

A Basi electrochemical workstation was used for cyclic voltammetry (CV). Initial CV measurements were performed in 0.1 M $TBAPF_6/CH_3CN$ solution at a scan rate of $100mVs^{-1}$ ranging from 800 mV to -1000 mV. All experiments were carried out at room temperature with three electrode system. A 1 mm diameter glassy carbon(GC) electrode was used as working electrode, the Ag/AgCl electrode as psuedoreference electrode, and platinum wire as the auxiliary electrode. Ferrocene was added to the solution and potentials were referenced against the Fc/Fc^+ redox couple.

Scan rate experiments were also undertaken using a Basi electrochemical workstation. Measurements were performed in 0.1 M $TBAPF_6$ solution and scan rate was varied from 20 mVs^{-1} to 300 mVs^{-1} between the voltage range of 560 mV to -1000 mV. Voltammograms were recorded for every 20 mVs^{-1} in scan rate. A 1 mm diameter glassy carbon(GC) electrode was used as working electrode, the Ag/AgCl electrode as psuedoreference electrode, and platinum wire as the auxiliary electrode. Ferrocene was added to the solution for reference, however only peak current data was used for further analysis.

Cyclic Voltammograms

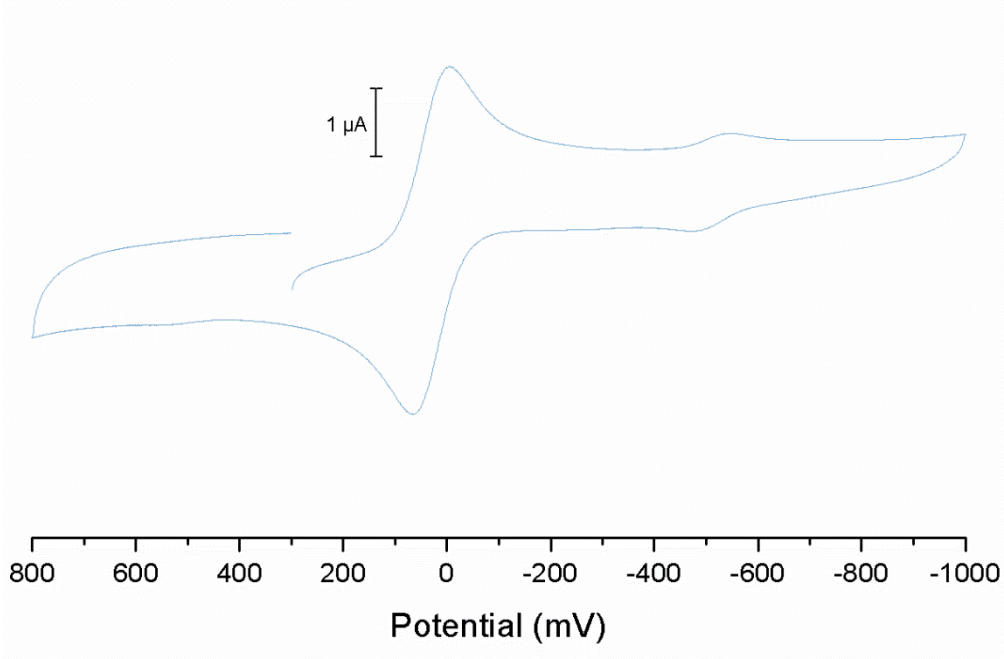

Figure 75. Cyclic Voltammogram of compound **5** 3,6-dioxo-*N*-phenylcyclohexa-1,4-diene-1-carboxamide at 100 mVs^{-1} in the presence of Fc/Fc^{+}.

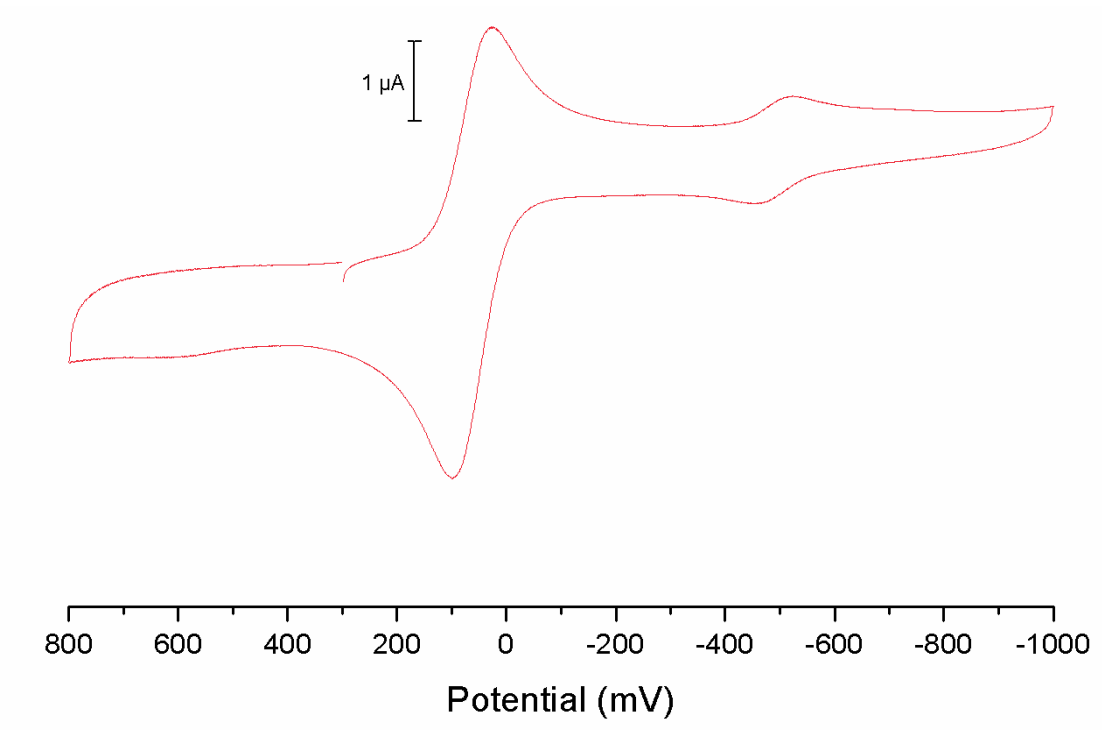

Figure 76. Cyclic Voltammogram of compound **6** 3,6-dioxo-N-(p-tolyl)cyclohexa-1,4-diene-1-carboxamide at 100 mVs^{-1} in the presence of Fc/Fc^{+}.

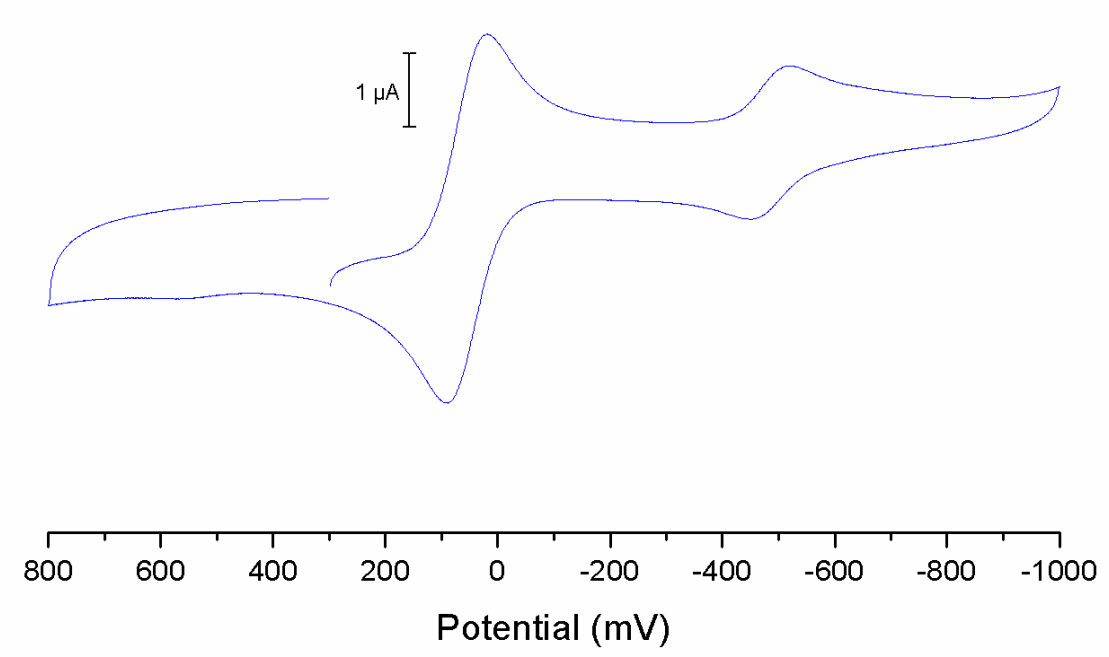

Figure 77. Cyclic Voltammogram of compound **7** *N*-(4-fluorophenyl)-3,6-dioxocyclohexa-1,4-diene-1-carboxamide at 100 mVs^{-1} in the presence of Fc/Fc^{+}.

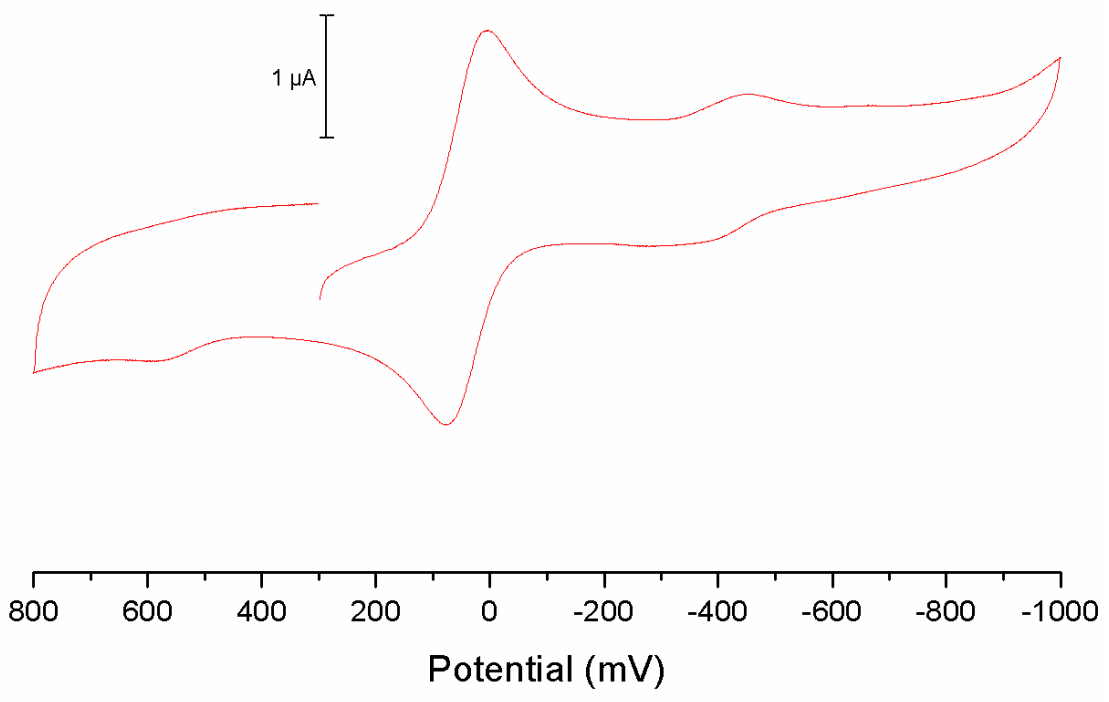

Figure 78. Cyclic Voltammogram of compound **8** *N*-(3,5-bis(trifluoromethyl)phenyl)-3,6-dioxocyclohexa-1,4-diene-1-carboxamide at 100 mVs^{-1} in the presence of Fc/Fc^{+}.

Scan Rate Experiments

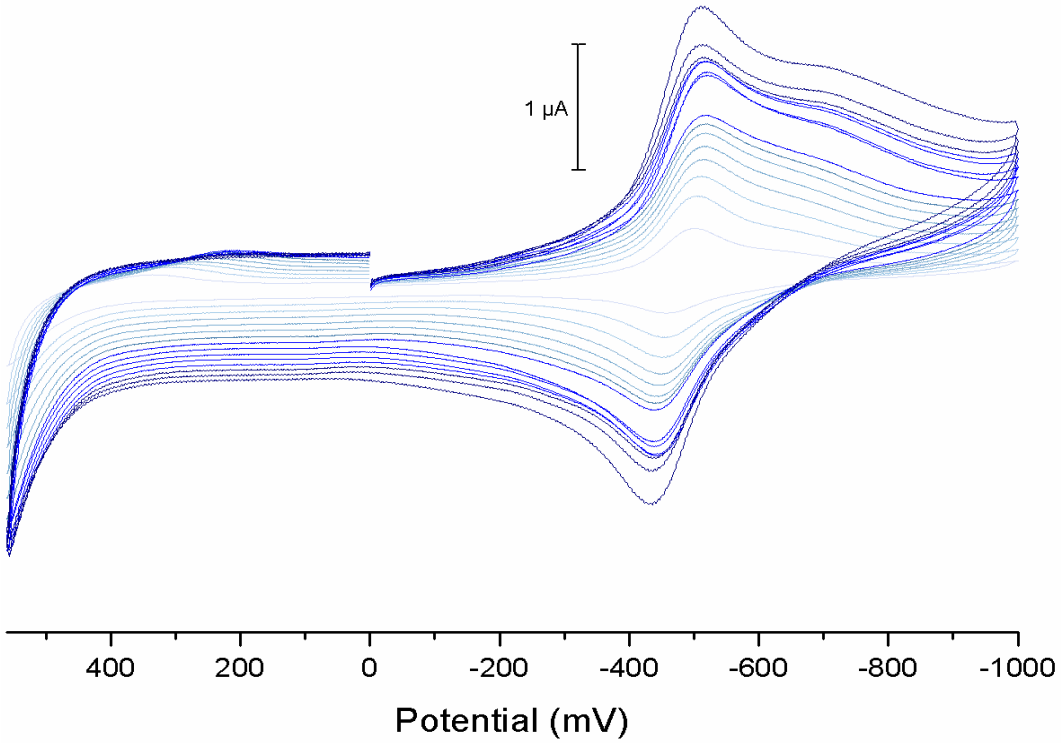

Figure 79. Series of cyclic voltammograms of compound **5** 3,6-dioxo-*N*-phenylcyclohexa-1,4-diene-1-carboxamide taken from scan rate 20 mVs^{-1} to 300 mVs^{-1}. The current response increases with faster scan rates.

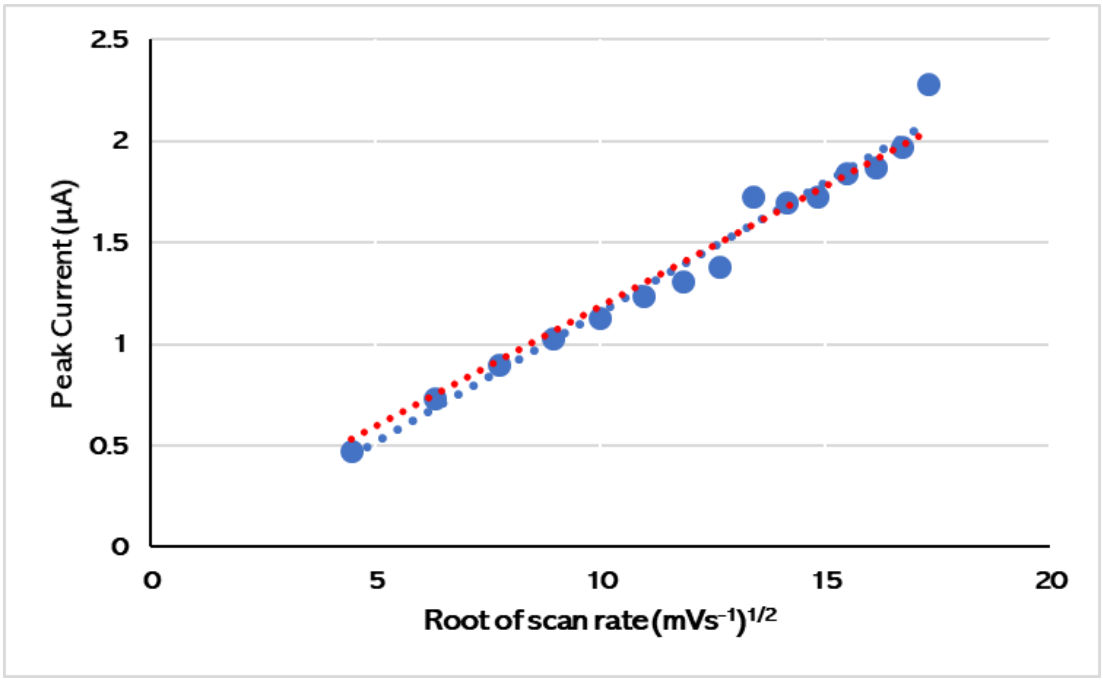

Figure 80. Plot of the root of scan rate ($v^{1/2}$) against peak current ($I_{p,c}$) for compound **5** 3,6-dioxo-*N*-phenylcyclohexa-1,4-diene-1-carboxamide. The red line shows the line of best fit through the origin, the blue line shows the true line of best fit.

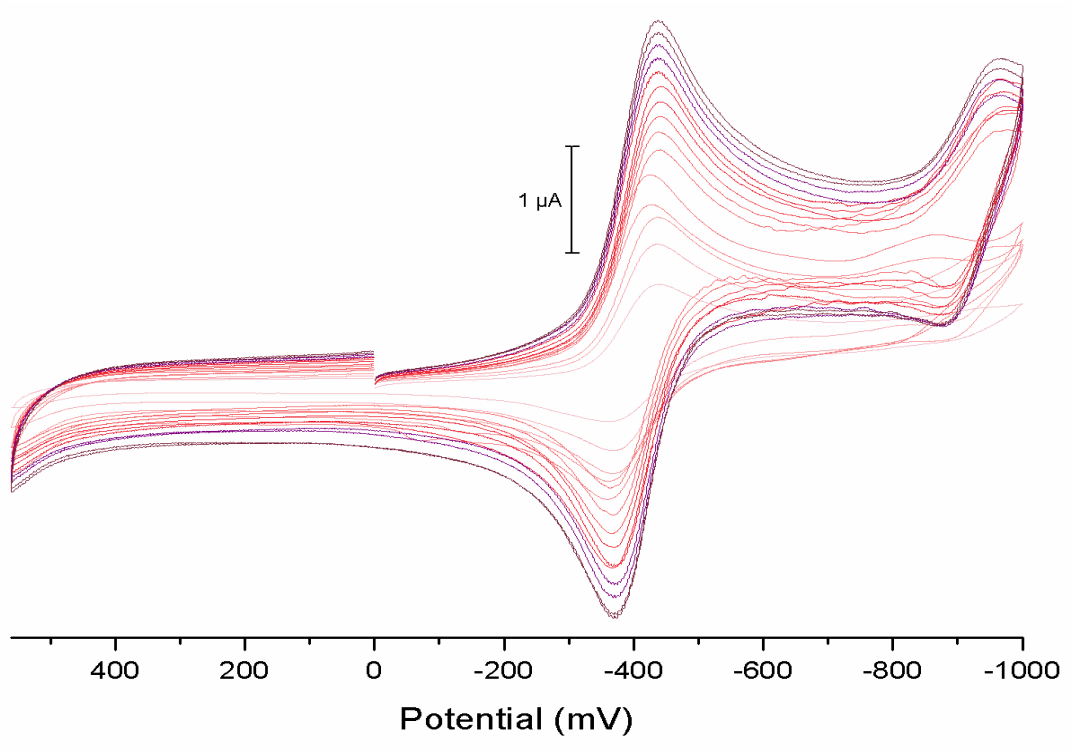

Figure 81. Series of cyclic voltammograms of compound **6** 3,6-dioxo-N-(p-tolyl)cyclohexa-1,4-diene-1-carboxamide taken from scan rate 20 mVs^{-1} to 300 mVs^{-1}. The current response increases with faster scan rates.

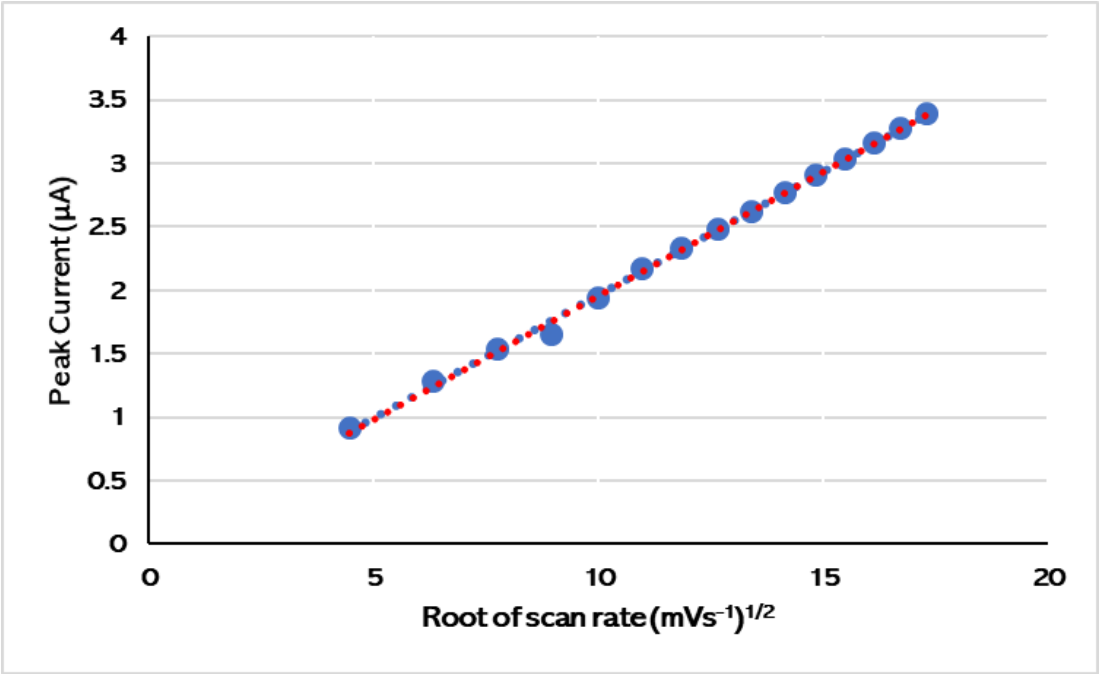

Figure 82. Plot of the root of scan rate ($v^{1/2}$) against peak current ($I_{p,c}$) for compound **6** 3,6-dioxo-N-(p-tolyl)cyclohexa-1,4-diene-1-carboxamide. The red line shows the line of best fit through the origin, the blue line shows the true line of best fit.

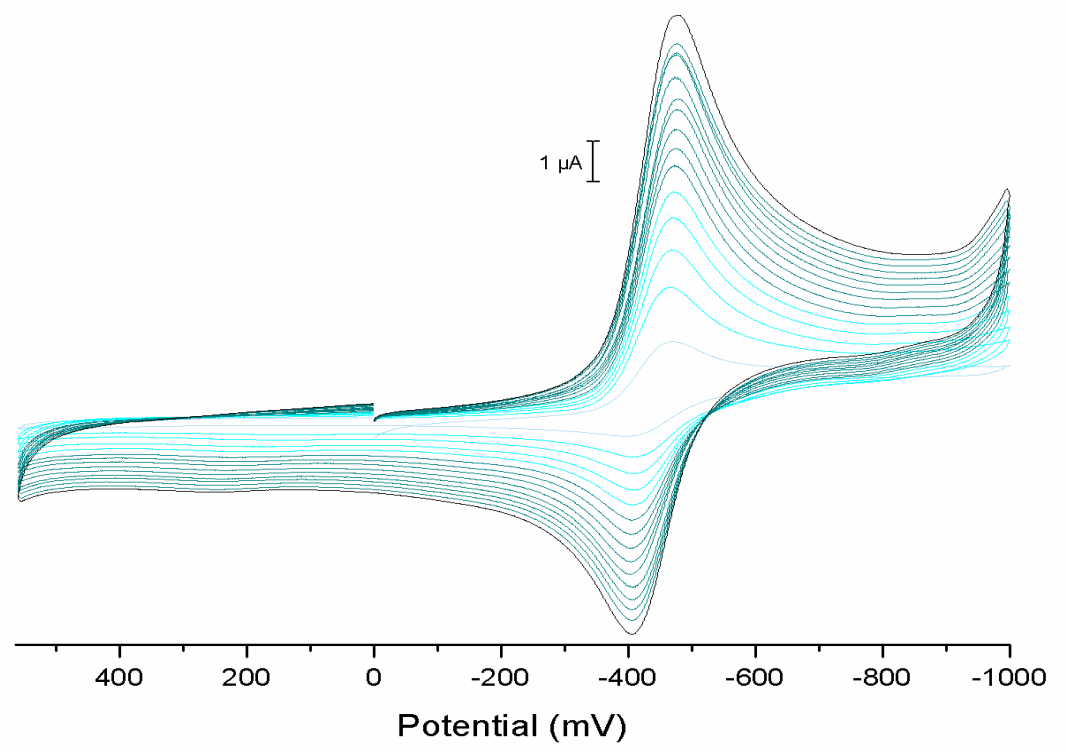

Figure 83. Series of cyclic voltammograms of compound **7** *N*-(4-fluorophenyl)-3,6-dioxocyclohexa-1,4-diene-1-carboxamide taken from scan rate 20 mVs^{-1} to 300 mVs^{-1}. The current response increases with faster scan rates.

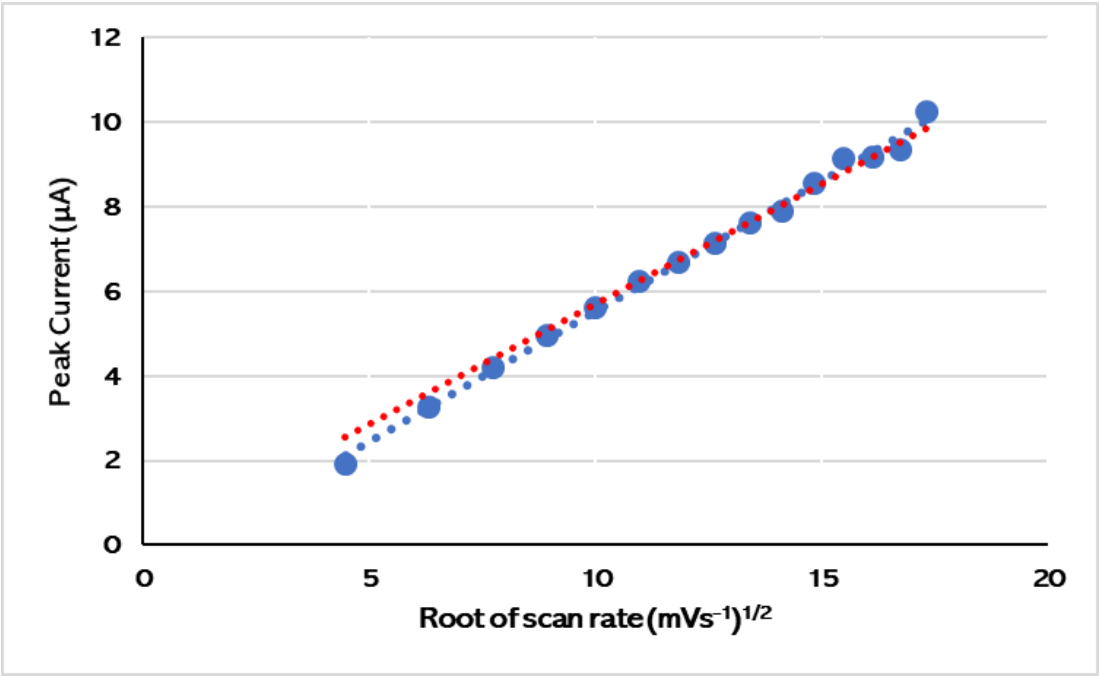

Figure 84. Plot of the root of scan rate ($v^{1/2}$) against peak current ($I_{p,c}$) for **7** *N*-(4-fluorophenyl)-3,6-dioxocyclohexa-1,4-diene-1-carboxamide. The red line shows the line of best fit through the origin, the blue line shows the true line of best fit.

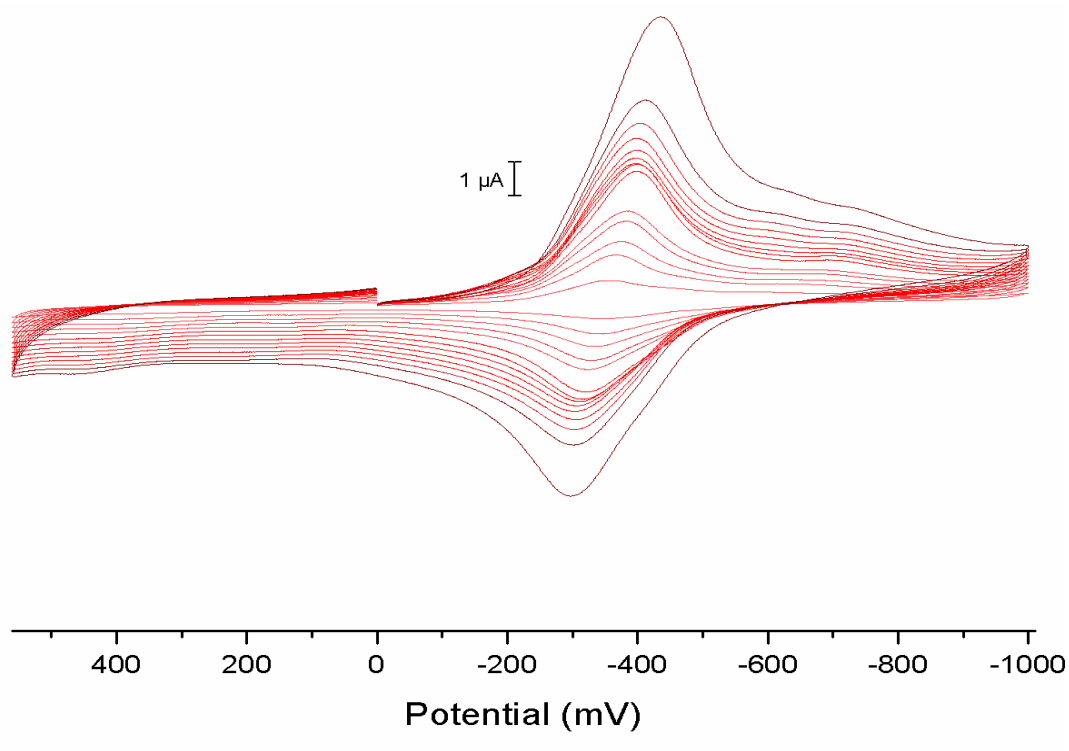

Figure 85. Series of cyclic voltammograms of compound **8** *N*-(3,5-bis(trifluoromethyl)phenyl)-3,6-dioxocyclohexa-1,4-diene-1-carboxamide taken from scan rate 20 mVs^{-1} to 300 mVs^{-1}. The current response increases with faster scan rates.

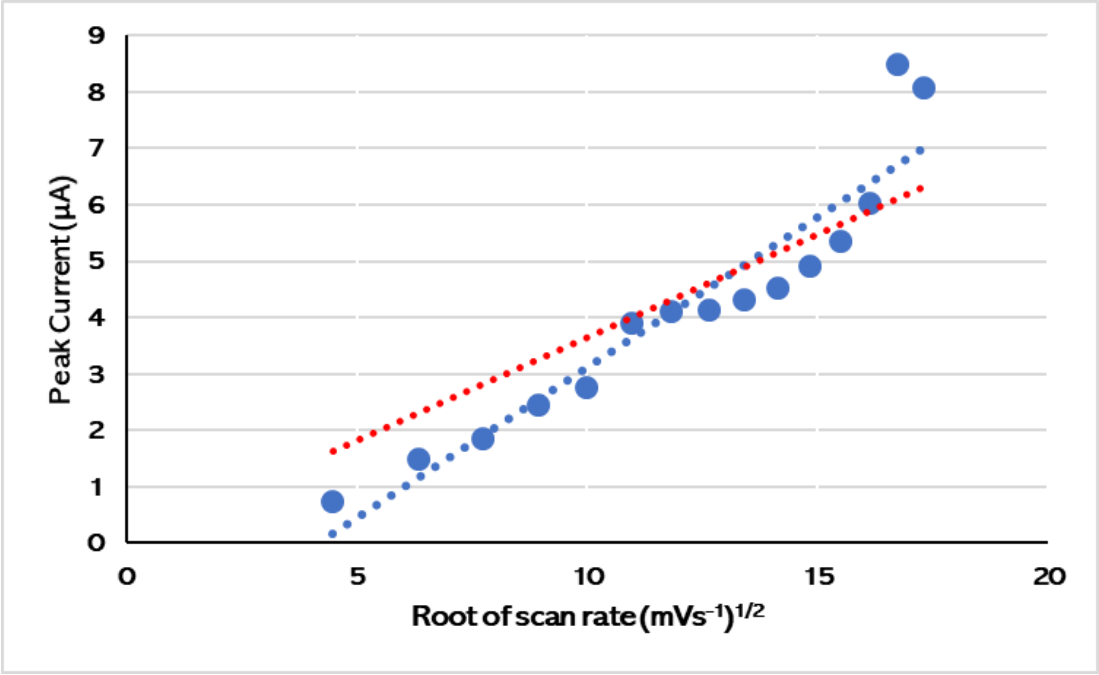

Figure 86. Plot of the root of scan rate ($v^{1/2}$) against peak current ($I_{p,c}$) for **8** *N*-(3,5-bis(trifluoromethyl)phenyl)-3,6-dioxocyclohexa-1,4-diene-1-carboxamide. The red line shows the line of best fit through the origin, the blue line shows the true line of best fit.

References

1. Wachter, V. Chemical synthesis of small molecule libraries around the p-benzoquinone scaffold 2007.